

*A new genus and new species of
Desmosomatidae Sars, 1897 (Isopoda) from
the eastern South Atlantic abyss described
by means of integrative taxonomy*

**Saskia Brix, Florian Leese, Torben Riehl
& Terue Cristina Kihara**

Marine Biodiversity

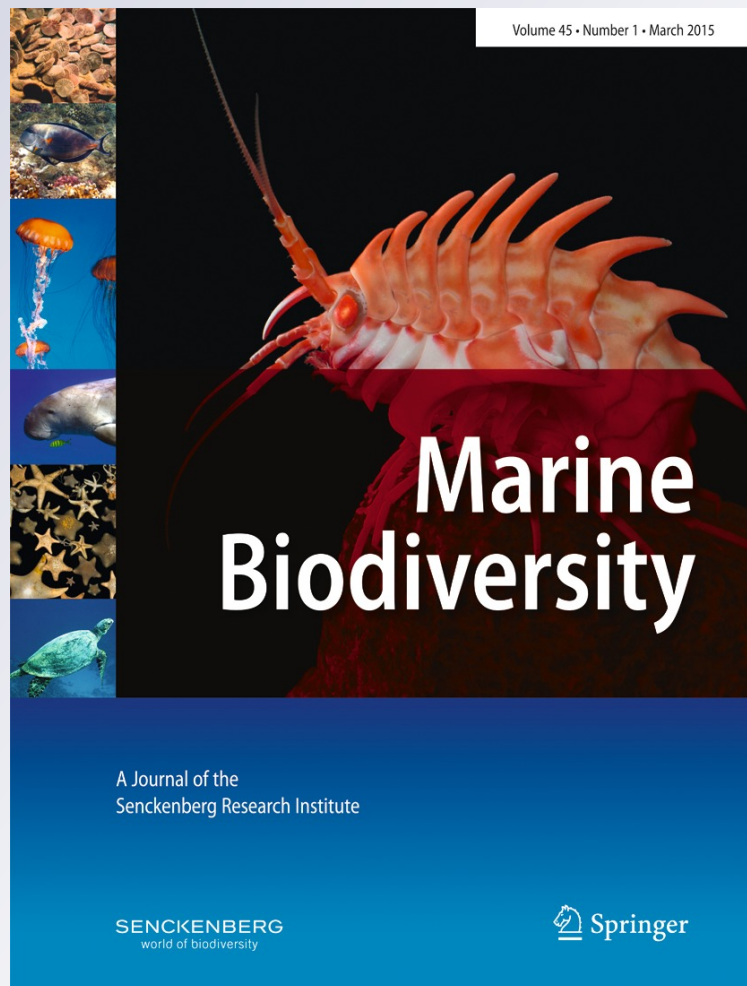
ISSN 1867-1616

Volume 45

Number 1

Mar Biodiv (2015) 45:7-61

DOI 10.1007/s12526-014-0218-3



Your article is protected by copyright and all rights are held exclusively by Senckenberg Gesellschaft für Naturforschung and Springer-Verlag Berlin Heidelberg. This e-offprint is for personal use only and shall not be self-archived in electronic repositories. If you wish to self-archive your article, please use the accepted manuscript version for posting on your own website. You may further deposit the accepted manuscript version in any repository, provided it is only made publicly available 12 months after official publication or later and provided acknowledgement is given to the original source of publication and a link is inserted to the published article on Springer's website. The link must be accompanied by the following text: "The final publication is available at link.springer.com".

A new genus and new species of Desmosomatidae Sars, 1897 (Isopoda) from the eastern South Atlantic abyss described by means of integrative taxonomy

Saskia Brix · Florian Leese · Torben Riehl ·
Terue Cristina Kihara

Received: 2 July 2012 / Revised: 22 February 2014 / Accepted: 23 February 2014 / Published online: 3 May 2014
© Senckenberg Gesellschaft für Naturforschung and Springer-Verlag Berlin Heidelberg 2014

Abstract We used a combined morphological and genetic approach for species delineation within desmosomatid isopods in the eastern South Atlantic. Based on morphological data from light, scanning electron, and confocal laser scanning, microscopy as well as on mitochondrial (COI, 16S) and nuclear (18S) DNA markers, we describe two new species and a new genus. *Chelator aequabilis* is reported from the Guinea Basin and the Angola Basin. High intraspecific genetic variability did not allow final conclusions about relationships and species status of all analysed individuals. Due to the patterns of genetic variation and the subtle variation in some morphological characters, we conclude that more than one species might be hidden in *C. aequabilis* north of the Walvis Ridge. *Chelator rugosus* is described from the Cape Basin; the new monotypic genus *Parvochelus* is erected with the description of *P. russus* from the Guinea and the Brazil Basins. In

Parvochelus, pereopod I bears a carpo-chela, especially the carpus is slender and long, its width is smaller than the merus width. The slender and long seta that is situated laterally to the carpo-propodal articulation is another characteristic feature. Despite the divergence within this species, shared lineages on both sides of the Mid-Atlantic Ridge suggest sporadic connectivity between populations on both sides. Our results document how molecular data can complement morphology in an integrative taxonomic approach elucidating biodiversity in the deep sea. Keys to the genera of Desmosomatidae and the species of *Chelator* are provided.

Keywords Isopoda · DIVA · Latitudinal gradient · DNA barcoding · Biogeography · Identification key

Introduction

Modern deep-sea sampling, setting the standard for present-day deep-sea biodiversity observations, started with pioneering studies in the 1960s (Sanders et al. 1965; Hessler and Sanders 1967; Sanders and Hessler 1969). Dozens of scientific cruises were conducted in the subsequent decades (Rex and Etter 2010), e.g. the DIVA expeditions (*Latitudinal Gradients of deep-sea BioDiversity in the Atlantic Ocean*) within the *Census of the Diversity of Abyssal marine Life* (CeDAMar) in the frame of the *Census of Marine Life* (CoML).

The deep sea harbours a high diversity of isopods including many undescribed species (e.g. Brandt et al. 2007; Wilson 2008a). The family Desmosomatidae (Sars 1897) is one of the most diverse families of deep-sea asellote isopods (Choudhury and Brandt 2007; Brandt et al. 2005, 2007; Svavarsson et al. 1993; Wilson 2008a). The family has been sampled in the Arctic and North Atlantic (Malyutina and Kussakin 1996; Svavarsson 1988; Wilson 2008a), South

S. Brix (✉)
Senckenberg am Meer, German Centre for Marine Biodiversity
Research (DZMB), Biocenter Grindel, Martin-Luther-King-Platz 3,
20146 Hamburg, Germany
e-mail: sbrix@senckenberg.de

F. Leese
Department of Animal Ecology, Evolution and Biodiversity, Ruhr
University Bochum, Universitätsstraße 150, 44801 Bochum,
Germany
e-mail: florian.leese@rub.de

T. Riehl
Biocenter Grindel, Zoological Museum, University of Hamburg,
Martin-Luther-King-Platz 3, 20146 Hamburg, Germany
e-mail: t.riehl@gmx.de

T. C. Kihara
Senckenberg am Meer, German Centre for Marine Biodiversity
Research (DZMB), Südstrand 44, 26382 Wilhelmshaven, Germany
e-mail: terue-cristina.kihara@senckenberg.de

Atlantic (Brix 2007), North Pacific (Birstein 1963), South Pacific (Brix 2006a; Brix and Bruce 2008), and Southern Ocean (Kaiser and Brix 2005; Brix 2006b; Choudhury 2009). The genus *Chelator* Hessler, 1970 occurs worldwide with seven currently described species, predominantly recorded from the North Atlantic Ocean and the Arctic Ocean (Table 1).

Recently, the family Desmosomatidae has been found to be among the most abundant isopod taxa in the eastern South Atlantic abyss (Brandt et al. 2005; Brix 2007). About 2,500 isopod specimens were sampled during DIVA-2 (Source: DZMB database, unpublished data), 650 of which were desmosomatids.

The eastern South Atlantic is divided into three deep-sea basins: the Guinea, Angola, and the Cape Basins. Based on its topography and contrasting hydrographic environments on either side, the Walvis Ridge has been postulated to represent a barrier to dispersal of benthic deep-sea species (Brandt et al. 2005). Isopods are brooders and lack free-swimming larvae. It can therefore be hypothesised that dispersal is likely to only occur over short distances (Wilson and Hessler 1987). Based on assumptions of Brökeland (2010a), however, Brix et al. (2011), found evidence for gene flow among haploniscid isopod populations on each side of the Walvis Ridge. The findings that the rises and ridges between the eastern South Atlantic deep-sea basins often are not barriers for taxa with planktonic larvae, such as polychaetes (Böggemann 2009; see also Wilson and Hessler 1987) or with the capability to passively drift with bottom currents, such as certain harpacticoid copepods (Menzel et al. 2011), seems also to be at least partly true for brooders like isopods. It has been shown recently, however, that, at least in some instances, strictly benthic isopods are capable of long-distance dispersal (Leese et al. 2010; Brix et al. 2011; Riehl and Kaiser 2012). How deep-sea isopods that live on soft-sediments are able to disperse across such distances remains to be investigated (see Wilson and Hessler 1987).

The aim of this study was to assess the species diversity of the genus *Chelator* in the three ocean basins of the eastern South Atlantic. We applied an integrative taxonomic approach, i.e. species diversity as inferred using both morphological and molecular approaches. We described two new

species of *Chelator* and a new monotypic genus. Furthermore, we compared patterns of haplotype diversity across marine mountain chains such as the Walvis Ridge and the Mid-Atlantic Ridge to investigate whether these may act as barriers to gene flow for benthic isopods. Identification keys to the subfamilies and genera of Desmosomatidae Sars, 1897 and to the species of *Chelator* Hessler, 1970 are provided.

Materials and methods

Specimens were sampled during recent expeditions (Fig. 1): DIVA-1–3, ANDEEP (*Antarctic benthic deep-sea biodiversity*), and IceAGE (*Icelandic marine Animals: Genetics and Ecology*). We focused on specimens sampled during DIVA-2 in 2005 (Tables 2 and 3) using an epibenthic sledge (EBS; Brenke 2005). For further details on the DIVA-1 and 2 sampling, see also Böggeman (2009), Brökeland (2010a, b), Brix et al. (2011) and Kröncke et al. (2013). All specimens used for molecular analyses are listed in Table 3.

Molecular methods

We sequenced the nuclear ribosomal small subunit (18S, complete sequence), the mitochondrial large ribosomal subunit (16S, fragment) and the mitochondrial cytochrome c subunit 1 gene (COI) for seven desmosomatid species. DNA extraction of freshly preserved specimens was performed as outlined by Brix et al. (2011). PCR was performed using primers 1471/1472 (Crandall and Fitzpatrick 1996), HCO2198/LCO1492 for COI (Folmer et al. 1994), 16A/16B for 16S (Palumbi et al. 1991) and 18A1neu/1800neu for 18S (Raupach et al. 2004). Protocols for PCR are listed in Table 4. An aliquot of 2–4 µl of undiluted DNA extraction was stored together with the voucher specimen at –20 °C. In the case of ZMH K–43204 (D2D072) only, we used the entire extracted DNA due to difficulties to obtain high quality sequences.

Sequences of 2–3 non-desmosomatid isopods obtained from GenBank were included as outgroup (see Table 3). Editing and assembly of contigs was performed using

Table 1 Distribution of *Chelator* species worldwide and their bathymetric range

| | | |
|--|-------------------|---------------|
| <i>C. brevicaudus</i> (Menziés & George, 1972) | Peru–Chile Trench | 1,238 m |
| <i>C. chelatus</i> (Stephensen, 1915) | Mediterranean | 0–126 m |
| <i>C. insignis</i> (Hansen, 1916) | N. Atlantic | 139–2,702 m |
| <i>C. stellae</i> Malyutina & Kussakin 1996 | Polar Sea | 230 m |
| <i>C. striatus</i> (Menziés, 1962) | Atlantic | 126 m |
| <i>C. verecundus</i> Hessler, 1970 | N. Atlantic | 1,150–2,500 m |
| <i>C. vulgaris</i> Hessler, 1970 | N. Atlantic | 2,496–4,833 m |
| <i>C. rugosus</i> Brix & Riehl sp. nov. | S. Atlantic | 5,054–5,055 m |
| <i>C. aequabilis</i> Brix & Leese sp. nov. | S. Atlantic | 5,047–5,415 m |

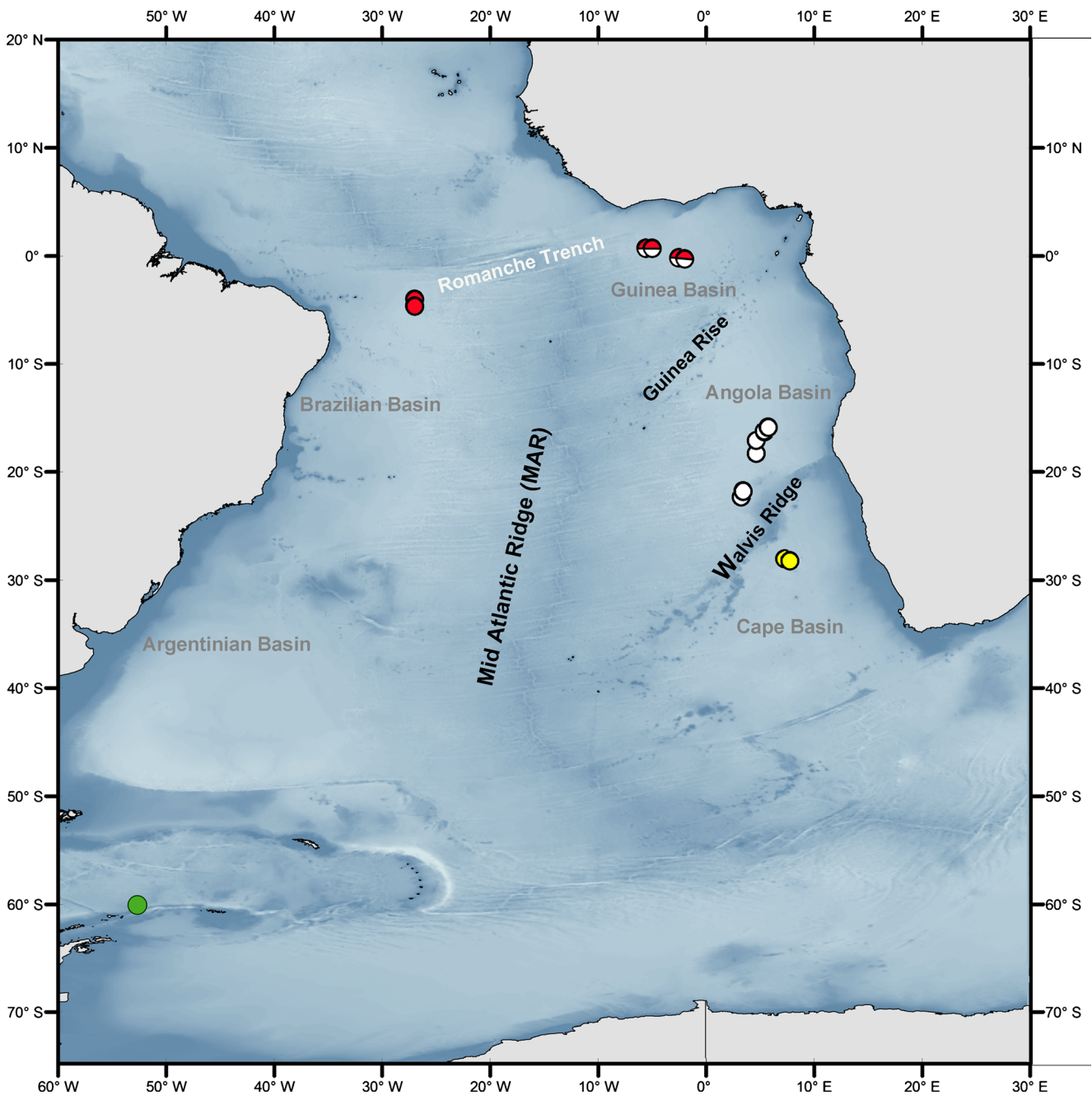


Fig. 1 South Atlantic DIVA stations, where the newly described species were found. Colours of dots indicating the presence of the single species: red *Parvochelus russus* sp. nov. Brix & Kihara, yellow *Chelator rugosus*

sp. nov. Brix & Riehl, white *Chelator aequabilis* sp. nov. Brix & Leese, green *Chelator* sp. from the Southern Ocean

Geneious 5.5 (Drummond et al. 2011). Sequence alignment was performed using MAFFT (Kato et al. 2002) with the L-INS-i (16S and COI) or the E-INS-i (18S) algorithm as implemented in Geneious 5.5. The most appropriate model of sequence evolution for each alignment was determined using jModeltest (Posada 2008) using both, the Akaike and the Bayesian Information Criterion (AIC and BIC, respectively). The models selected for the calculation of phylogenetic trees with MrBayes were: COI: GTR+I+G (AIC) and HKY+G

(BIC), respectively; and 16S: GTR+I+G (AIC), 18S GTR+I+G (both criteria). However, since the resulting trees differed only marginally in the support values but not in their topology, we used the model reported from the AIC for the remainder of this study.

To remove the ambiguously aligned hypervariable expansion segment from the 18S alignment, we used Gblocks (Castresana 2000), allowing smaller blocks, fewer strict flanking regions and gaps in the final alignment. A Bayesian

Table 2 List of DIVA stations, were specimens were sampled (Brix 2007; Brökeland 2010a, b)

| Expedition | Station | Date | Lat | Long | Depth (m) | Trawling distance (m) |
|------------|---------|------------|------------|------------|-----------|-----------------------|
| DIVA-1 | 318-1 | 09.07.2000 | 22°20.0'S | 03°18.3'E | 5,144 | 3,147 |
| DIVA-1 | 320-2 | 10.07.2000 | 22°19.9'S | 03°17.8'E | 5,126 | 2,446 |
| DIVA-1 | 340-9 | 22.07.2000 | 18°18.3'S | 04°41.3'E | 5,395 | 3,985 |
| DIVA-1 | 344-10 | 25.07.2000 | 17°06.20'S | 04°41.70'E | 5,415 | 4,475 |
| DIVA-1 | 348-11 | 28.07.2000 | 16°18.10'S | 05°27.20'E | 5,390 | 4,599 |
| DIVA-1 | 350-12 | 29.07.2000 | 16°14.30'S | 05°26.80'E | 5,389 | 3,179 |
| DIVA-2 | 40-1 | 04.03.2005 | 28°3.07'S | 07°19.81'E | 5,055 | 1,620 |
| DIVA-2 | 41-2 | 04.03.2005 | 28°3.98'S | 07°20.49'E | 5,054 | 1,368 |
| DIVA-2 | 63-4 | 15.03.2005 | 0°8.79'S | 02°28.75'W | 5,047 | 4,176 |
| DIVA-2 | 64-5 | 15.03.2005 | 0°13.27'S | 02°29.91'W | 5,054 | 2,520 |
| DIVA-2 | 89-6 | 20.03.2005 | 0°42.95'N | 05°31.29'W | 5,142 | 3,132 |
| DIVA-2 | 90-7 | 20.03.2005 | 0°40.49'N | 05°29.71'W | 5,142 | 1,440 |
| DIVA-3 | 604-7 | 05.08.2009 | 03°57.67'S | 28°05.36'W | 5,180 | 2,550 |
| DIVA-3 | 605-8 | 06.08.2009 | 03°57.49'S | 28°04.67'W | 5,189 | 2,340 |

consensus tree was calculated using MrBayes v.3.2. Search parameters consisted of four independent runs with four chains each. Results were checked for convergence and the first 25 % of the trees were discarded as burnin. ML trees were calculated with Phyml (Guindon et al. 2010) and the parameters of the model reported from jModeltest. Bootstrap support was calculated using 1,000 replicates. All DNA sequences assigned to species of the present paper can be retrieved from GenBank and are indicated in the description below. Alignments are deposited in TreeBASE under Accession number S 12946 (<http://purl.org/phylo/treebase/phyloids/study/TB2:S12946>).

Morphological methods

Line drawings were made as described in Brix (2007) using a Leica DM 2500 compound microscope with a camera lucida. Specimens were oriented according to Hessler (1970) and Wilson (2008b), where possible without damaging specimens (exceptions are marked in the figure captions). For the terminology of most important setae types, see Hessler (1970), Brix (2007) and Riehl and Brandt (2010). Figures were inked manually. They were digitised and assembled as plates using Adobe Photoshop CS5. Holotypes were used for habitus drawings. Where available, appendages were dissected from paratypes only.

Specimen handling for SEM

Sixteen specimens were used for scanning-electron microscopy (SEM) as indicated in the descriptions below. They were cleaned in an ultrasonic bath for 10 s and dehydrated in a series of ethanol concentrations, transferred to 100 % acetone

and critical point dried. After drying they were sputter coated with gold (DIVA-1 specimen ZMH K-43209, VVK2.6) or graphite (DIVA-2 specimens). The specimens were photographed in a Leo 1525 SEM.

Confocal Laser Scanning Microscopy (CLSM)

Four specimens were used for CLSM as indicated in the descriptions below. Before dissection, two adult specimens of *Chelator aequabilis* Brix & Leese sp. nov. (ZMH K-43207 female and ZMH K-43208 male) were stained with Congo Red and other two specimens of *Parvochelus russus* Brix & Kihara sp. nov. (ZMH K-43244 female and ZMH K-43245 male) were stained with Acid Fuchsin, using procedures adapted from Michels and Büntzow (2010)).

The whole specimens were temporarily mounted onto slides with glycerine, and self-adhesive plastic reinforcement rings were used to support the coverslip (Kihara and Rocha 2009; Michels and Büntzow 2010). When required, specimens were dissected in glycerine under a Leica MZ12 stereomicroscope. Dissected parts were mounted on slides using glycerine as mounting medium, and pieces of coverslip with appropriate thickness were mounted between the slide and coverslip, so that the parts were not compressed.

The material was examined using a Leica TCS SP5 equipped with a Leica DM5000 B upright microscope and 3 visible-light lasers (DPSS 10 mW 561 nm; HeNe 10 mW 633 nm; Ar 100 mW 458, 476, 488 and 514 nm), combined with the software LAS AF 2.2.1. (Leica Application Suite Advanced Fluorescence).

Different lenses were used, depending on the size of the material scanned (Table 5). Images were obtained using only

Table 3 List of voucher specimens used for the genetic study located at the Zoological Museum Hamburg (ZMH) or the German Centre of Marine Biodiversity Research (DZMB HH) and all available information (GB Guinea Basin, CB Cape Basin, AB Angola Basin, BB Brazilian Basin, IB Iceland Basin); all other specimens used for species description and comparative specimens are listed in the species descriptions

| Expedition | Deep-sea basin | Taxon (type status) | Seqs | GenBank accession number(s) | DZMBHH &/or ZMH catalogue number | Expedition identification number | Sex/stage |
|-------------|----------------|---|---------------|-----------------------------------|----------------------------------|----------------------------------|---------------|
| DIVA-2 | CB | <i>Chelator rugosus</i> (holotype) | COI, 18S | KJ578683 KJ578676 | ZMH K-43228 | D2D002 | Female/prep |
| DIVA-2 | CB | <i>Chelator rugosus</i> (paratype) | COI, 16S, 18S | KJ578686 KJ578667 KJ578678 | ZMH K-43229 | D2D003 | Male/adult |
| DIVA-2 | CB | <i>Chelator rugosus</i> (paratype) | COI, 16S | KJ578684 KJ578668 | ZMH K-43230 | D2D012 | Juvenile |
| DIVA-2 | CB | <i>Chelator rugosus</i> (paratype) | COI, 18S | KJ578687 KJ578677 | ZMH K-43230 | D2D013 | Juvenile |
| DIVA-2 | CB | <i>Chelator rugosus</i> (paratype) | COI, 16S | KJ578685 KJ578665 | ZMH K-43230 | D2D014 | Juvenile |
| DIVA-2 | CB | <i>Chelator rugosus</i> (paratype) | COI, 16S | KJ578688 KJ578666 | ZMH K-43230 | D2D016 | Juvenile |
| DIVA-2 | GB | <i>Chelator aequabilis</i> (holotype) | COI, 16S | KJ578689 KJ578662 | ZMH K-43203 | D2D023 | Female/prep |
| DIVA-2 | GB | <i>Chelator aequabilis</i> (paratype) | COI, 16S, 18S | KJ578690 KJ578663 KJ578675 | ZMH K-43205 | D2D051 | Juvenile |
| DIVA-2 | GB | <i>Chelator aequabilis</i> (paratype) | 16S, 18S | KJ578664 KJ578681 | ZMH K-43204 | D2D072 | Male/subadult |
| IceAGE1 | IB | <i>Chelator insignis</i> | COI | KJ578692 | DZMB HH 19905 | IDesm059 | Female/prep |
| IceAGE1 | IB | <i>Chelator insignis</i> | COI, 16S | KJ578693 KJ578670 | DZMB HH 19917 | IDesm071 | Female/prep |
| IceAGE1 | IB | <i>Chelator insignis</i> | 16S | KJ578669 | DZMB HH 19910 | IDesm064 | Female/prep |
| DIVA-2 | GB | <i>Parvochelus russus</i> (holotype) | COI, 16S | KJ578695 KJ578671 | ZMH K-43238 | D2D031 | Female/prep |
| DIVA-2 | GB | <i>Parvochelus russus</i> (paratype) | COI | KJ578696 | ZMH K-43239 | D2D035 | Female/prep |
| DIVA-2 | GB | <i>Parvochelus russus</i> (paratype) | COI, 16S | KJ578697 KJ578672 | ZMH K-43240 | D2D044 | Female/prep |
| DIVA-3 | BB | <i>Parvochelus russus</i> (paratype) | COI | KJ578694 | DZMB HH 9381 | D3D156 | Female/prep |
| DIVA-3 | BB | <i>Parvochelus russus</i> (paratype) | COI, 18S | KJ578698 KJ578674 | DZMB HH 9392 | D3D157 | Female |
| OUTGROUP(s) | | | | | | | |
| DIVA-2 | GB | <i>Eugerdella huberti</i> (holotype) | COI, 16S, 18S | HQ214677, HQ214679 KJ578682 | ZMH K-42422 | D2D053 | Female |
| DIVA-2 | GB | <i>Eugerdella theodori</i> | COI, 16S | KJ578699 KJ578673 | ZMH K-43212 | D2D050 | Female |
| DIVA-2 | GB | <i>Eugerdella theodori</i> | 18S | KJ578680 | ZMH K-43212 | D2D063 | Female |
| DIVA-2 | GB | <i>Eugerdella theodori</i> | 18S | KJ578679 | ZMH K-43212 | D2D064 | Female/oov. |
| DIVA-2 | CP | <i>Haploniscus rostratus</i> (paratype) | COI | JF283474 | ZMH K-42635 | DIVA2-HA456 | Unknown |
| ANDEEP | | <i>Haploniscus sp.</i> | 16S | AY693420 | | | |
| ANDEEP | 42-2 | <i>Haploniscus cucullus</i> | 18S | AY461465 | ZMH K-40760 | HA56 | |
| ANDEEP | 46-7 | <i>Chelator sp.</i> | COI, 18S | KJ57891 AY461460 | | DE1 | |
| ANDEEP | | <i>Betamorpha fusiformis</i> | 16S | EF116500 | | | |
| | | <i>Lipomerinae sp.</i> | COI | EF682297 | | | |
| | | <i>Paropsurus giganteus</i> | COI | EF682287 | | | |
| | | <i>Paropsurus giganteus</i> | 18S | EF682253 | | | |

561-nm excitation wavelength with acousto-optic tunable filter (AOTF) ranging between 30 and 80 %. Series of stacks were obtained, collecting overlapping optical sections throughout the whole preparation with optimal number of sections according to the software. The acquisition resolution was 2,048×2,048 pixels and the settings applied for the preparations are given in Table 5.

Final images were obtained by maximum projection, and CLSM illustrations were composed and adjusted for contrast and brightness using the software Adobe Photoshop CS4.

Abbreviations used in the recent study

A1 = antennula; A2 = antenna; Ip = Incisior process; lMd = left mandible; rMd = right mandible; lm = lacinia mobilis; mp = molar process; Op = operculum; PI–PVII = pereopods I–VII; Plt = pleotelson; Prn1–7 = pereonites 1–7; Up = uropods; ZMH = Zoological Museum, Hamburg; USNM = United States National Museum of Natural History, Washington; AMNH = American Museum of Natural History; ZMUC = Zoologisk Museum, University of Copenhagen; AM = Australian Museum

Comparative material

| | |
|--------------|---|
| USNM 125089 | <i>Chelator verecundus</i> Hessler, 1970, holotype female |
| USNM 125090 | <i>Chelator vulgaris</i> Hessler, 1970, holotype female |
| USNM 120963 | <i>Chelator brevicaudus</i> (Menzies & George, 1972), holotype male [1] |
| AMNH 12121 | <i>Chelator striatus</i> (Menzies, 1962), holotype** |
| AM P59160 | <i>Chelator vulgaris</i> Hessler, 1970, paratype female |
| AM P58856 | <i>Chelator insignis</i> Hessler, 1970, paratype female |
| ZMUC CRU-510 | <i>Chelator chelatus</i> (Stephensen, 1915), holotype* female |
| ZMUC CRU | plus 14 specimens deposited as “other material” (nontype Isopoda, blue label, no number) det. E. Fresi as <i>Desmosoma chelatus</i> , Ischia, Italy, 110 m, 16 May 1968 |
| ZMUC CRU-588 | <i>Chelator insignis</i> (Hansen, 1916)*, lectotype |
| ZMUC CRU-589 | <i>Chelator insignis</i> (Hansen, 1916)*, paralectotype |

*Types are deposited as *Desmosoma*.

**The type specimen is in very bad condition.

Results

Taxonomy

Family Desmosomatidae Sars, 1897

Subfamily Eugerdelatinae Hessler, 1970

Genus *Chelator* Hessler, 1970

Diagnosis

Anterior part of body (Prn1–4) compact (Prn1 higher than Prn5), cephalon with transverse ridge on frons and with frons-clypeal furrow, Prn5 and Plt of similar height. PI enlarged (carpus width about 2.0 PII carpus width), carpo-propodochelate with propodus rotating against a pronounced robust claw seta articulating distoventrally on carpus and the dactylus partly opposing the propodus and closing off the “hand” formed by propodus and carpal seta distally; propodus broad proximally and narrower distally; carpus flexor margin with minor setation (setae length less than

0.5 claw-seta length) or aetose; carpus produced distoventrally at base of claw-seta. Plt in females without posterolateral spines, small spines may be present in males (sexual dimorphism).

Remarks

In all Eugerdelatinae, sensu Hessler (1970), PI is enlarged compared to the PII. Apomorphies of *Chelator* distinguishing the genus from *Prochelator* are the production of the carpus at the base of the claw and the presence of at most only small setae behind the claw-seta. The posterolateral spines in *Chelator*, although absent in females, are variable in the males and therefore problematic as diagnostic characters. The uniramous condition of the uropods of *Chelator* spp. is shared with two species of *Prochelator* (*P. angolensis* and *P. incomitatus*). Clear apomorphies of *Chelator* thus remain only the character states of the PI as discussed in Brix and Bruce (2008).

Table 4 Main protocols for PCR of DIVA-2 extractions for all three markers

| PCR mix volumes (μl) | COI | 18S | 16S |
|---------------------------------------|-------|------------|-------|
| EPPENDORF® HotMasterMix (2.5×) | 10 | 25 | 10 |
| ddH ₂ O (μl) | 9 | 19 | 9 |
| Primer 1 (10–12 μM) | 1 | 1 (100 μM) | 1 |
| Primer 2 (10–12 μM) | 1 | 1 (100 μM) | 1 |
| Template DNA (μl) | 4 | 4 | 4 |
| Total volume (μl) | 25 | 50 | 25 |
| <i>PCR protocol</i> | | | |
| Preheated lid | Yes | No | Yes |
| Initial denaturation time (min) | 02:00 | 02:00 | 02:00 |
| Initial denaturation temperature (°C) | 94 | 94 | 94 |
| Denaturation time (min) | 00:45 | 00:30 | 00:45 |
| Denaturation temperature (°C) | 94 | 94 | 94 |
| Annealing time (min) | 00:45 | 00:50 | 00:45 |
| Annealing temperature (°C) | 50 | 52 | 50 |
| Elongation time (min) | 01:20 | 03:20 | 01:20 |
| Elongation temperature (°C) | 72/65 | 72/65 | 72/65 |
| Cycle number | 35 | 36 | 35 |
| Final elongation time (min) | 07:00 | 10:00 | 07:00 |

Synonymy

See Kussakin (1999)

Chelator aequabilis Brix & Leese sp. nov.

Material

A total of 119 specimens from 10 stations (DIVA-1 and 2) were determined and compared for the species description. Only specimens with DNA sequence available, those from the same locality as the holotype and those analysed with the SEM and CLSM are described and listed as types. All other specimens are listed as “other material.”

Holotype Female, preparatory, 2.9 mm; ZMH K–43203 (D2D023); designated here

Type locality Guinea Basin, start position: 0°13.27'S, end trawl: 2°29.91'W, depth 5,054 m; RV “Meteor” M63/2; station 64-5; gear: EBS; 15 March 2005.

Paratypes 1 male, subadult, 1.3 mm; ZMH K–43204 (D2D072); 20 March 2005; 1 juvenile, 2.2 mm; ZMH K–43205 (D2D051); 20 March 2005; – Guinea Basin, start position: 0°42.95'N, end position: 5°31.29'W, depth 5,142 m; RV “Meteor” M63/2; station 89-6; gear: EBS.

ZMH K-43206 (4 specimens), same locality as holotype. CLSM specimens:

DIVA-1: ZMH K-43207 (VH13) female; ZMH K–43208 (VH19) male; 28 July 2000; – Angola Basin, start position: 16°18.1'S, end position: 5°27.2'E, depth 5,390 m; RV “METEOR” M48/1; station 348-11; gear: EBS.

SEM specimens

DIVA-1: ZMH K–43209 (VVK2.6), 25 July 2000; – Angola Basin, start position: 17°06.2'S, end position: 4°41.7'E, depth 5,415 m; RV “METEOR” M48/1; station 344-10; gear: EBS.

DIVA-2: ZMH K–43210 (D2D233) male, ZMH K–43211 (D2D271) female, 15 March 2005; – Guinea Basin, start position: 0°8.79', end position: 2°28.75'W, depth 5,047 m; RV “METEOR” M63/2; station 63-2; gear: EBS. ZMH K–43213 (D2D450) male, ZMH K–43214 (D2D435) female, ZMH K–43215 (D2D464) juvenile, 15 March 2005; same locality as holotype. ZMH K–43216 (D2D549) male, 20 March 2005 – Guinea Basin, start position: 0°42.95'N, end position: 5°31.29'W, depth 5,142 m; RV “METEOR” M63/2; station 89-6; gear: EBS. ZMH K–43217 (D2D722) female, ZMH K–43218 (D2D647) male, 20 March 2005; – Guinea Basin, start position: 0°40.49'N, end position: 5°29.71'W, depth 5,142 m; RV “METEOR” M63/2; station 90-7; gear: EBS.

Table 5 List of specimens examined by CLSM with information on objectives and settings

| Preparation | Objective | Detected emission wavelength (nm) | Electronic zoom | Pinhole aperture (μm) |
|---|---|-----------------------------------|-----------------|-----------------------|
| ZMH K–43207 and ZMH K–43208 Habitus (Fig. 14a–d) and cuticle (Fig. 15b, e) | HCX PL APO CS 10.0X/0.40 DRY UV | 573–641 | 1.0 | 45.0–56.1 |
| ZMH K–43207 and ZMH K–43208 Dissected parts (Fig. 14a, c, d, f) | HCX PL APO CS 20.0X/0.70 IMM UV HCX PL APO CS 63.0X/1.40 OIL UV | 573–775 | 1.0–1.4 | 60.7–115.7 |
| ZMH K–43244 and ZMH K–43245 Habitus (Fig. 31a–d) and oostegite (Fig. 32d) | HGX PL APO CS 10.0X/0.40 DRY UV | 595–702 | 1.5–2.0 | 44.2–94.8 |
| ZMH K–43244 and ZMH K–43245 Dissected parts (Fig. 32a, c–e) | HGX APO U-V-I 40.0X/0.75 DRY UV HCX PL APO CS 20.0X/0.70 IMM UV HCX PL APO CS 63.0X/1.40 OIL UV | 571–775 | 1.3–3.0 | 55.8–117.9 |

Other material ZMH K–43219 (26 specimens), DIVA-1, station 318; ZMH K–43220 (2 specimens), DIVA-1, station 320; ZMH K–43221 (5 specimens), DIVA-1, station 340; ZMH K–43222 (12 specimens), DIVA-1, station 344; ZMH K–43223 (17 specimens), DIVA-1, station 348; ZMH K–43224 (15 specimens), DIVA-1, station 350; ZMH K–43225 (13 specimens), DIVA-2, station 63–4; ZMH K–43226 (6 specimens), DIVA-2, station 89–6; ZMH K–43227 (4 specimens), DIVA-2, station 90–7

Etymology

The species name refers to the “aequabilis” (Lat. uniform) appearance of the species which makes it difficult to distinguish from *Chelator rugosus* Brix & Riehl sp. nov.

Diagnosis

Body covered with subtle cuticular folds, predominantly head and pl. Lateral margins of Prn 1–7 smooth, Plt without posterolateral spines in female and male. Mxp scale tip without “hook” and fine setae, only one simple seta present. A1 of five articles. Lm with three teeth. Urp uniramous, claw of PII with simple conate seta in adult stage. Op with two small setae at posterior margin.

Description of female

Habitus (ZMH K–43203 Fig. 2, ZMH K–43207 Fig. 14a, b) body ZMH K–43203 2.9 mm long, 3.8 longer than width of Prn2. Head free, with surface structure (folds; Fig. 15b) like on Prns and Plt, 0.7 longer than wide. Prn1 length 1.2 Prn2 length. Lateral margins of Prn1–4 convex. Prn5 width 1.2 length, anterior margin straight, lateral margins of Prn5 straight. Coxae 1–4 anteriorly produced, tipped with stout setae. Plt length equal width. Posterolateral spines absent. Lateral margins slightly convex, posterior margin convex.

Antennula (ZMH K–43203; Fig. 5f) 0.5 mm long, length 0.2 body length, with 5 articles. Article 1 with 7 broom setae and 1 simple seta. Article 2 length 6.9 width, 4.2 article 1 length; distally with 2 large broom setae. Article 4 with 1 small seta, distally with 1 broom seta (broken off). Article 5 with 1 small broom seta, 2 long slender setae, 1 aestetasc.

Antenna (ZMH K–43203; Fig. 5g) broken off.

Mandibles (ZMH K–43203; Fig. 3a, b) first article of Md palp with 1 seta each, second article of distally with 2 setulate setae, marginally fringed with numerous fine setae, apical article with 2 setulate setae and combs of fine setae. Ip with 4 teeth. Lm of lMd with 3 teeth, lm like structure of rMd distally serrated, spine row with 7 spines. Mp with 10–11 setae.

Maxillula (ZMH K–43203; Fig. 3c) Outer lobe terminally with 12 strong spines, marginally with several small setae.

Maxilla (ZMH K–43203; Fig. 3d) with 3 lobes. Medial lobe slightly broader and shorter than outer lobes, ventrobasally with 5 long slender setae and marginally with numerous fine setae, terminally with 2 serrated setae and 4 simple setae. Outer lobes length 6.5 width, terminally with 1 long, serrated seta and 3 simple setae, dorsolaterally with 7 pairs of fine setae and 3 rows of 3 setae, ventrolaterally with row of 16 triangular shaped setae.

Maxilliped (ZMH K–43203; Fig. 3e) epipodite length 3.4 width, length 1.3 endite length, outer margin fringed with numerous fine setae, distally 1 slender seta on inner margin. Endite with 2 coupling hooks, terminally with fine setae, 2 fan setae and 2 simple setae, on distolateral margin with several pairs of fine setae. Outer margins of palp articles 1 and 2 fringed with fine setae. Palp article 2 with 2 setae on inner margin and 1 seta on outer margin. Article 3 with 10 setae on inner margin and 1 seta on outer margin. Article 4 with 2 setae, article 5 with 5 setae.

Pereopod I (ZMH K–43203; Fig. 2c, c'; ZMH K–43207; Fig. 15a, a') basis length 4.3 width, dorsally with 5 setae, ventrally with 4 setae. Ischium length 1.6 width, ventrally with 2 small setae, distodorsally with 2 setae. Merus length 0.6 width, distodorsally with 1 seta, distoventrally with 1 seta. Carpus produced at base of claw-seta, length 1.9 width, ventromedially with 1 small seta, distoventrally with 3 simple setae close to claw-seta, distodorsally with 1 small simple seta. Propodus length 3.3 width, ventrally fringed with combs of setae in a cuticular membrane. Dactylus distomedially with 3 simple slender setae close to claw. Claw of dactylus consisting of 2 conate setae with 2 slender setae inserting in between them.

Pereopod II (ZMH K–43203; Fig. 4a) basis length 4.8 width, dorsally with 3 small setae and 1 small broom seta, ventrally with 5 distally setulate setae. Ischium length 2.2 width, dorsally with 1 seta, ventrally with 2 setae. Merus length 0.9 width, distodorsally with 3 setae (1 distally setulate and 2 small setae), ventrally with 2 composed setae and 1 small seta. Carpus length 3 width, dorsomedially with row of 8 setae, distodorsally with 11 composed seta, ventrally with row of 14 composed (a` unequally bifid distally setulate) setae increasing in size towards propodus. Propodus length 3.3 width, dorsally with row of 4 setae, distodorsally with 1 composed (unequally bifid, distally setulate) seta and 1 small broom seta, ventrally with row of 13 composed (unequally bifid, distally setulate) setae increasing in size towards dactylus, distoventrally 1 slender seta. Dactylus (a`) ventrally with comb of fine setae, distomedially 3 small slender setae close to claw. Claw of dactylus consisting of 1 large and 1 small simple conate seta, with 2 slender setulate setae inserting in between.

Pereopod III (ZMH K–43203; Fig. 4b) basis length 5.0 width, dorsally with 2 broom setae and 1 small seta, ventrally with 4 distally setulate setae and 3 small setae, distoventrally 1 additional setulate seta. Ischium length 2.2 width,

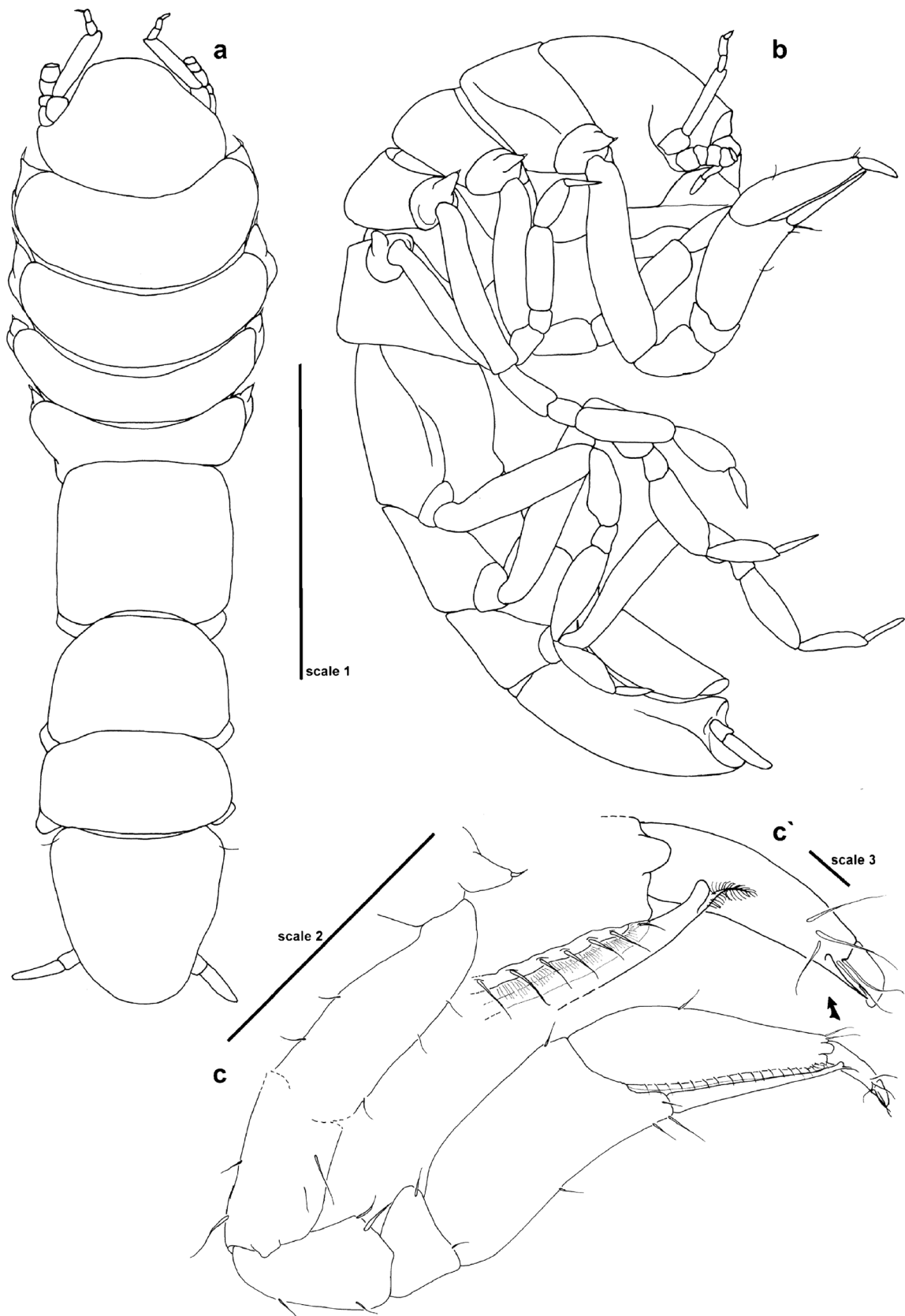


Fig. 2 ZMH K-43203 *Chelator aequabilis* sp. nov., female (holotype): **a** habitus lateral; **b** habitus dorsal; **c** left PI (Scale 1 1 mm, scale 2 0.1 mm, scale 3 0.01 mm)

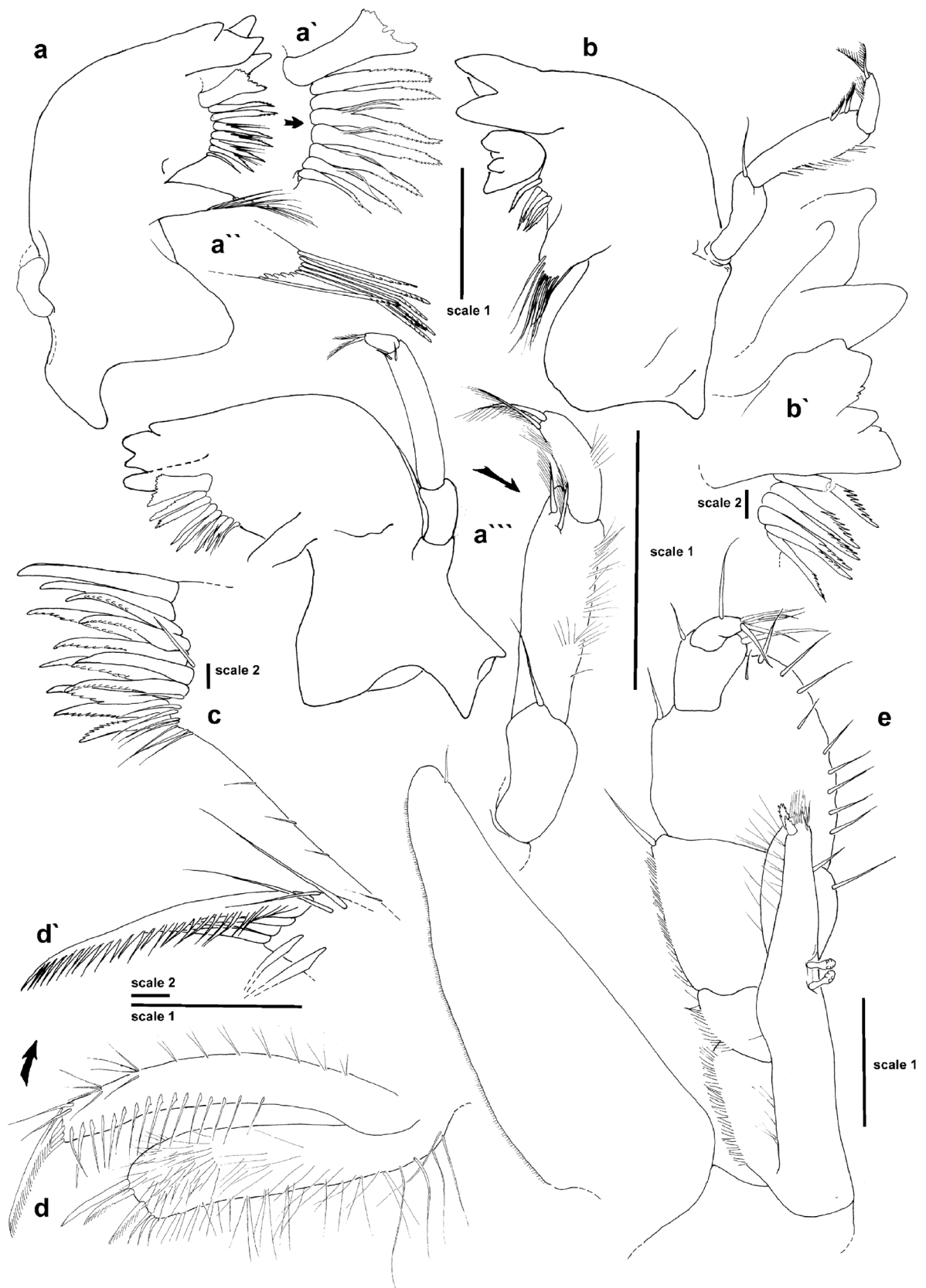


Fig. 3 ZMH K-43203 *Chelator aequabilis* sp. nov., female (holotype): **a** MdR, **a'** enlargement spine row, **a''** enlargement seta type mp, **a'''** MdR different view, **b** MdL, **b'** enlargement spine row and Lm MdL, **c** left Mx1; **d** left Mx2; **e** left Mxp (Scales 1 0.1 mm, scales 2 0.01 mm)

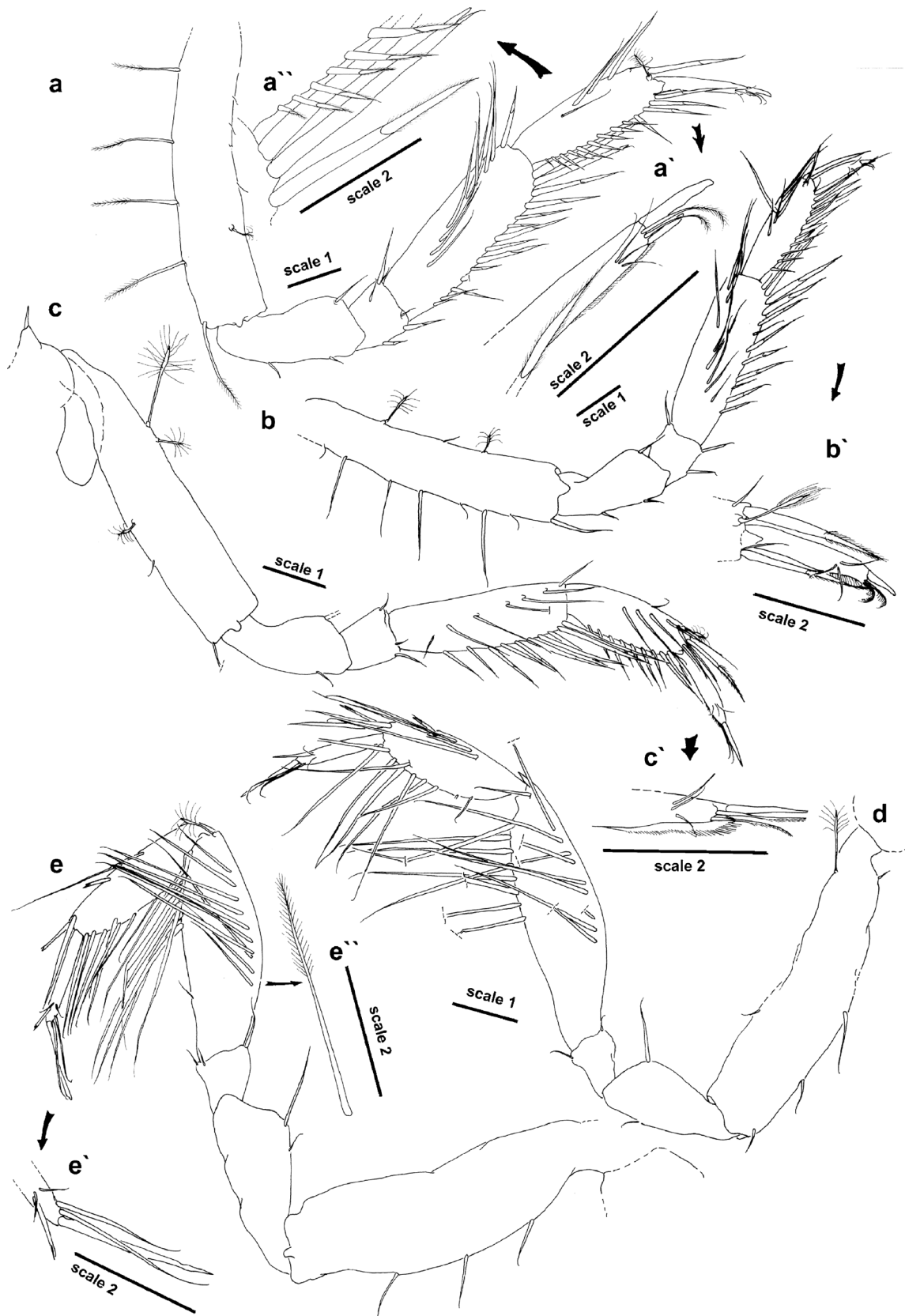


Fig. 4 ZMH K-43203 *Chelator aequabilis* sp. nov., female (holotype): **a, a', a''** right PII; **b, b'** left PIII; **c, c'** right PIV; **d** right PV; **e, e', e''** right PVI (Scales 1 0.1 mm, scales 2 0.01 mm)

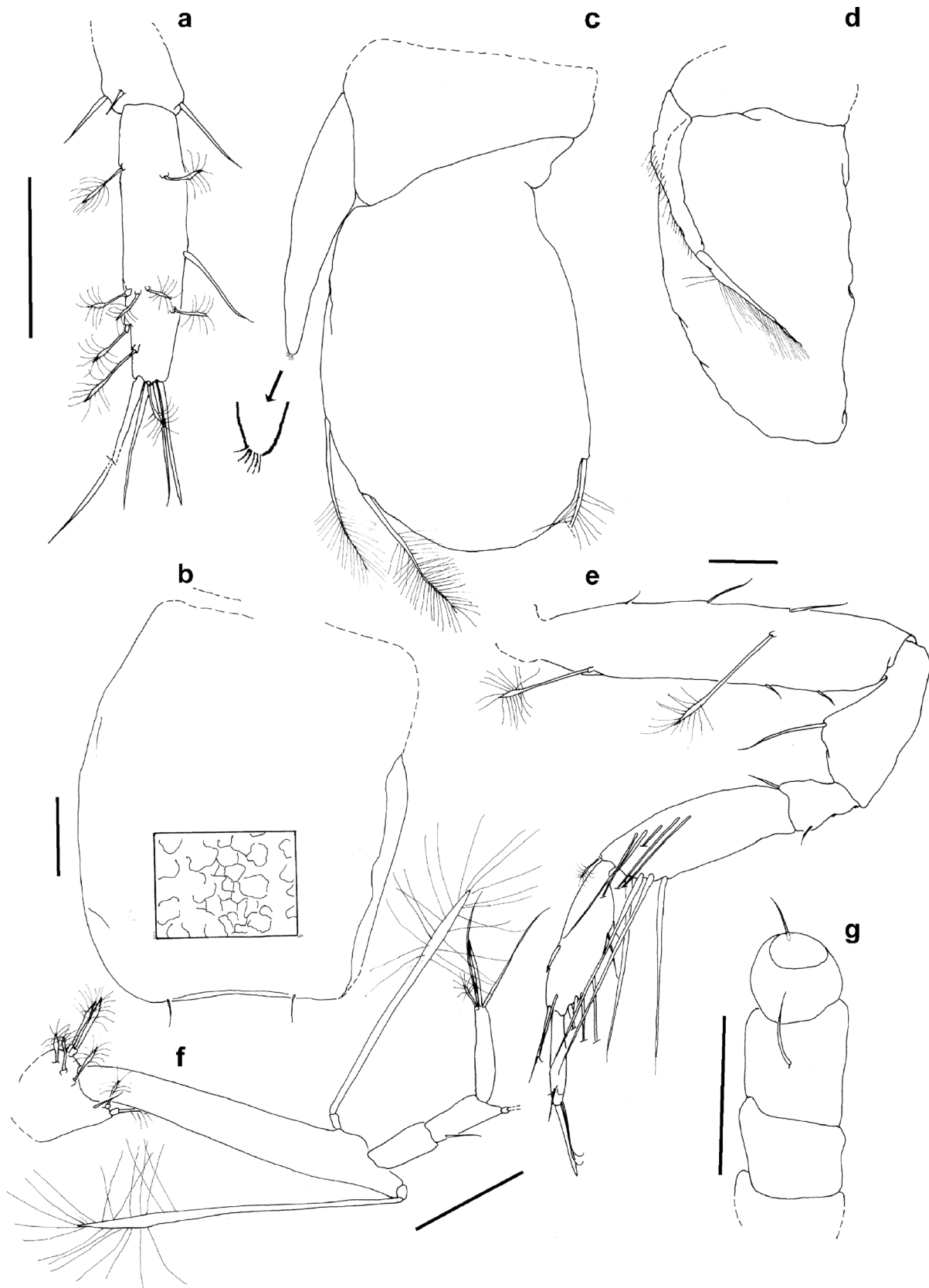


Fig. 5 ZMH K-43203 *Chelator aequabilis* sp. nov., female (holotype): **a** left Ur; **b** Op; **c** right Plp 3; **d** right Plp4; **e** right PVII; **f** A1; **g** A2 pedicular articles only (Scales 0.1 mm)

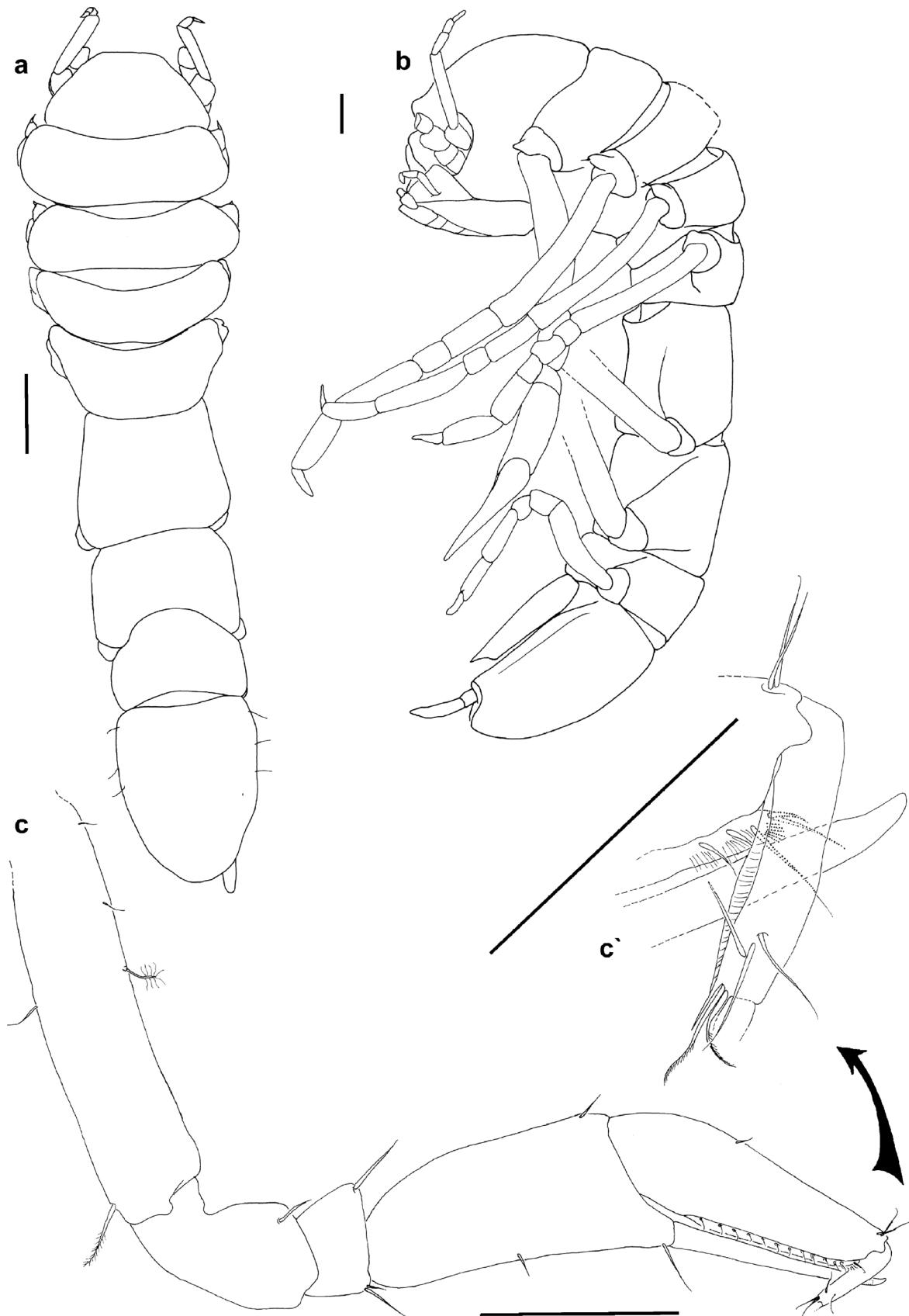


Fig. 6 ZMH K-43205 *Chelator aequabilis* sp. nov., juvenile (paratype): **a** habitus lateral; **b** habitus dorsal; **c**, **c'** PI (Scales 0.1 mm)



Fig. 7 ZMH K-43205 *Chelator aequabilis* sp. nov., juvenile (paratype): **a** MdL, **a'** enlargement spine row; **b** MdR, **b'** enlargement spine row; **c** left Mx1; **d**, **d'** left Mx2; **e**, **e'**, **e''** left Mxp; **f** A1 (Scales 0.1 mm)

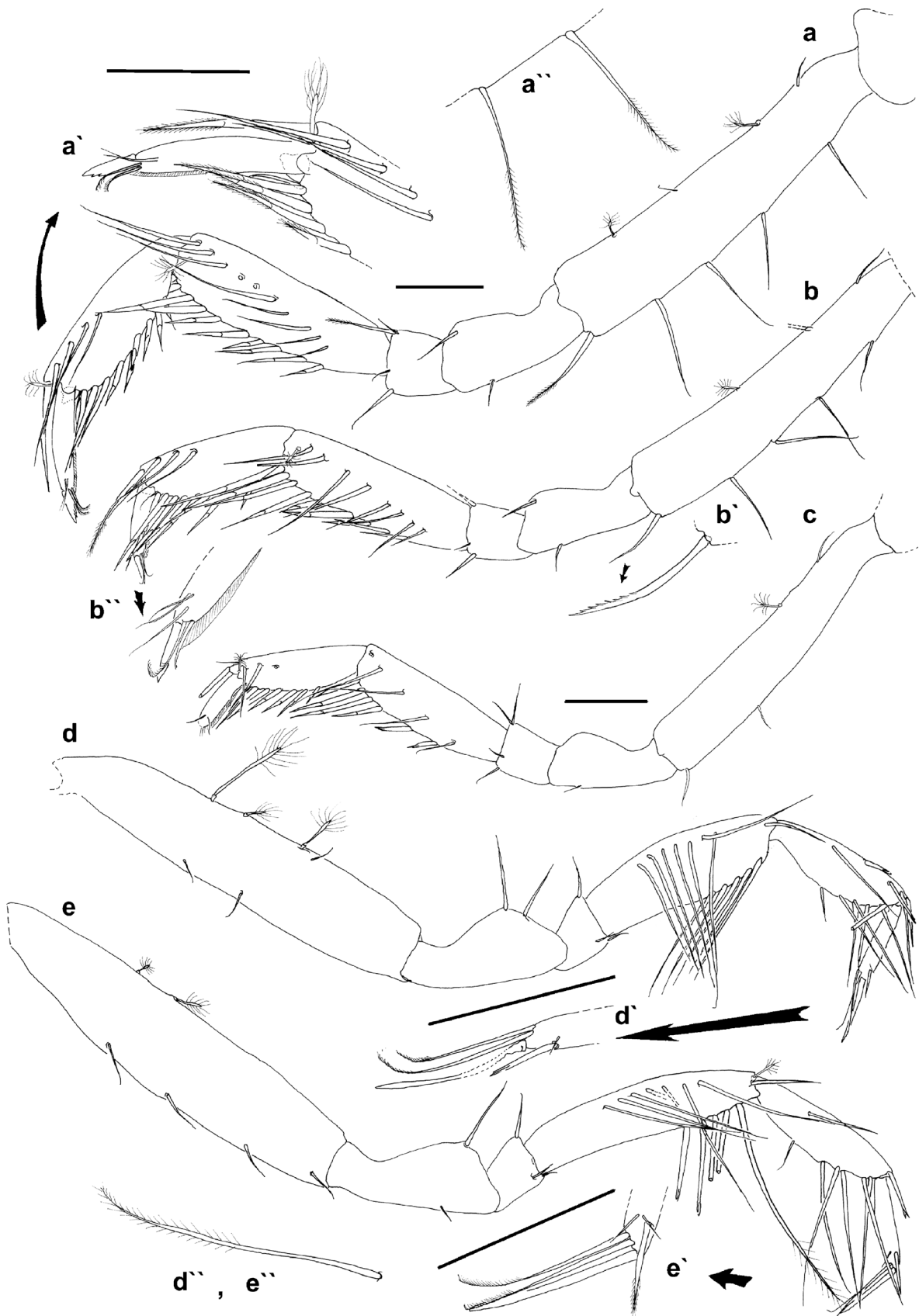


Fig. 8 ZMH K-43205 *Chelator aequabilis* sp. nov., juvenile (paratype): a, a', a'' PII; b, b', b'' PIII; c PIV; d, d', d'' PV; e, e', e'' PVI (Scales 0.1 mm)

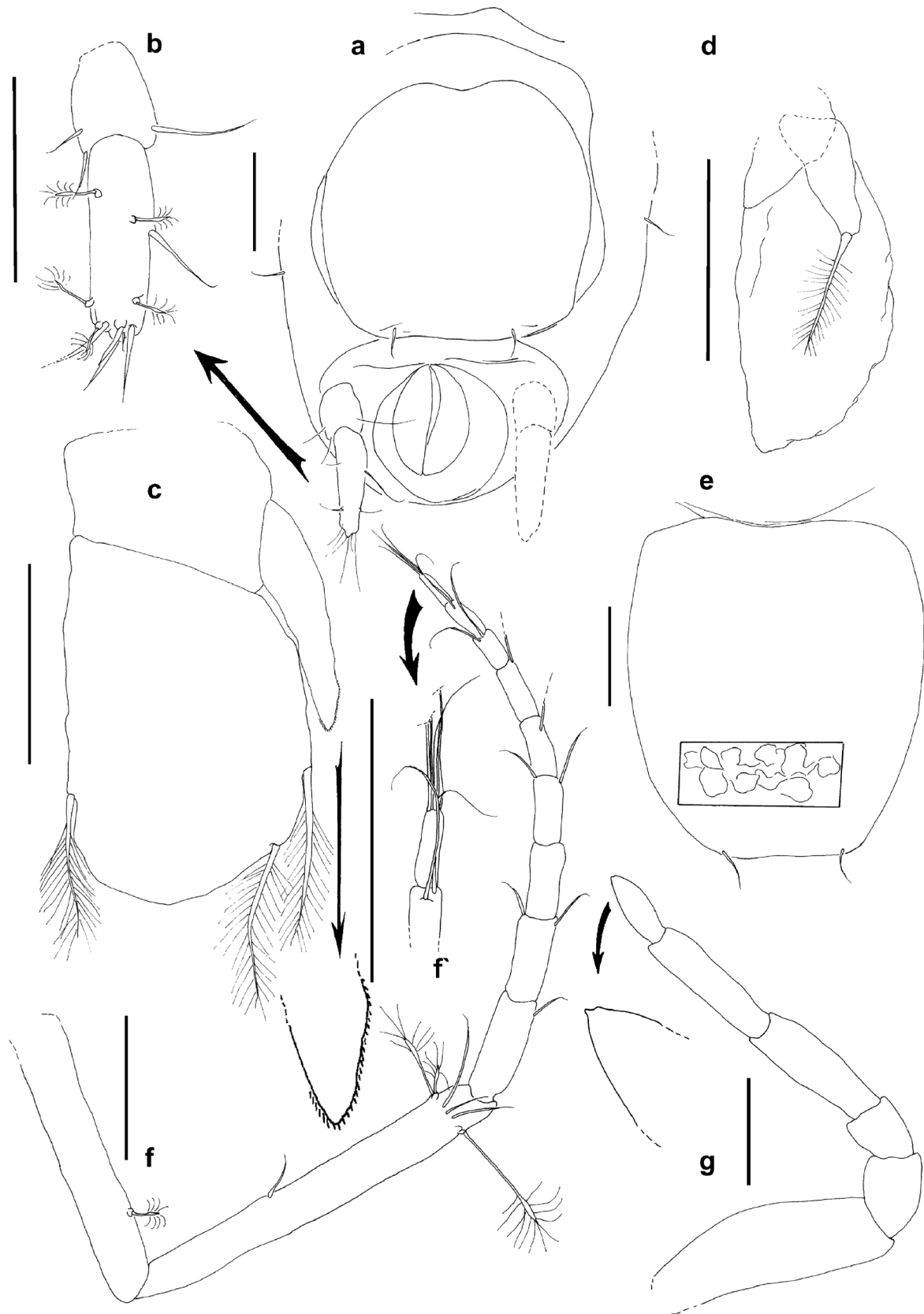


Fig. 9 ZMH K-43205 *Chelator aequabilis* sp. nov., juvenile (paratype): **a** Plt ventral view; **b** right Ur; **c** Plp 3; **d** Plp 4; **e** Op, **f**, **f** A2; **g** PVII (Scales 0.1 mm)

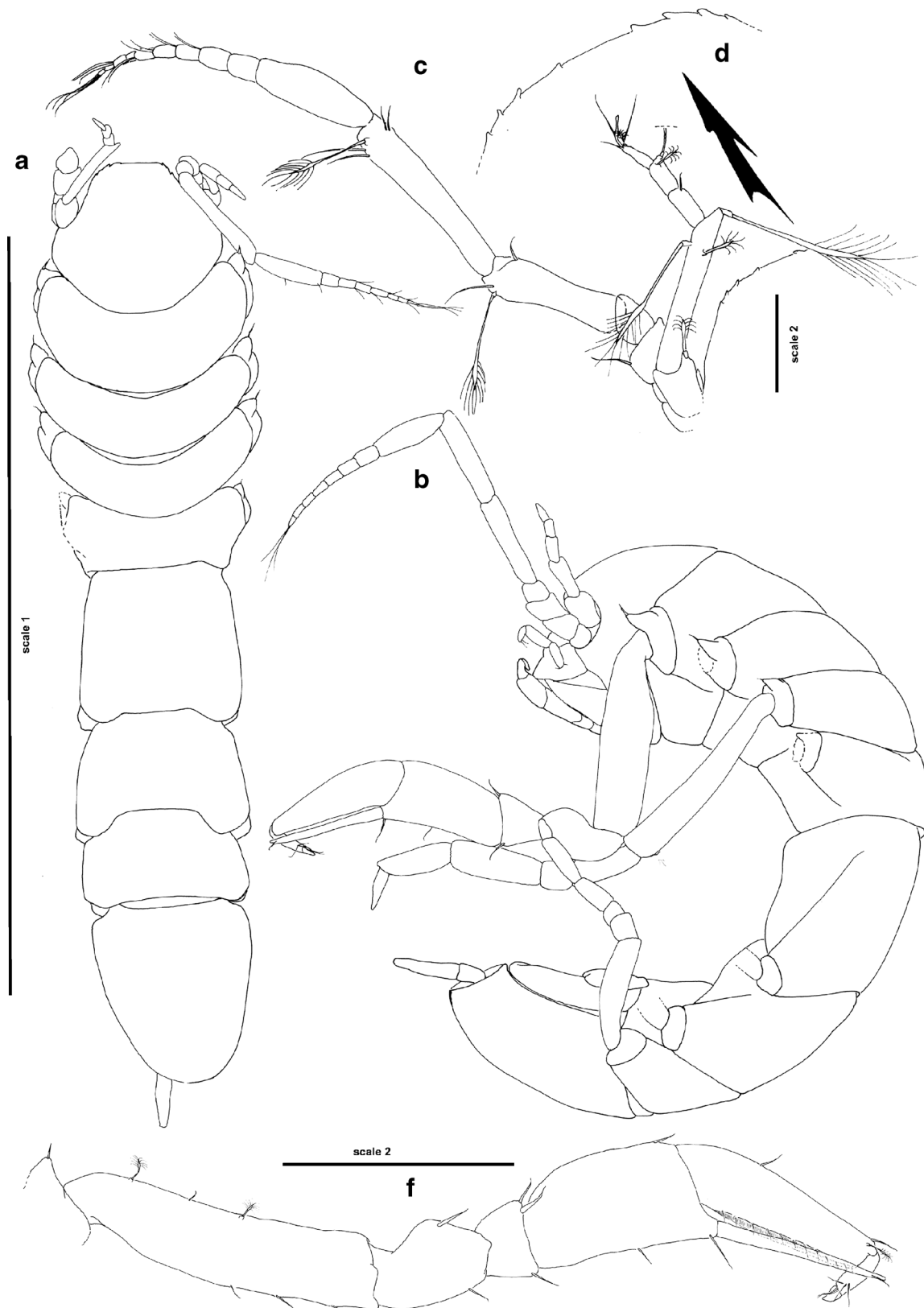


Fig. 10 ZMH K–43204 *Chelator aequabilis* sp. nov., male subadult (paratype): **a** habitus dorsal; **b** habitus lateral; **c** A2 and A1; **d** enlargement of dorsal view on front of cephalon; **e** right PI (Scale 1 1 mm, scale 2 0.1 mm)

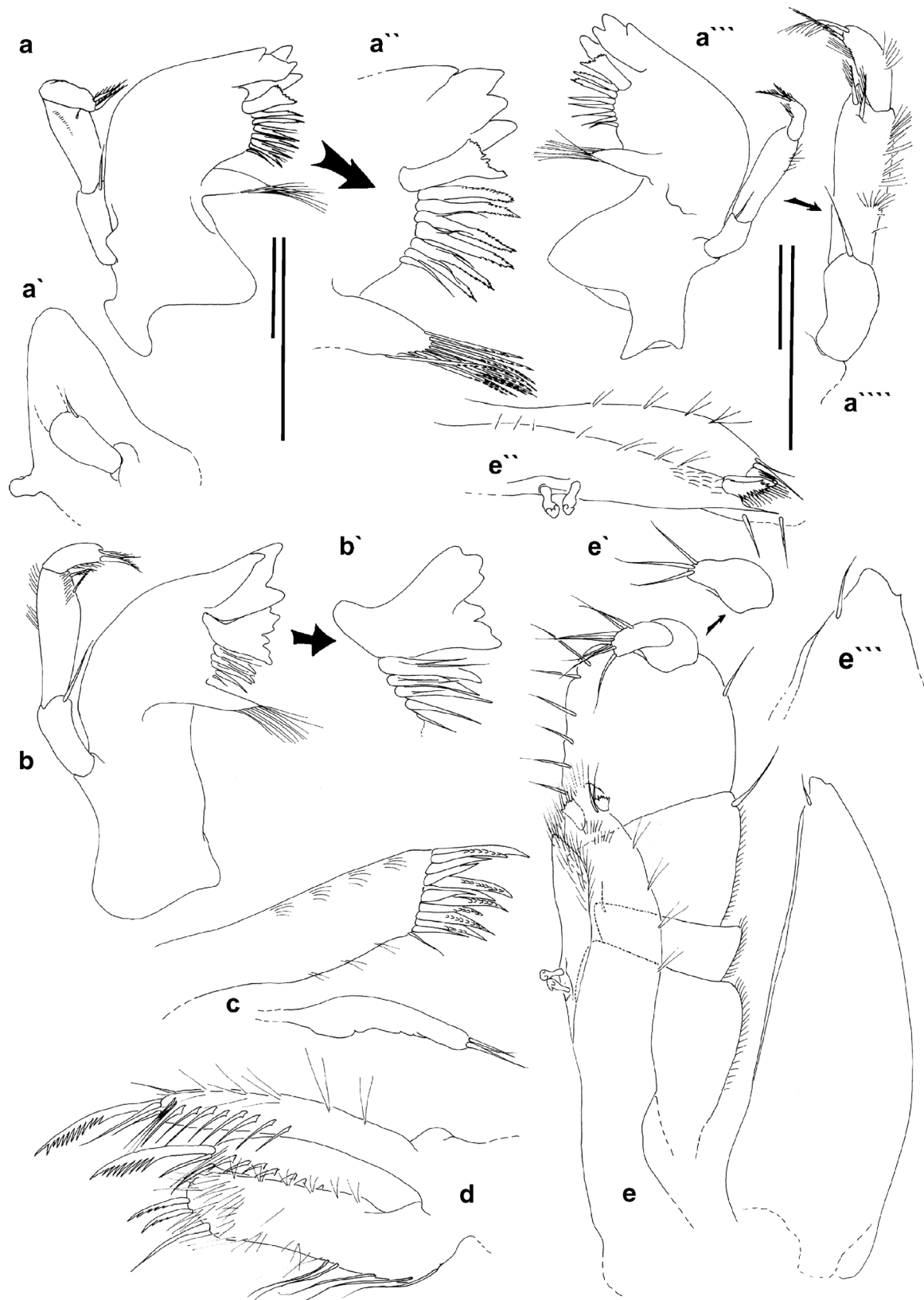


Fig. 11 ZMH K-43204 *Chelator aequabilis* sp. nov., male subadult (paratype): **a** MdR, **a'** different view MdR, **a''** enlargement spine row, **a'''** different view MdR, **a''''** enlargement mandibular palp; **b** MdL, **b'** enlargement spine row MdL; **c** left Mx1; **d** left Mx2; **e**, **e'**, **e''**, **e'''** left Mxp (Scales 0.1 mm)



Fig. 12 ZMH K-43204 *Chelator aequabilis* sp. nov., male subadult (paratype): **a** left PII; **b**, **b'** right PIII (damaged); **c** PV; **d** PVI; **e**, **e'** PVII (Scales 0.1 mm)

distodorsally with 1 seta, ventrally with 2 setae. Merus length 0.8 width, dorsally with 1 seta, ventrally with 2 composed (unequally bifid distally setulate) setae. Carpus length 3.1 width, dorsomedially with row of 11 setae, ventrally with row of 12 (unequally bifid distally setulate) setae increasing in size towards propodus. Propodus length 3.1 width, dorsally with row of 6 setae, distodorsally with 1 broom seta, ventrally with row of 11 (unequally bifid distally setulate) setae, distoventrally 1 slender seta. Dactylus (b') distomedially with 3 small slender setae close to claw, ventrally fringed with fine setae in cuticular membrane. Claw of dactylus consisting of 1 simple conate setae and 2 slender setulate setae inserting in between them.

Pereopod IV (ZMH K-43203; Fig. 4c) basis length 4.5 width, dorsally with 2 boom setae, ventrally with 1 broom and 1 small seta, distoventrally additionally 1 seta (broken off). Ischium length 2.1 width, dorsally with 1 seta (broken off), ventrally with 1 seta. Merus length equal width, distodorsally with 1 small seta, ventrally with 2 setae. Carpus length 3.2 width, dorsomedially with row of 7 setae, ventrally with row of 10 composed (unequally bifid distally setulate) setae. Propodus length 3.4 width, dorsally with row of 5 setae and 1 small seta, distodorsally with 1 broom and 1 composed (unequally bifid, distally setulate) seta, ventrally with row of 9 (unequally bifid distally setulate) setae, distoventrally with 1 slender seta. Dactylus ventrally with comb of fine setae in cuticular membrane, distomedially 3 small slender setae close to claw. Claw of dactylus (c') consisting of 1 simple conate seta and 2 slender setulate setae.

Pereopod V (ZMH K-43203; Fig. 4d) basis length 4.7 width, dorsally with 1 broom and 1 small seta, ventrally

with 1 proximal small seta and 3 distally setulate setae. Ischium length 2.1 width, dorsally with 1 distally setulate seta, ventrally with 1 small seta. Merus damaged, distodorsally with 1 small seta, distoventrally with 1 seta. Carpus length 3.6 width, dorsally with row of 9 slender distally setulate setae, distodorsally 1 composed seta, ventrally with row of 8 long slender distally setulate setae. Propodus length 2.8 width, dorsally with row of 5 slender distally setulate setae and 2 unequally bifid setae (1 medially, 1 distally), ventrally with row of 10 long slender setae. Dactylus with 1 unequally bifid seta and 2 small simple setae inserting close to claw. Claw of dactylus consisting of 1 long simple conate seta and 2 slender setae, which are slightly longer than the conate seta.

Pereopod VI (ZMH K-43203; Fig. 4e) basis length 3.7 width, ventrally with 3 distally setulate setae. Ischium length 2.5 width, dorsally with 1 small and 1 distally setulate seta. Merus length 0.8 width, 1 seta distodorsally, 2 setae distoventrally. Carpus length 3.3 width, dorsally with row of 10 long slender distally setulate setae (e''), distodorsally 1 small broom seta, ventrally with row of 7 long slender setae. Propodus length 3.4 width, dorsally with 2 long slender setae and 2 unequally bifid setae, ventrally row of 6 slender setae. Dactylus with 1 unequally bifid seta and 2 small simple setae inserting close to claw. Claw of dactylus (e') consisting of 1 long simple conate seta and 2 slender setae, which are slightly longer than the conate seta.

Pereopod VII (ZMH K-43203; Fig. 5e) basis length 5 width, with 2 large broom seta, dorsally 2 small setae, ventrally 1 small and 2 distally setulate setae. Ischium length 1.8 width, dorsally 1 distally setulate setae. Merus length 1.6 width, distodorsally with 1 seta, distoventrally with 1 seta. Carpus length 2.9 width, dorsally with row of 5 long slender distally setulate setae, distodorsally 1 small broom seta, ventrally with row of 4 long slender setae. Propodus length 3.4 width, dorsally with 1 slender seta and 2 unequally bifid setae, ventrally with row of 6 long slender setae. Dactylus with 1 unequally bifid seta and 2 small simple setae inserting close to claw. Claw of dactylus consisting of 1 long simple conate seta and 2 slender setae, which are slightly longer than the conate seta.

Pleopod 2, operculum (ZMH K-43203; Fig. 5b (distorted preparing the slide); 15c) length 1.1 width. Lateral margins slightly convex, distal margin slightly concave. Lateral margins without seta and distal margin with two small setae. Surface structure (folds) present (ZMH K-43207; Fig. 15c).

Pleopod 3 (ZMH K-43203; Fig. 5c) endopod length 1.5 width, distally with 3 plumose setae. Exopod length 0.6 endopod length, terminally with several small fine setae.

Pleopod 4 (ZMH K-43203; Fig. 5d) endopod oval, length 1.8 width. Exopod length 8.8 width, 0.5 endopod length, lateral margin fringed with fine setae, terminally with 1 plumose seta.

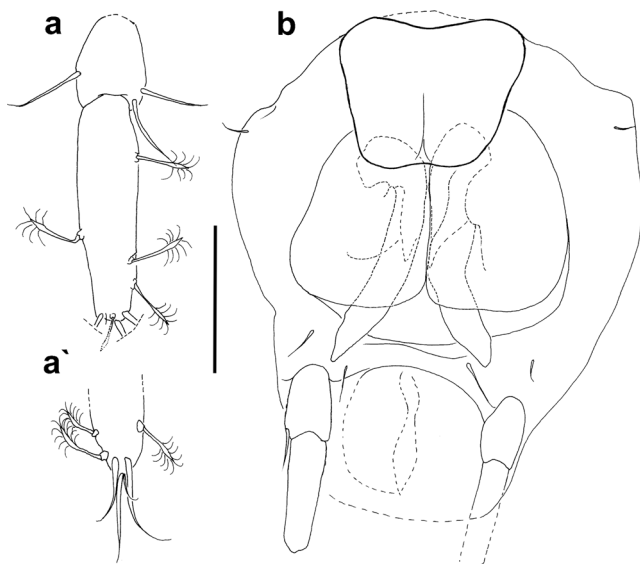


Fig. 13 ZMH K-43204 *Chelator aequabilis* sp. nov., male subadult (paratype): **a** Ur (right, **a'** left in enlargement); **b** Plt ventral view (Scale 0.1 mm)

Fig. 14 *Chelator aequabilis* sp. nov., confocal laser scanning microscopy images. ZMH K–43207, female: **a** habitus dorsal, **b** habitus lateral. ZMH K–43208, male: **c** habitus dorsal, **d** habitus lateral (Scales 400 μ m)



Uropods (ZMH K–43203; Fig. 5a) uniramous. Protopod with 3 simple setae. Endopod length 3.3 protopod length, endopod length 4.5 width, with 9 broom setae and 5 long simple setae.

Description of juvenile

Habitus (ZMH K–43205; Fig. 6a, b) stage juvenile 1 according to Hessler (1970), body 2.2 mm long, length 4.0 Prn2 width. Frons clypeal furrow and transverse ridge on frons present. Prn1 width 1.3 cephalon width. Prn1 length 1.2

Prn2 length, equal Prn2 width. Lateral margins of Prn1–4 convex. Prn5 width 1.2 length, lateral margins of Prn5 straight. Coxae 1–4 produced, tipped with stout setae. Plt rounded, length 1.2 width, no posterolateral spines present.

Antennula (ZMH K–43205; Fig. 7f) 0.4 mm long, length 0.2 body length, with 5 articles. Article 1 with 3 broom setae. Article 2 length 6.9 width, 3.7 article 1 length; distally with 3 long and 1 small broom setae. Article 4 distally with 1 broom seta. Setation of distal article broken off, with at least 3 setae.

Fig. 15 *Chelator aequabilis* sp. nov., confocal laser scanning microscopy images. ZMH K–43207, female: **a** PI, **a'** PI chela detail, **b** cephalon cuticle detail, **c** Plt ventral ZMH K–43208, male. **d** PI, **d'** PI chela detail, **e** cephalon cuticle detail, **f** Plt ventral (*Scales* (**a**, **b**, **c**, **e**, **f**) 100 μ m, (**a'**, **d**, **d'**) 40 μ m)



Antenna (ZMH K–43205; Fig. 9f) about about 1 mm long, length 0.45 body length, with 15 articles. Article 5 marginally with 1 broom seta. Article 6 distally with 3 broom and 3 slender setae. Flagellar articles distally with 1 or 2 slender setae, distal flagellar article terminally with 4 long slender setae.

Mandible (ZMH K–43205; Fig. 7a, b) first article of Md palp with 1 seta, second article marginally with combs of fine setae, distally with 2 setulate setae, apical article with 2 setulate setae. Ip with 4 teeth. Lm of lMd (a') with 3 teeth, lm like structure of rMd (b') distally serrated, spine row containing 4–5 spines. Mp triangular with 10 setae.

Maxillula (ZMH K–43205; Fig. 7c, c') terminally with 4 setae, marginally with 4 slender setae. Outer lobe length 3.6 width, terminally with 12 strong spines, marginally with pairs or combs of fine setae.

Maxilla (ZMH K–43205; Fig. 7d) with 3 lobes. Medial lobe broken off. Outer lobes terminally with 1 long serrated seta and 2 simple setae, dorsolaterally with rows of fine setae, ventrolaterally with 11 triangular shaped setae.

Maxilliped (ZMH K–43205; Fig. 7e) epipodite length 4.0 width, length subsimilar endite length, lateral margin fringed with fine setae, tipped with 1 slender seta. Endite with 2 coupling hooks, terminally with numerous fine setae, 2 star-shaped conate

Fig. 16 ZMH K–43209 *Chelator aequabilis* SEM pictures: **a** habitus lateral, **b** PI carpo-chela, **c** PI claw, **d** Plt and Ur lateral view (Scales **a** 1 mm, **b** 0.1 mm, **c–d** 0.01 mm)



setae, marginally with numerous fine setae. Outer margins of palp articles 1 and 2 fringed with fine setae. Palp article 2 with 2 setae on medial margin and 1 on lateral margin. Article 3 with 8 setae on inner margin and 1 seta on outer margin. Article 4 terminally with 2 setae, article 5 with 3 setae.

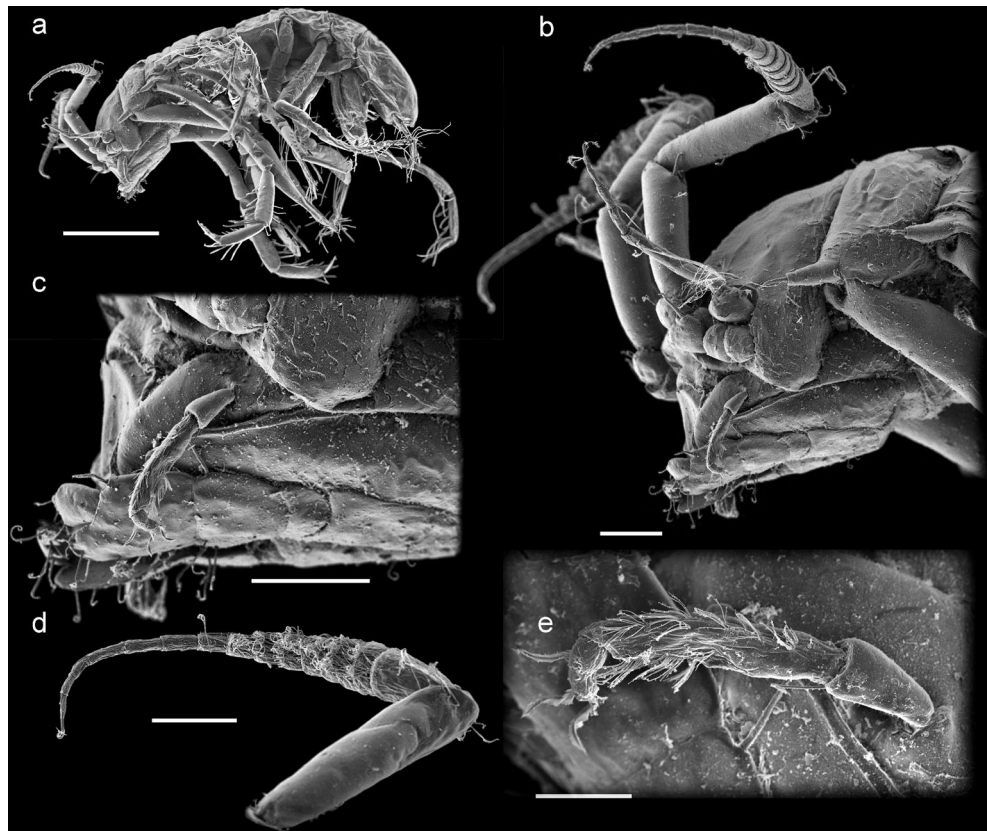
Pereopod I (ZMH K–43205; Fig. 6c) basis length 4.2 width, dorsally with 2 small setae and 1 broom seta, ventrally with 1 seta, distoventrally additionally 1 distally setulate seta. Ischium length 1.8 width, ventrally proximal to merus dorsally 1 seta. Merus length 0.6 width, distodorsally with 1 distally setulate setae, ventrally with 2 setae. Carpus length 2.2 width, on ventral side medially 1 small seta and proximal to claw-seta 1 slender seta, distodorsally with 1 small seta. Propodus length 3.3 width, distodorsally with 2 slender setae. Dactylus ventrally with comb of fine setae in cuticular membrane and 3 slender setae close to claw. Claw of dactylus consisting of 2 conate setae (one small, one large) and 2 slender setulate setae inserting in between.

Pereopod II (ZMH K–43205; Fig. 8a) basis length 4.8 width, dorsally with 2 broom setae and 2 small setae, ventrally

with 4 distally setulate setae (a''), distoventrally additionally 1 distally setulate seta. Ischium length 2.3 width, dorsally with 1 distally setulate seta, ventrally with 1 small seta. Merus length 1.1 width, distally with 3 setae. Carpus length 3.5 width, dorsomedially with row of 10 setae, distodorsally 1 small broom seta, ventrally with row of 10 composed (unequally bifid, distally setulate) setae. Propodus length 3.1 width, dorsally with row of 4 setae, distodorsally 1 composed and 1 broom seta, ventrally with row of 10 composed (unequally bifid, distally setulate) setae and 1 small seta. Dactylus ventrally fringed with fine setae in cuticular membrane, distally 2 slender setae inserting close to claw. Claw of dactylus (a') consisting of 1 serrated conate seta and 2 slender setulate setae.

Pereopod III (ZMH K–43205; Fig. 8b) basis length 5.4 width, dorsally with 2 broom setae and 1 distally setulate seta, ventrally with 4 distally setulate setae, distoventrally 1 additional setulate seta (b'). Ischium length 2.3 width, dorsally with 1 seta, ventrally with 1 seta. Merus length equal width, distally with 3 setae. Carpus length 3.5 width, dorsomedially

Fig. 17 ZMH K–43210 *Chelator aequabilis* male SEM pictures: **a** habitus lateral, **b** head lateral view, **c** mouthparts lateral view, **d** antenna medial view, **e** Md palp (Scales (a) 0.5 mm, (b–d) 0.1 mm, e 0.05 mm)



with row of 8 setae and 1 small broom seta, ventrally with row of 9 composed (unequally bifid distally setulate) setae. Propodus length 2.9 width, dorsally with row of 3 setae, distodorsally with 1 composed seta. Dactylus ventrally fringed with fine setae in cuticular membrane, distally with 3 slender setae inserting close to claw. Claw of dactylus consisting of 1 simple conate seta and 2 slender setulate setae.

Pereopod IV (ZMH K–43205; Fig. 8c) basis length 5.6 width, dorsally with 1 broom seta and 1 distally setulate seta, ventrally with 2 distally setulate setae. Ischium length 2.2 width, ventrally with 1 small seta. Merus length equal width, distodorsally with 2 distally setulate setae, ventrally with 2 simple setae. Carpus length 3.2 width, dorsolaterally with row of 5 setae, ventrally with row of 6 composed (unequally bifid distally setulate) setae. Propodus length 3.4 width, dorsally with 4 composed setae, 1 broom seta and 1 slender seta. Claw of dactylus broken off.

Pereopod V (ZMH K–43205 Fig. 8d) basis length 5.1 width, dorsally with 3 broom setae and 1 simple seta, ventrally with 2 setae. Ischium length 2.4 width, dorsally with 2 distally setulate setae. Merus length 0.8 width, distodorsally with 1 seta, distoventrally with 2 setae. Carpus length 3.2 width, dorsally with row of 7 long slender setae, distodorsally 1 distally setulate seta, ventrally with row of 5 long slender distally setulate setae. Propodus length 3.1 width,

dorsally with 3 slender and 2 unequally bifid setae, ventrally with row of 7 long slender distally setulate setae (d''). Dactylus with 1 unequally bifid seta and 1 small seta inserting close to claw. Claw of dactylus (d') consisting of 1 long conate seta and 2 slender setulate setae.

Pereopod VI (ZMH K–43205 Fig. 8e) basis length 4.7 width, dorsally with 2 small broom setae, ventrally with 4 distally setulate setae. Ischium length 2.5 width, dorsally 1 long distally setulate seta, ventrally 1 small seta. Merus length equal width, distodorsally 1 distally setulate seta, ventrally 2 small setae. Carpus length 4.6 width, dorsally with row of 7 long slender distally setulate (e'') setae, distodorsally 1 small broom seta and 1 composed seta, ventrally with row of 5 (two long unequally bifid, 3 long slender distally setulate) setae. Propodus length 3.3 width, dorsally with 1 slender and 1 unequally bifid seta, ventrally with row of 6 long slender setae. Dactylus with 1 unequally bifid seta and 1 small seta inserting close to claw. Claw of dactylus (e') consisting of 1 long conate seta and 2 slender setulate setae.

Pereopod VII (ZMH K–43205; Fig. 9g) without setae, juvenile condition.

Pleopod 2, operculum (ZMH K–43205; Fig. 9a, e) length 1.1 width. Lateral margins slightly convex and distal margin straight. Distal margin with 2 setae. Surface structure present.

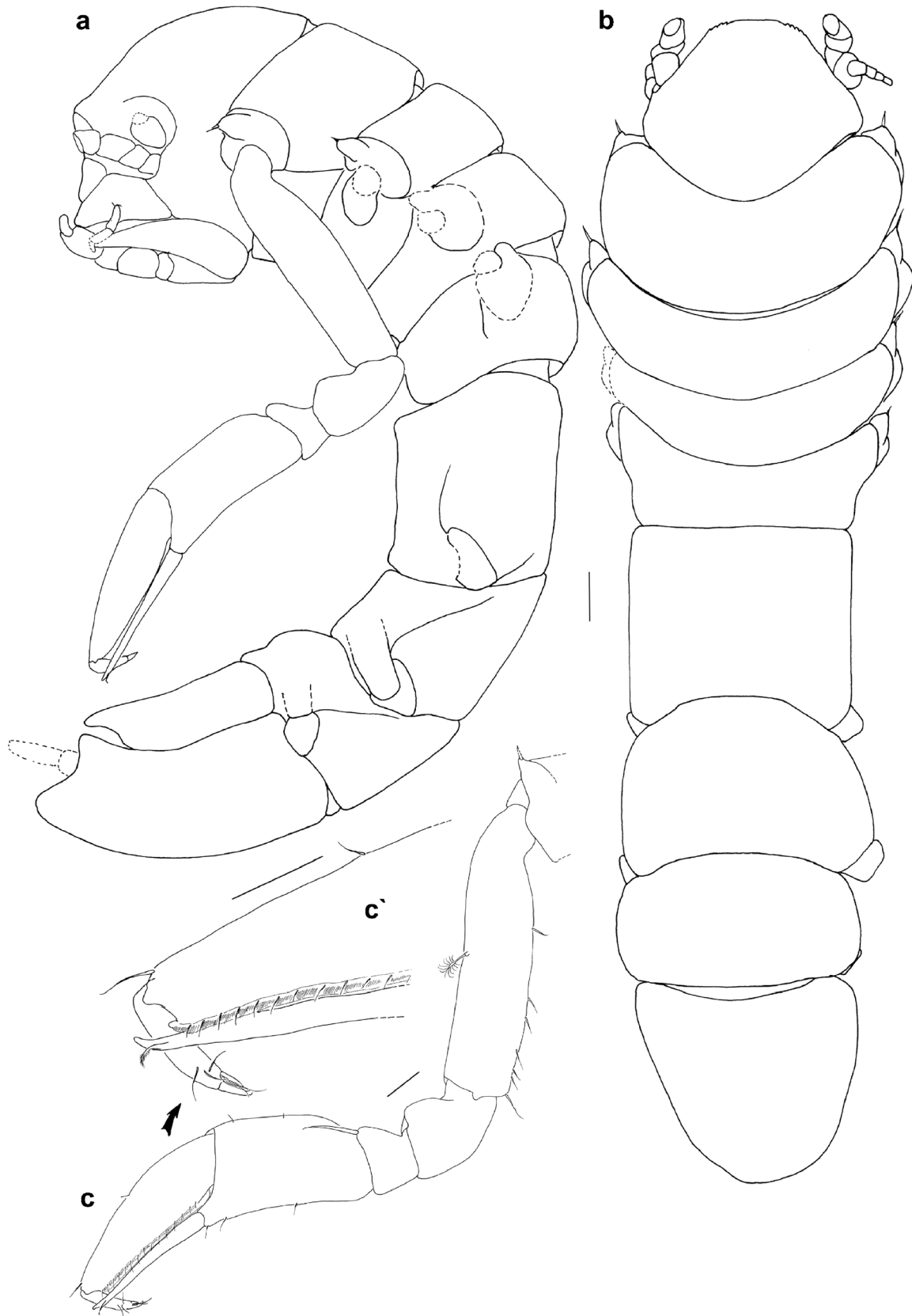


Fig. 18 ZMH K-43228 *Chelator rugosus* sp. nov., female (holotype): **a** habitus lateral; **b** habitus dorsal (Plt distorted, not perfectly stretched); **c, c'** right PI (Scales 0.1 mm)



Fig. 19 ZMH K-43228 *Chelator rugosus* sp. nov., female, (holotype): a Op; b Plp 3; c Plp 4; d A1; e, e' MdL; f, f, f' MdR; g, g' Mx1; h, h' Mx2; j, j', j'' Mxp (Scales 0.1 mm)

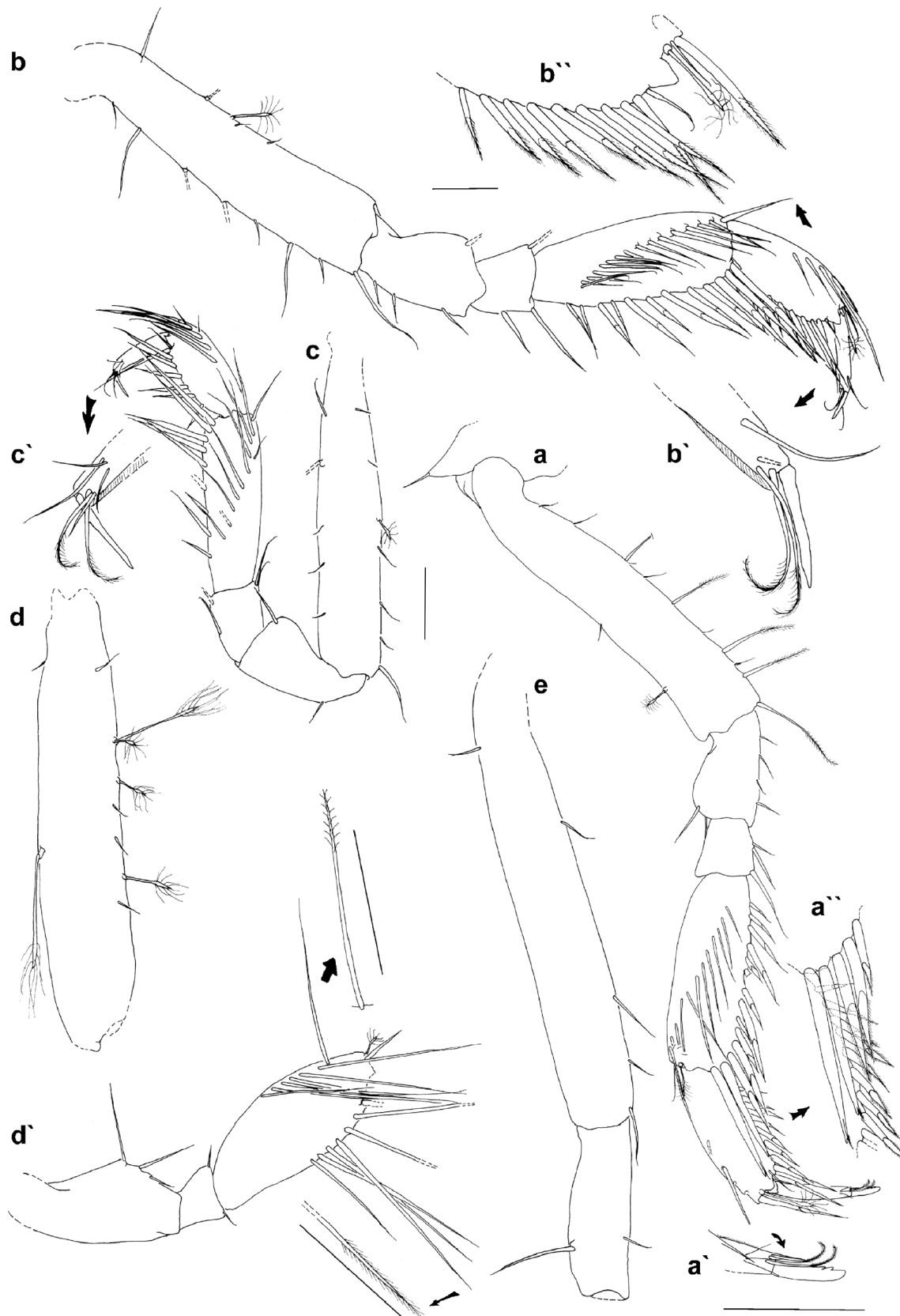


Fig. 20 ZMH K-43228 *Chelator rugosus* sp. nov., female, (holotype): **a, a', a''** right PII; **b, b'** right PIII **b''** detail ventral setal row of carpus PIII; **c, c'** right PIV; **d, d'** right PV ischium, merus and carpus; **e** left PVI basis and ischium (Scales 0.1 mm)

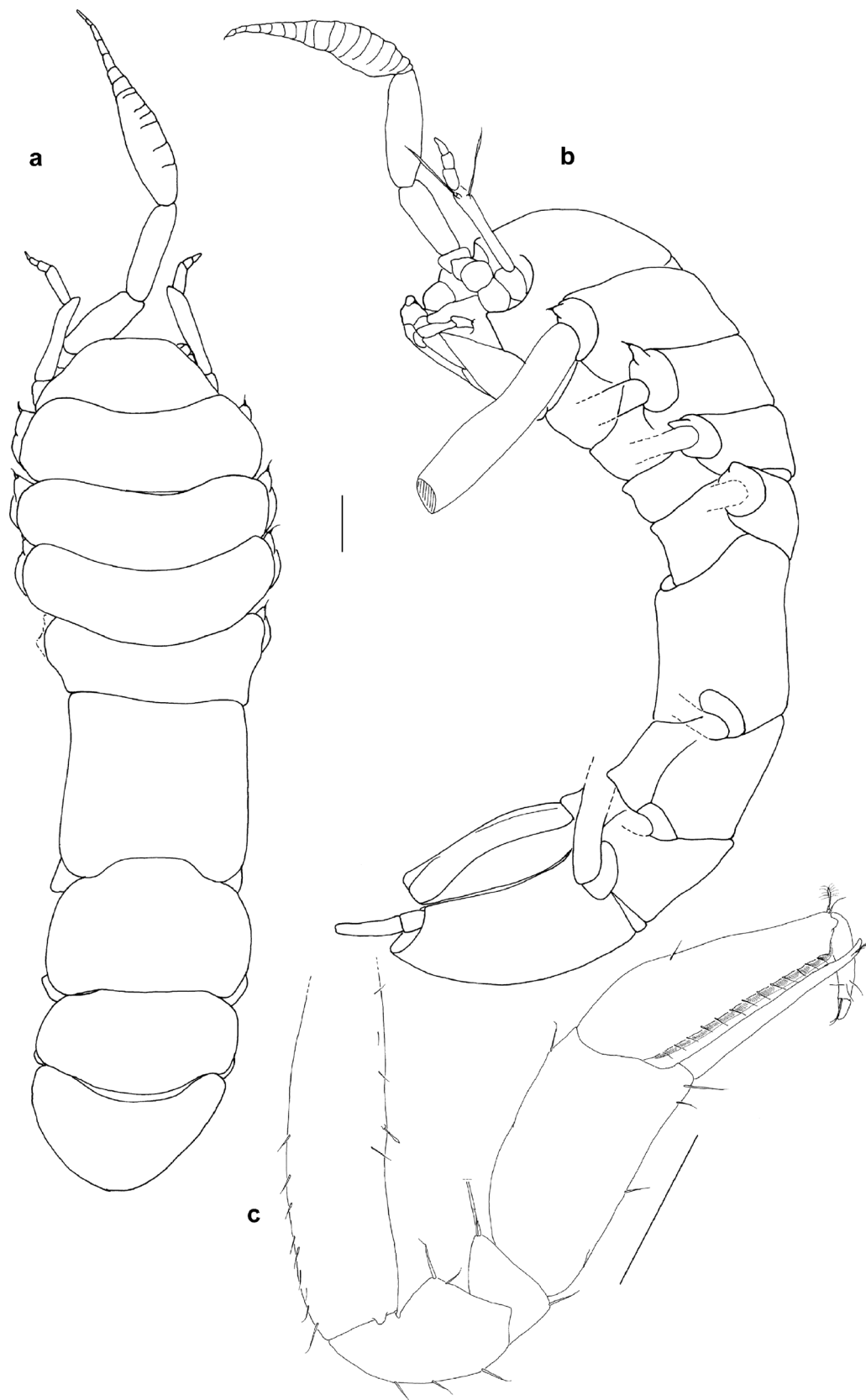


Fig. 21 ZMH K-43228 *Chelator rugosus* sp. nov., male (paratype): **a** habitus lateral; **b** habitus dorsal (distorted, not completely stretched); **c** right PI (Scales 0.1 mm)



Fig. 22 ZMH K-43229 *Chelator rugosus* sp. nov., male (paratype): **a** MdR, **b** MdL, **c** Mx1, **d** Mx2, **e** Mxp (Scales 0.1 mm)

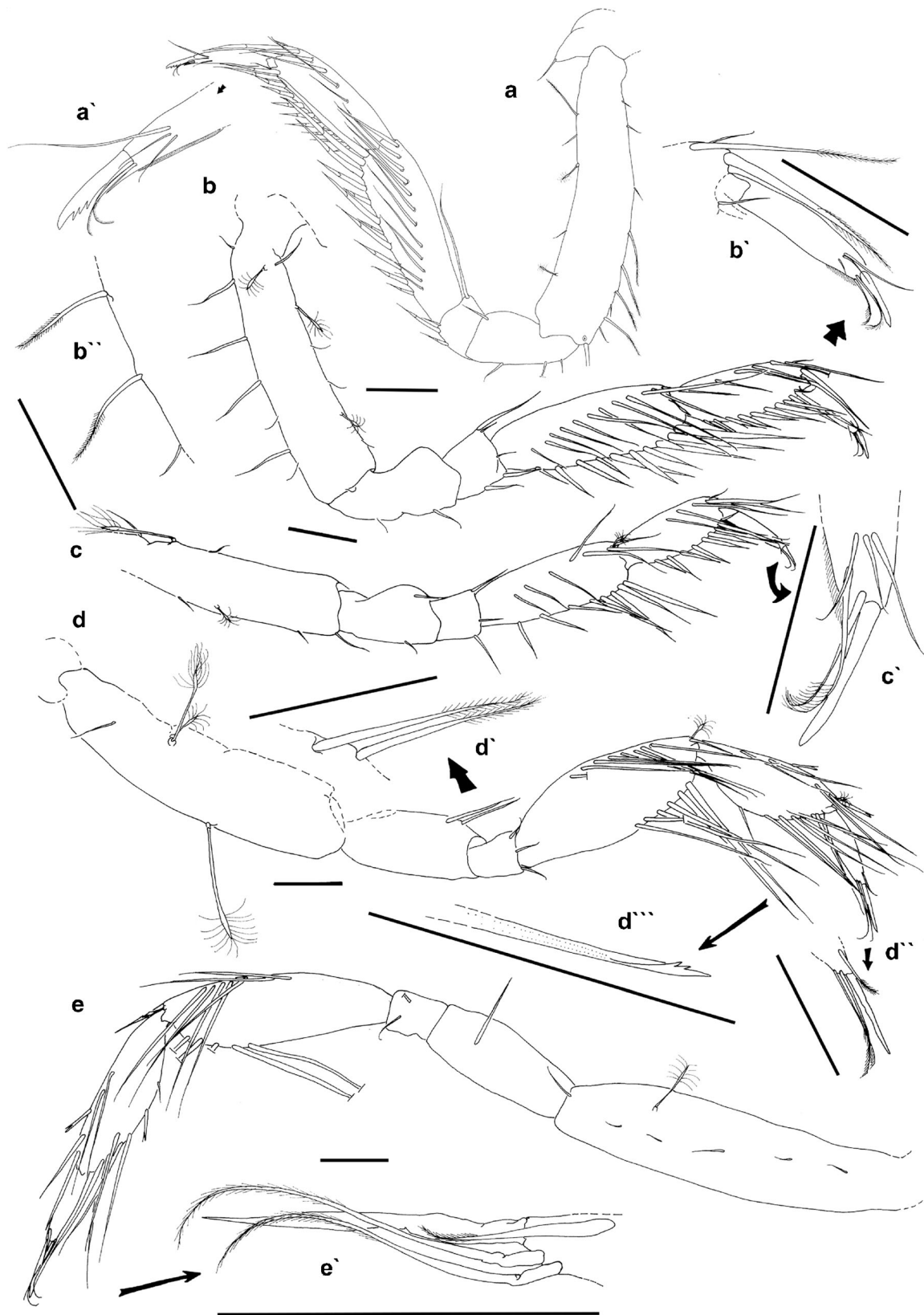


Fig. 23 ZMH K-43229 *Chelator rugosus* sp. nov., male (paratype): a, a' right PII; b, b', b'' right PIII; c, c' right PIV; d, d', d'', d''' right PV; e, e' right PVI. (Scales 0.1 mm)

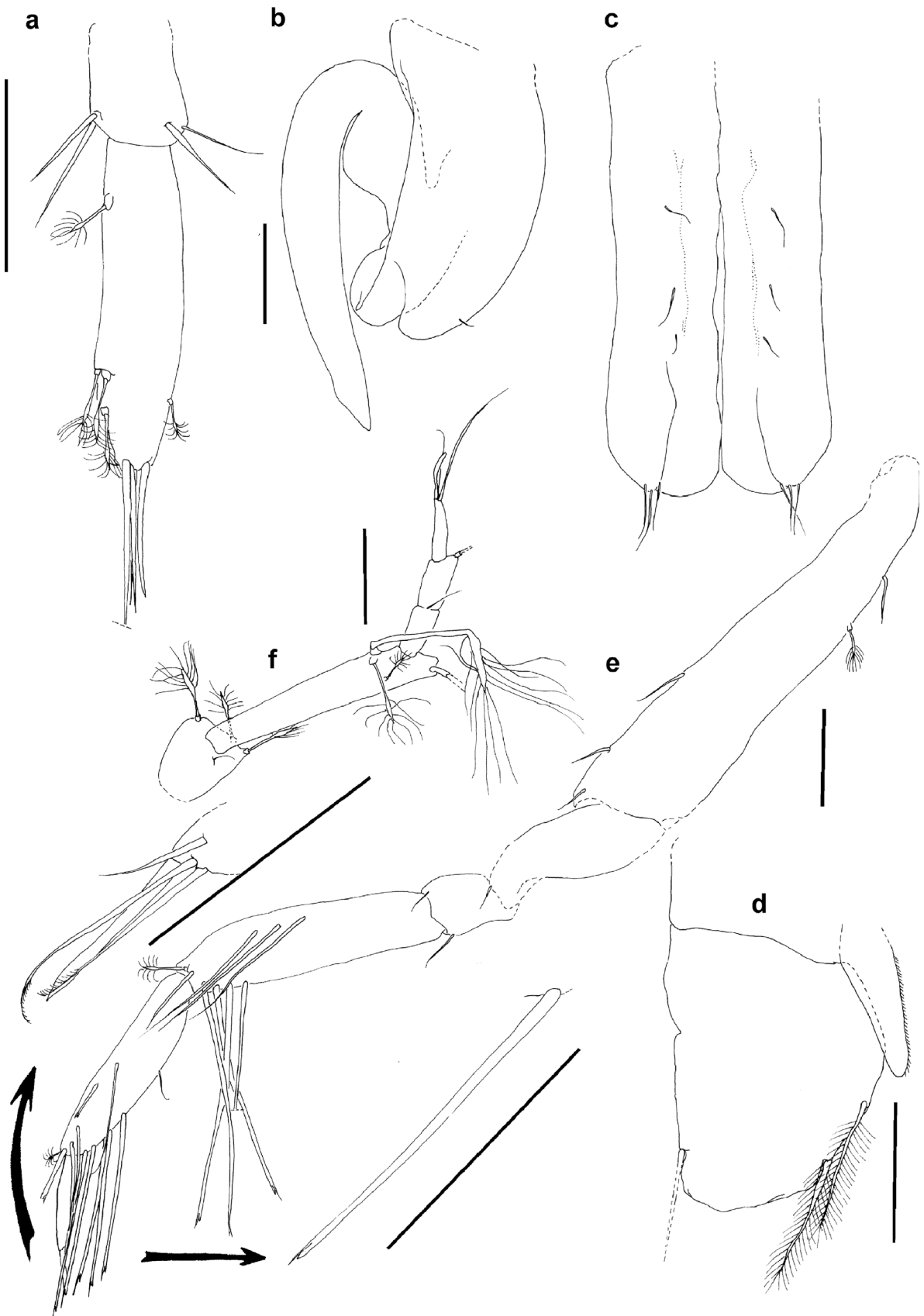


Fig. 24 ZMH K-43229 *Chelator rugosus* sp. nov., male (paratype): **a** left Ur, **b** left Plp 2, **c** Plp 1; **d** left Plp 3; **e** left PVII; **f** AI. (Scales 0.1 mm)

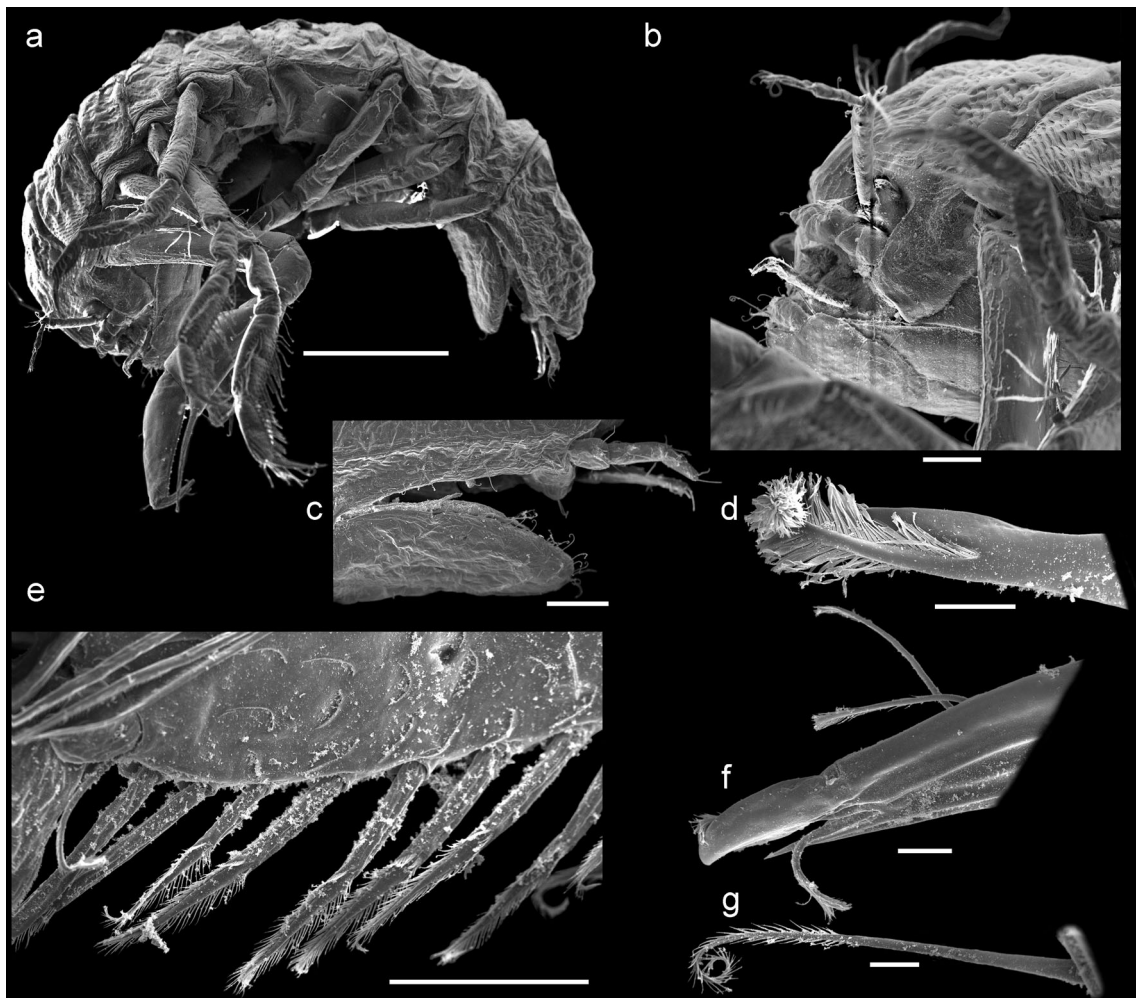


Fig. 25 ZMH K–43231 *Chelator rugosus* female SEM pictures: **a** habitus lateral, **b** head lateral view, **c** operculum lateral view, **d** PI tip of cla-seta, **e** PII propodus ventral setal row, **f** PI claw, **g** PII propodus seta in dorsal setal row (Scales (**a**) 0.5. mm, (**b–c**) 0.1 mm, (**d, f–g**) 0.01 mm, (**e**) 0.05 mm)

Pleopod 3 (ZMH K–43205; Fig. 9c) endopod length 1.4 width, distally with 3 plumose setae. Exopod length 0.6 of endopod length, outer margin terminally fringed with fine setae.

Pleopod 4 (ZMH K–43205; Fig. 9d) endopod oval-shaped, length 1.8 width. Exopod 0.5 endopod length, terminally with 1 plumose seta.

Uropods (ZMH K–43205; Fig. 9a, b) uniramous. Protopod with 1 inner lateral and 5 apical (4 simple and 1 small seta). Endopod length 2.1 protopod length, endopod length 3.3 width, with 5 broom setae and 4 simple setae and 1 small seta.

Description of male

Habitus (ZMH K–43204; Fig. 10a, b, subadult male; ZMH K–43208; Fig. 14c, d, adult male) length ZMH K–43204 1.3 mm, 4.4 Prn2 width. Cephalon with cuticular folds arranged as ring of small “horns” from dorsal view (detail Fig. 10d). Frons clypeal furrow and transverse ridge on frons

present. Prn1 width 1.2 cephalon width. Prn1 length 0.8 Prn2 length, 0.97 Prn2 width. Lateral margins of Prn1–4 convex. Prn5 width 0.9 length, anterior margin straight, lateral margins of Prn5 almost straight, slightly convex. Coxae 1–4 produced, tipped with stout setae. Plt rounded, length 1.2 width. Posterolateral spines absent.

Antennula (ZMH K–43204; Fig. 10c) 0.3 mm long, with 5 articles. Article 1 length 0.9 width, with 1 broom seta. Article 2 length 7.2 width, 3.6 article 1 length; distally with 2 large broom setae and 1 small broom seta. Article 3 distally with 1 small seta. Article 4 distally with 2 small broom setae. Article 5 distally with 3 slender setae (partly broken off), 1 aestetasc (broken off).

Antenna (ZMH K–43204; Fig. 10c) about 0.7 mm long, length 0.5 body length, with 16 articles. Article 5 distally with 1 long broom seta and 2 small slender setae, article 6 distally with 1 broom seta and 4 simple setae. Flagellar articles distally with few setae, distal flagellar article terminally with several long slender setae.

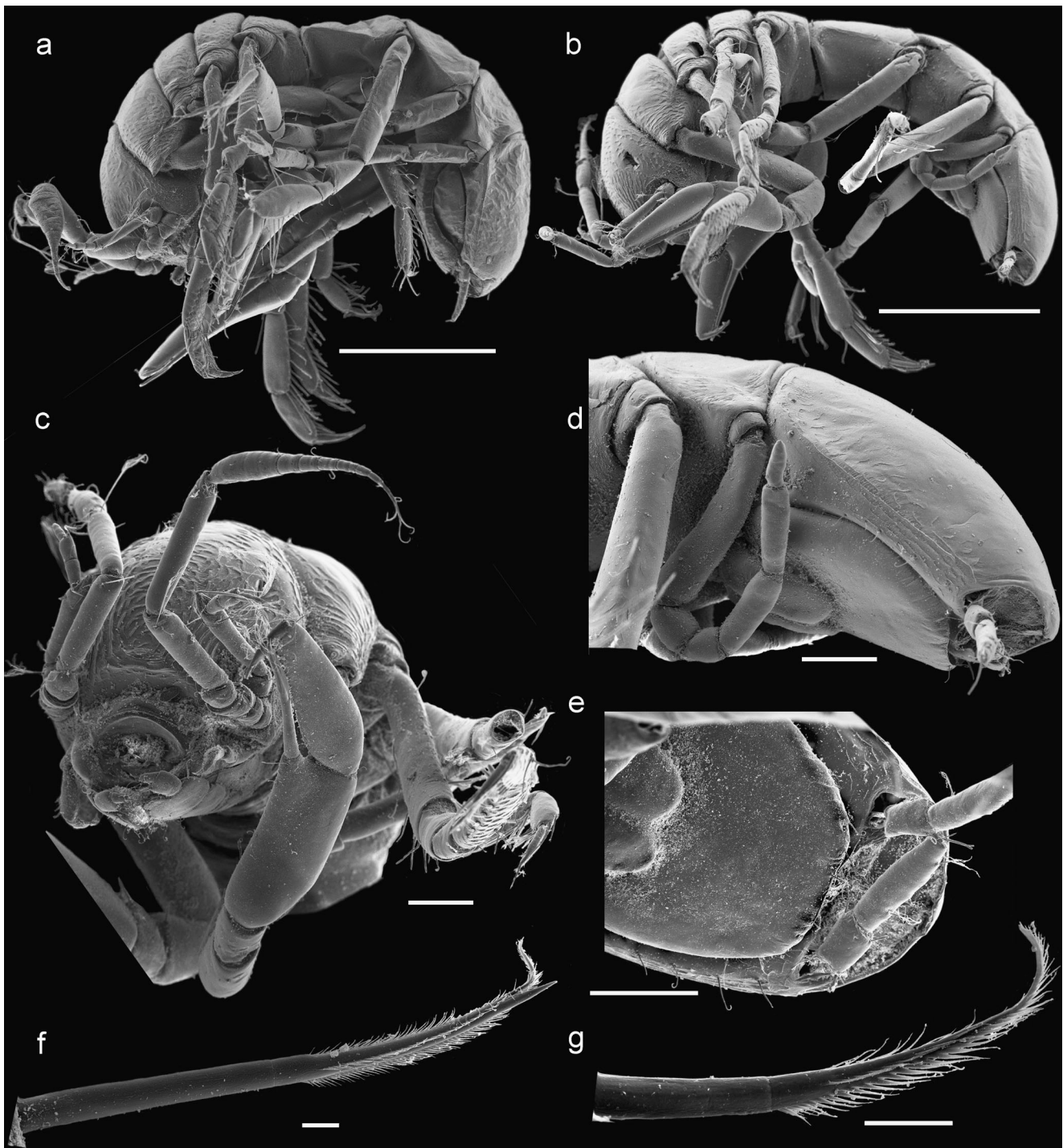


Fig. 26 ZMH K-43233 *Chelator rugosus* adult male and ZMH K-43234 subadult male SEM pictures: **a** ZMH K-43234 habitus lateral, **b** ZMH K-43233 habitus lateral, **c** ZMH K-43234 head frontal, **d** ZMH K-43233 Plt. lateral view, **e** ZMH K-43233 Plt. ventral view, **f** ZMH K-43234 PIII carpus seta in ventral row, **g** ZMH K-43233 PII carpus seta in ventral row (Scales (**a–c**) 0.5 mm, (**d, e**) 0.1 mm, (**f, g**) 0.01 mm)

Mandible (ZMH K-43204; Fig. 11a, b) first article of Md palp with 1 seta, second article distally with 2 setulate setae, marginally fringed with numerous fine setae, apical article with 2 setulate setae and combs of fine setae. Ip with 4 teeth. Lm of IMd

(b') with 3 teeth, lm like structure of rMd distally serrated (a''), spine row containing 5–7 spines. Mp triangular with 10 setae.

Maxillula (ZMH K-43204; Fig. 11c) terminally with 3 setae. Outer lobe, terminally with 12 strong spines, ventrally

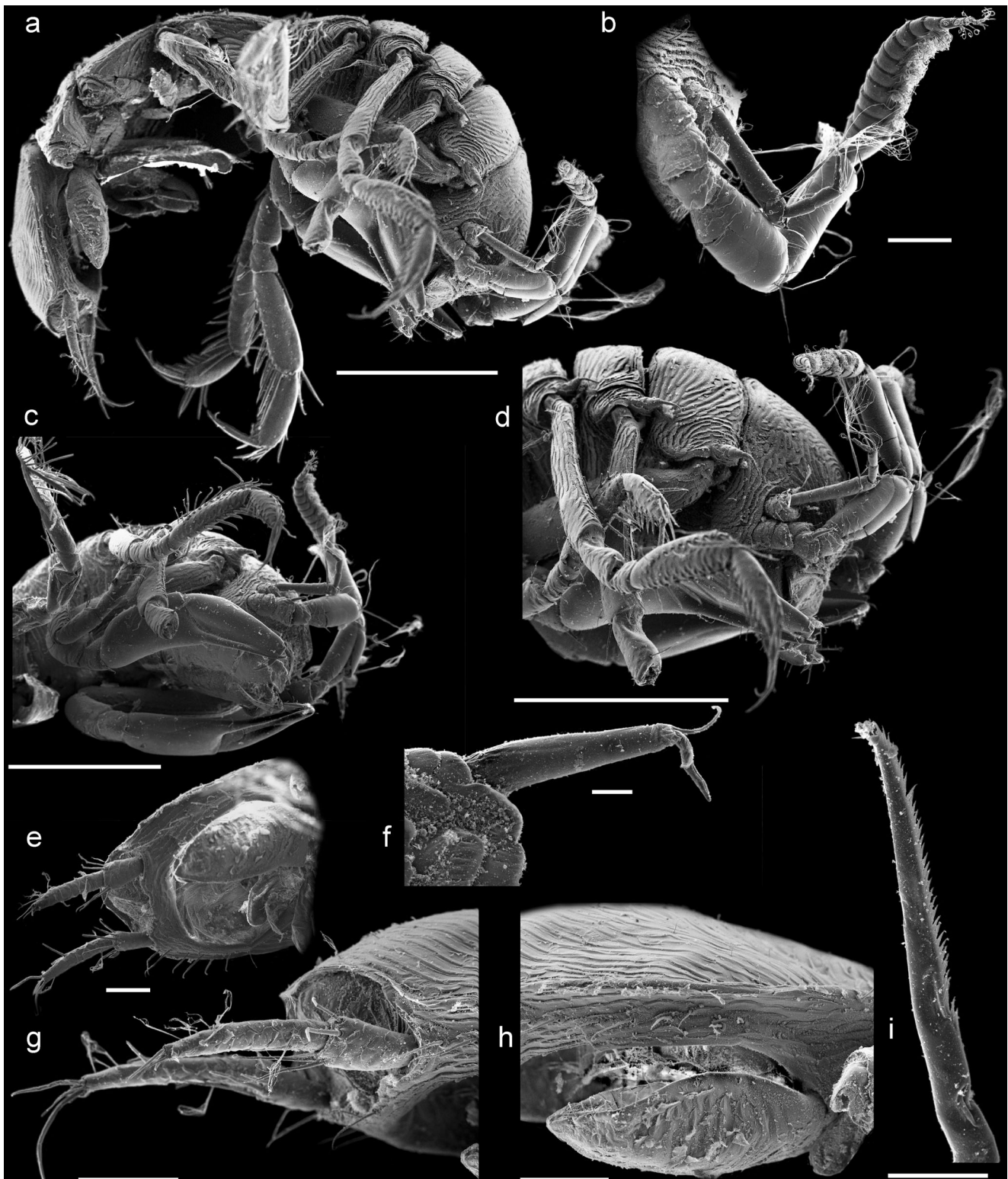


Fig. 27 ZMH K-43232 *Chelator rugosus* adult male SEM pictures: **a** habitus lateral, **b** antennae ventrolateral view, **c** head ventral view, **d** head lateral view, **e** Plt. ventral view, **f** A1 spine-like bifid seta on peduncular

article 3, **g** Ur lateral view, **h** Plt. lateral view, **i** Ur tip serrated seta (Scales (a, c, d) 0.5 mm, (b, e, g, h) 0.1 mm, (f, i) 0.01 mm)

with 3 pairs of fine setae, dorsally 4 rows of fine setae with 4 setae each.

Maxilla (ZMH K-43204; Fig. 11d) with 3 lobes. Medial lobe slightly broader than outer lobes, ventrally with 5 long

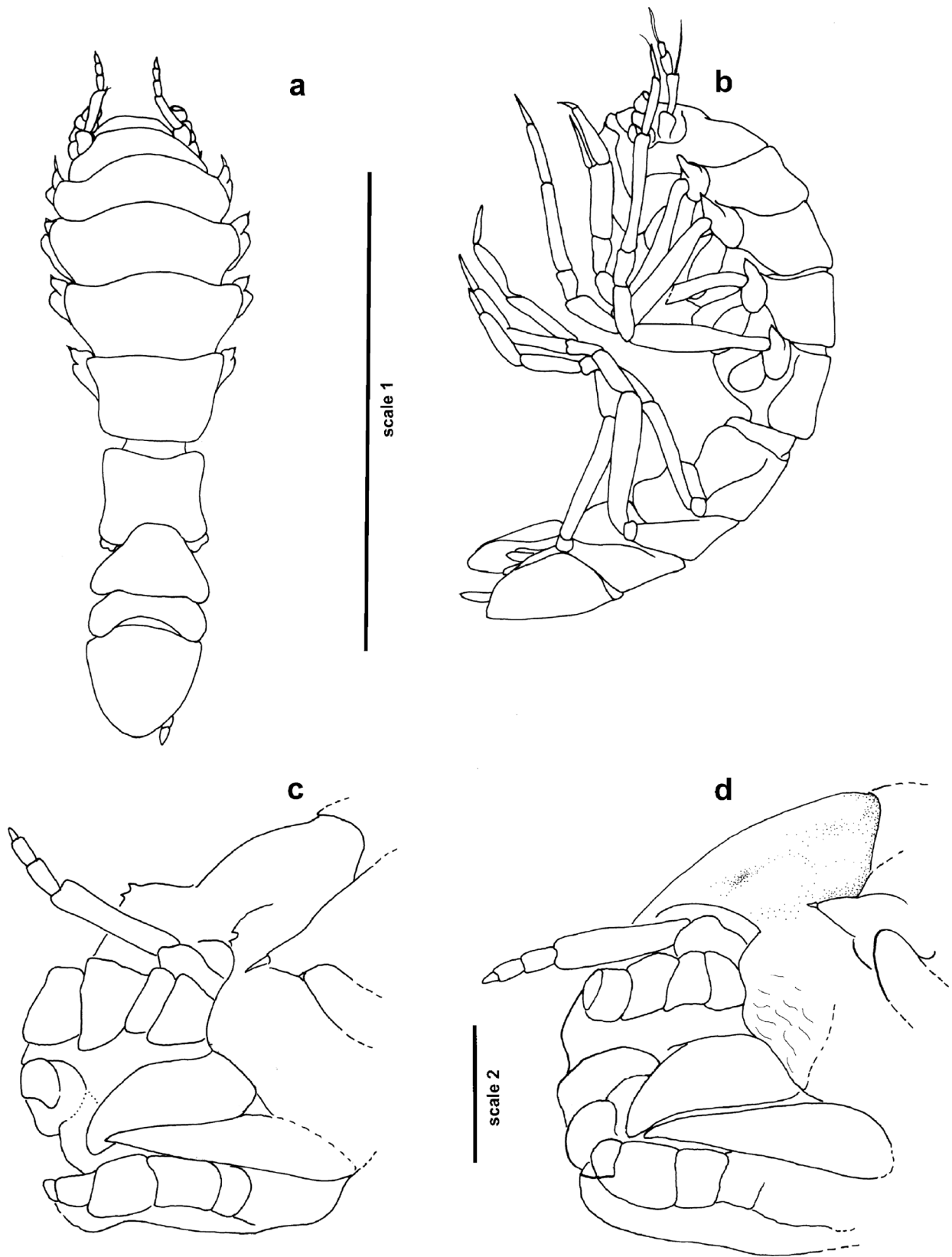


Fig. 28 ZMH K-43238 *Parvochelus russus* sp. nov., female (holotype): **a** habitus dorsal, **b** habitus lateral; **c** ZMH K-43242 head female, **d** ZMH K-43243 head male (Scale 1 1 mm, scale 2 100 μ m)

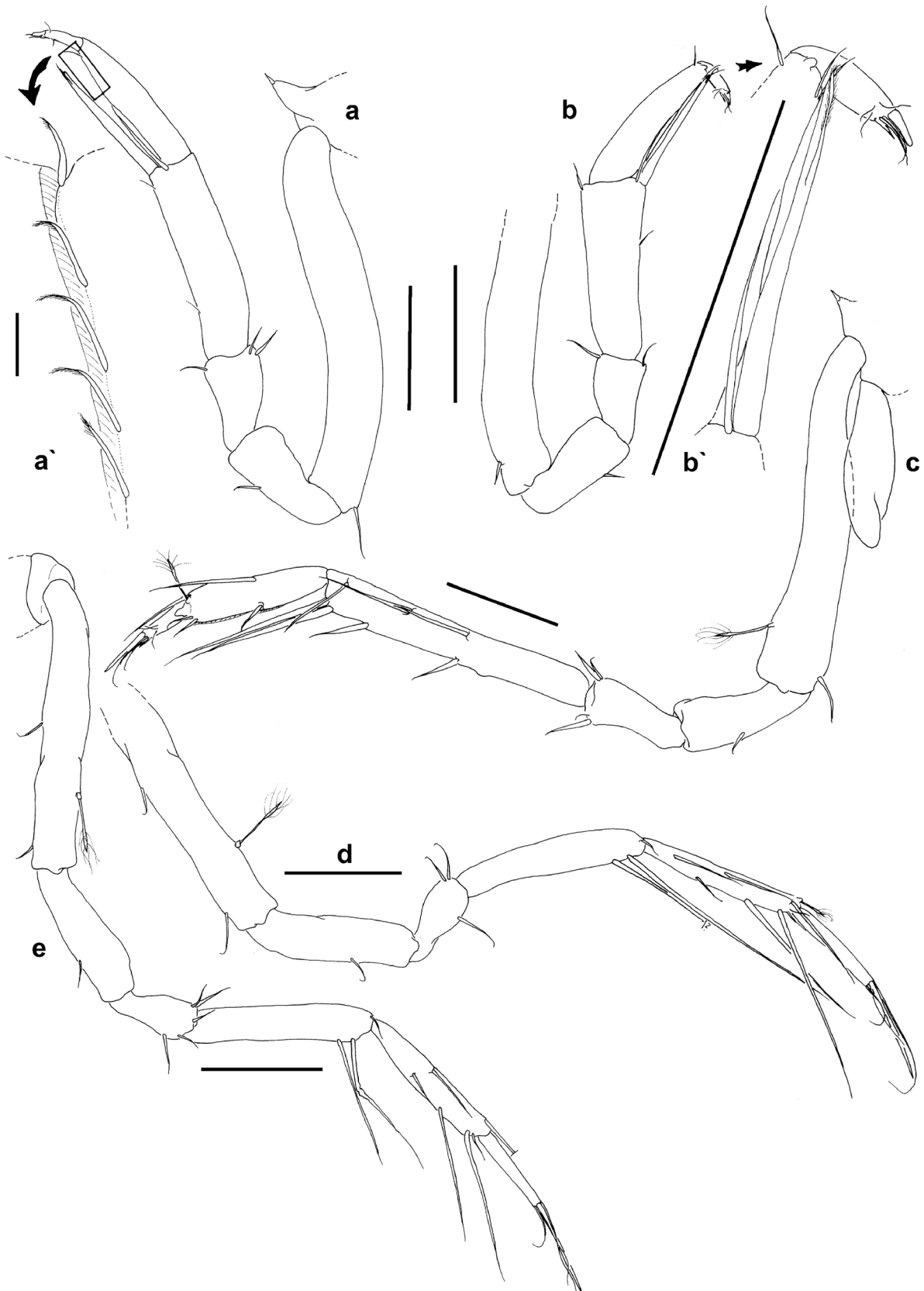


Fig. 29 *Parvocheilus russus* sp. nov., female: **a, a'** ZMH K–43238 PI; **b, b'** ZMH K–43240 PI, **c** ZMH K–43238 PII, **d** ZMH K–43238 PV, **e** ZMH K–43238 PVI (all Scales 0.1 mm except (**a'**) 0.01 mm)

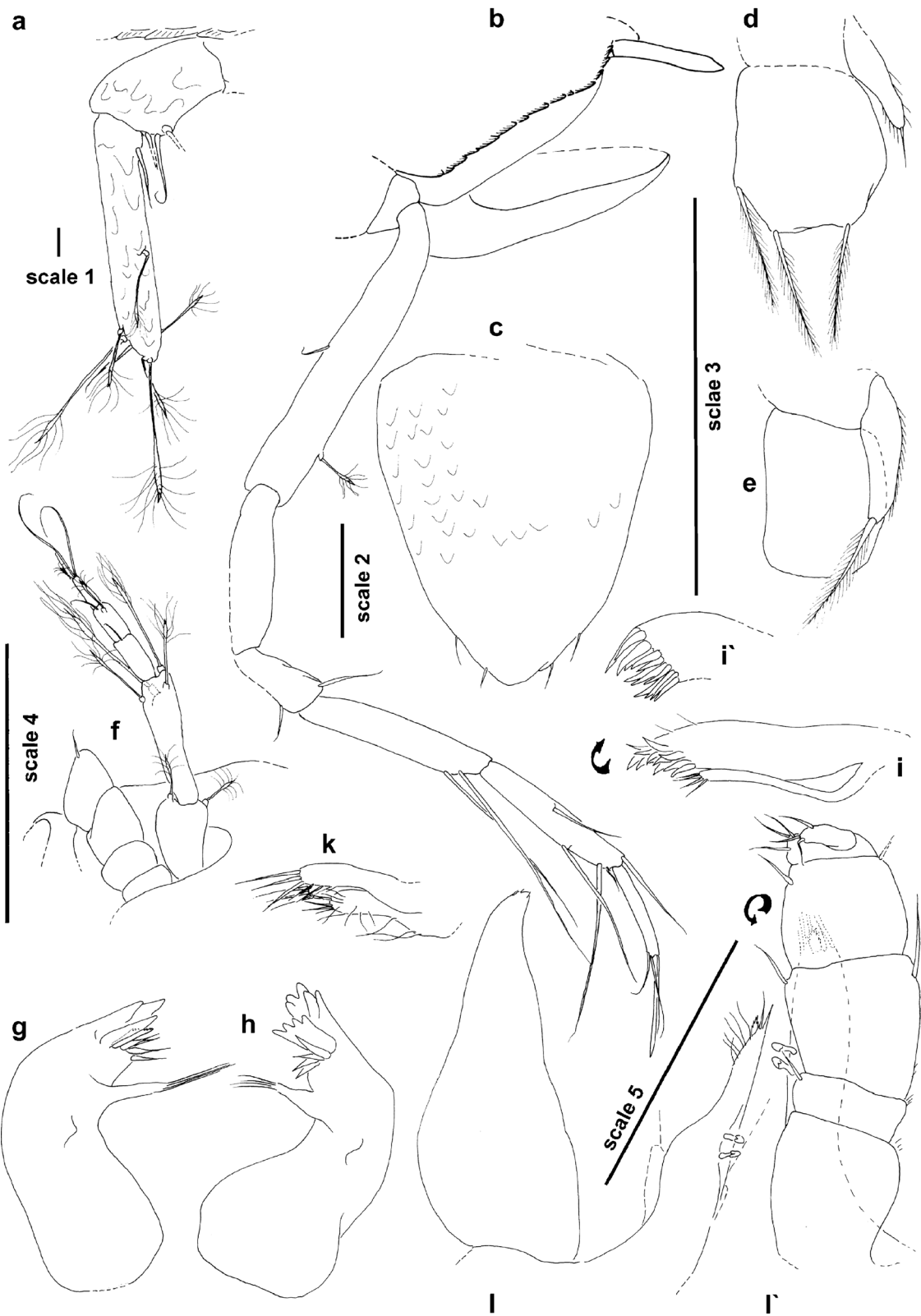
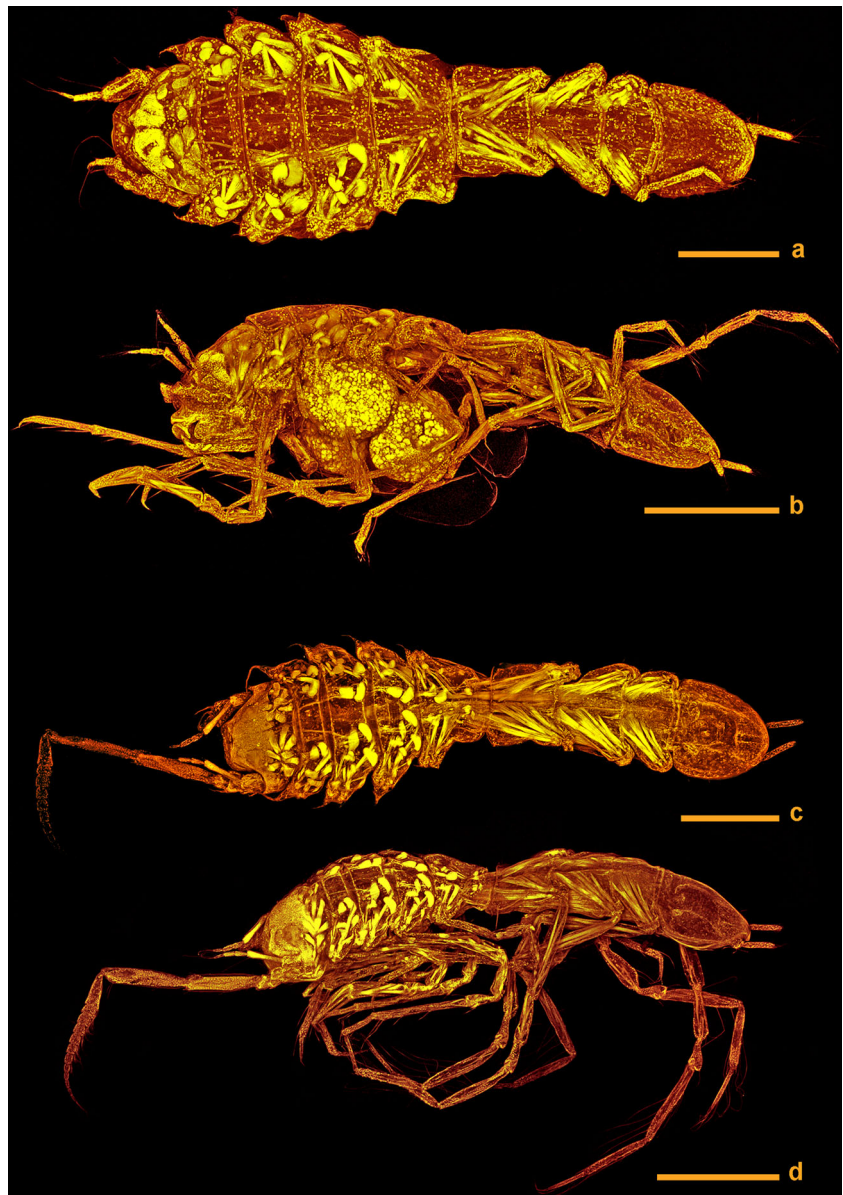


Fig. 30 *Parvochelus russus* sp. nov., female: **a** ZMH K-43242 right uropod; **b** ZMH K-43238 Plt margin and P VII, **c** ZMH K-43240 Op, **d** ZMH K-43240 Plp 3, **e** ZMH K-43240 Plp 4; **f** ZMH K-43238 A1 and

basis A2, **g** ZMH K-43240 M dR; **h** ZMH K-43240 M dL, **i, i'** ZMH K-43240 M x1; **k** ZMH K-43240 M x2, **l, l'** ZMH K-43240 M xp inner and outer view (Scale 1 10 μ m, scale 2–5 0.1 mm)

Fig. 31 *Parvocheilus russus* sp. nov., confocal laser scanning microscopy images. ZMH K–43244 female: **a** habitus dorsal, **b** habitus lateral ZMH K–43245 male. **c** habitus dorsal, **d** habitus lateral (Scales (**a**, **c**) 200 μ m, (**b**, **d**) 300 μ m)



slender setae and marginally numerous fine setae, terminally with 2 serrated setae and 1 simple seta. Outer lobes length 6.8 width, terminally with 1 long serrated setae and 3 simple setae, dorsolaterally with 5 rows of fine setae, ventrolaterally with row of 8 triangular shaped setae.

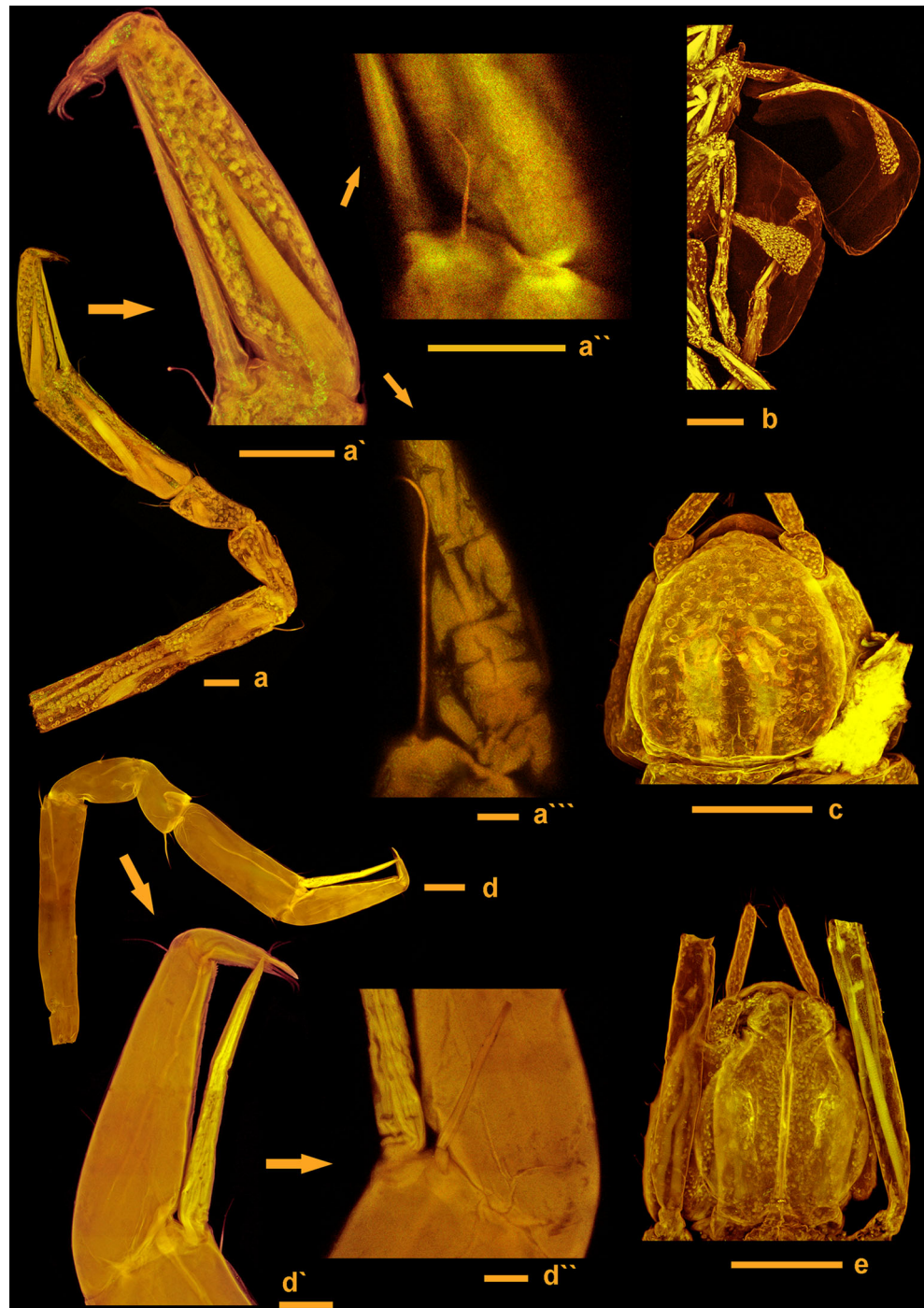
Maxilliped (ZMH K–43204; Fig. 11e) epipodite inner margin fringed with fine setae in cuticular comb, distally 1 slender seta and margin pointed (e''). Endite with 2 coupling hooks, terminally with numerous fine setae, 2 fan setae, marginally with numerous fine setae. Palp articles 1 and 2 lateral margins of fringed with fine setae, article 2 outer margin tipped with 1 seta. Palp article 3 with 6 setae on medial margin and 1 seta on lateral margin. Article 4 terminally with 4 setae, article 5 (e') with 3 setae.

Pereopod I (ZMH K–43204; Fig. 10f) basis length 4.5 width, dorsally with 1 small and 2 broom setae, ventrally with

3 small seta, distoventrally additionally 1 small seta. Ischium length 1.5 width, ventrally with 1 seta, dorsally 1 seta. Merus length 0.7 width, distodorsally with 2 setae, ventrally with 1 seta. Carpus produces at base of claw-seta length 1.7 width, distodorsally with 1 small seta, midventrally 1 small seta and 1 slender seta close to claw-seta. Propodus length 3.4 width, dorsally with 1 small seta, distodorsally with 1 small seta and 1 broom seta. Dactylus with 3 small slender setae close to claw. Claw of dactylus consisting of 2 conate setae and 2 slender setae inserting in between.

Pereopod II (ZMH K–43204; Fig. 12a) basis length 4.6 width, dorsally with 3 broom setae, ventrally with 3 distally setulate setae, distoventrally with 1 distally setulate seta. Ischium length 2.1 width, dorsally with 1 seta, ventrally with 2 setae. Merus length 0.9 width, distodorsally with 2 setae

Fig. 32 *Parvochelus russus* sp. nov., confocal laser scanning microscopy images. ZMH K-43244, female: **a** PI, **a'** PI chela detail, **a''** PI chela detail, enlargement seta, **a'''** PI chela detail, enlargement seta, **b** oostegites detail, **c** Plt ventral. ZMH K-43208, male: **d** PI, **d'** PI chela detail, **d''** PI chela detail, enlargement seta, **e** Plt ventral (Scales (a, a', a'', d') 30 μ m, (a''', d'') 10 μ m, (b, c, e) 100 μ m, (d) 40 μ m)



(broken off), ventrally with 2 composed setae. Carpus, propodus and dactylus broken off.

Pereopod III (ZMH K-43204; Fig. 12b) basis and ischium damaged. Merus length subsimilar width, distodorsally with 1 small and 1 distally setulate seta, ventrally with 1 distally setulate seta. Carpus length 2.9 width, mediodorsally with row of 9 setae, ventrally with row of 7 composed (unequally bifid, distally setulate) setae. Propodus length 2.6 width, dorsally with row of 3 setae, distodorsally with 1 slender, 1 composed and 1 small broom seta. Dactylus with 3 small

slender setae inserting close to claw. Claw of dactylus consisting of 1 simple conate seta and 2 slender setulate setae.

Pereopod IV (ZMH K-43204) broken off.

Pereopod V (ZMH K-43204; Fig. 12c) basis and ischium damaged (distorted) on slide. Merus length subsimilar width, distodorsally with 1 small seta, distoventrally with 1 small seta. Carpus length 3.0 width, dorsally with row of long slender distally setulate setae, distodorsally 1 small broom seta, ventrally with row of 5 long slender distally setulate setae. Propodus length 2.9 width, dorsally with 2 slender, 2 unequally

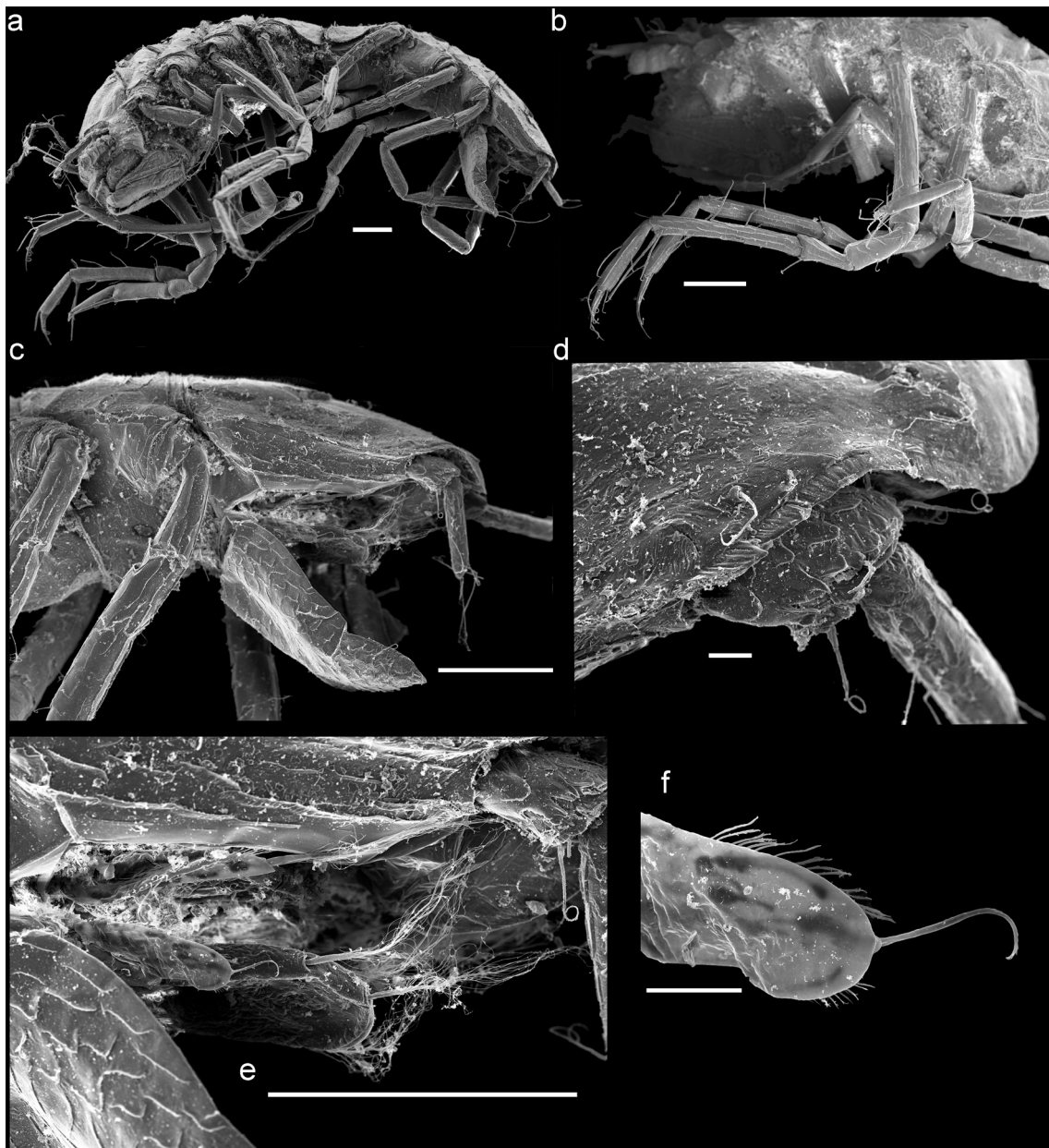


Fig. 33 ZMH K–43242 *Parvochelus russus* sp. nov., female SEM pictures: **a** habitus lateral, **b** PIII and PIV, **c** Plt. lateral, **d** Ur detail, **e** Plp3, f Plp3 detail exopod (Scales (a–c, e) 0.1 mm, (d) 0.01 mm, (f) 10 μ m)

bifid setae and 1 small broom seta, ventrally with row of 5 long slender, distally setulate setae. Dactylus with 2 small slender setae and 1 unequally bifid seta (broken) inserting close to claw. Claw of dactylus consisting of 1 long conate seta and 2 slender setulate setae of same length as conate seta.

Pereopod VI (ZMH K–43204; Fig. 12d) basis length 3.6 width, dorsally with 3 broom setae, ventrally with 1 broom seta and distoventrally 1 seta. Ischium length 2.7 width, dorsally with two distally setulate setae, ventrally with 1 seta. Merus length subsimilar width, distodorsally with 1 distally setulate seta, ventrally 2 small setae. Carpus length 3.0 width, dorsally with row of 6 slender, distally setulate setae, distodorsally with 1 small broom seta, ventrally with row of

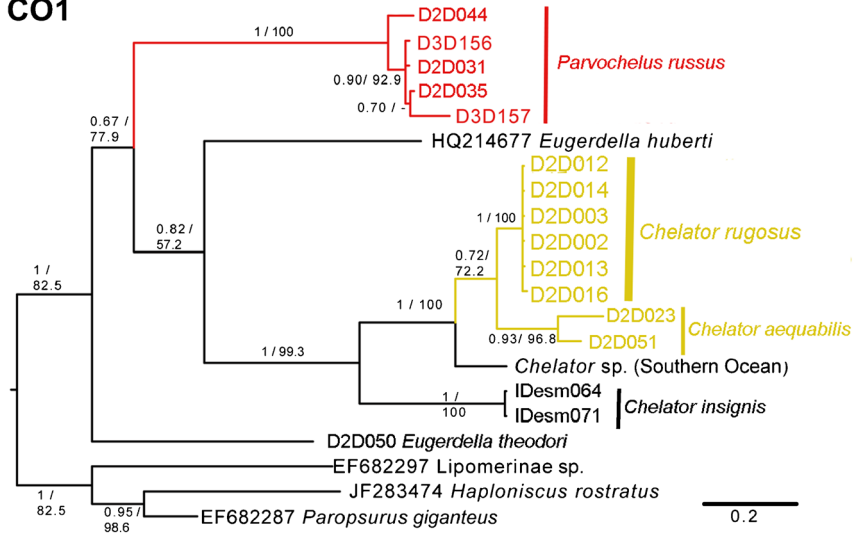
5 long slender, distally setulate setae. Propodus length 2.9 width, dorsally with 3 slender setae and 1 unequally bifid seta, ventrally with row of 5 long slender, distally setulate setae. Claw of dactylus consisting of 1 long simple conate seta and 2 slender setulate setae of similar length.

Pereopod VII (ZMH K–43204; Fig. 12e) basis with 1 broom seta, further articles without setae, juvenile condition.

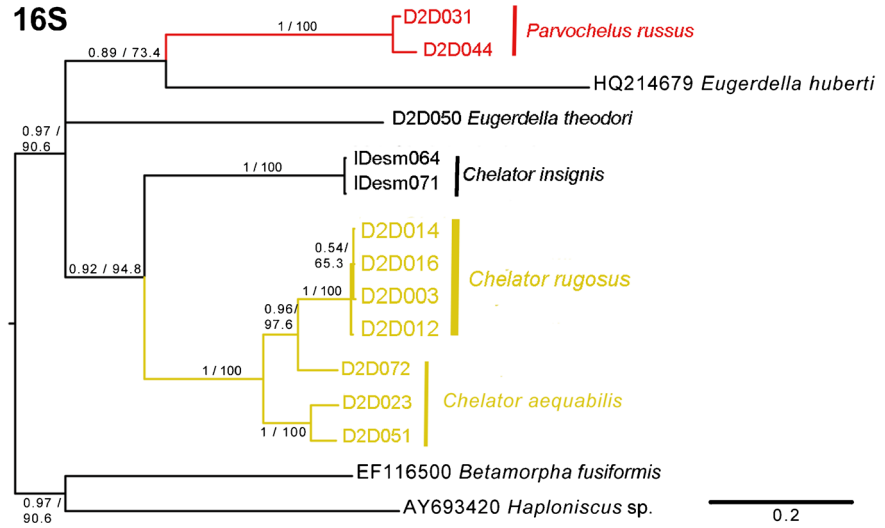
Pleopod 1 (ZMH K–43204; Fig. 13b) illustrated in situ, subadult condition. Length 0.9 width. Pleopod of adult male (ZMH K–43208) documented as CLSM picture (Fig. 15f). Lateral margins slightly concave, distal margin convex on each half with each ending with four slender setae. Surface ventrally with few small slender setae on each half.

Fig. 34 Trees (a COI, b 16S, c 18S)

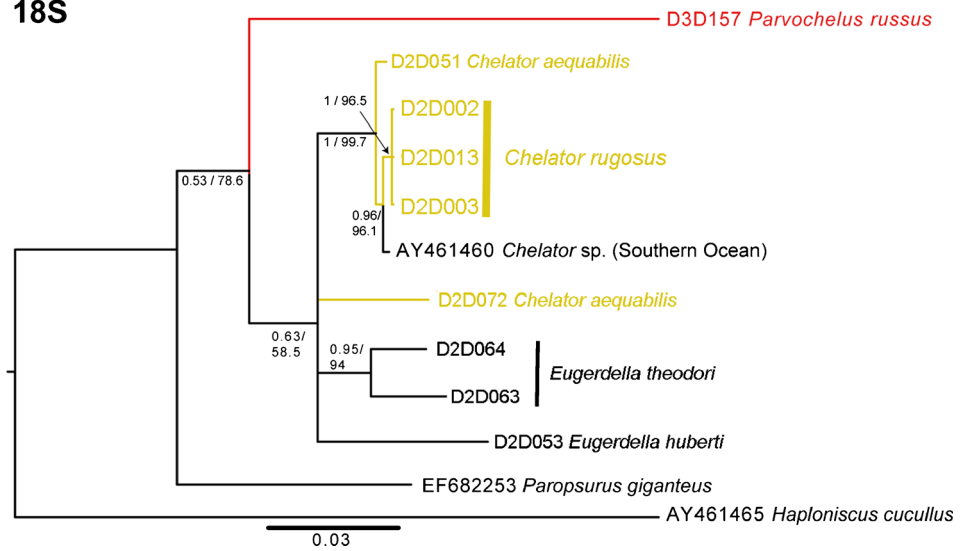
a COI



b 16S



c 18S



Pleopod 2 (ZMH K–43204; Fig. 13b) length 1.5 width, oval form.

Pleopod 3, 4 (ZMH K–43204; Fig. 13b) not dissected to avoid damage of the pleotelson.

Uropods (ZMH K–43204; Fig. 13a) uniramous. Protopod length 1.1 width, with 3 simple setae. Endopod length 2.8 protopod length, endopod length 3.6 width, with 5 broom setae and 3 slender setae located distally (Figs. 14, 15, 16 and 17).

Remarks

Pereopod I of *Chelator aequabilis* shows the projection at the base of the claw seta and can thus be allocated to *Chelator*. It differs from *C. insignis*, *C. chelatus* and *C. stellae* by the shape of pereonite 5 (equal width or less width of pleotelson while in the former three species it is broadest with lateral extensions). While the antennula of *C. chelatus* and *C. brevicaudus* possess six articles, the remaining *Chelator* species including *C. aequabilis* possess 5 articles. *C. aequabilis* differs from *C. vulgaris* by the setation of PI (carpus with more small setae ventrally). Pereopod I of *C. aequabilis* resembles *C. verecundus*, but the new species differs by the higher number of setae in the setal rows on carpus and propodus of PII (12–16 vs. 5–7) and carpus more heavily built in *C. aequabilis*.

Minor differences between the specimens of *C. aequabilis* from different stations (64-5 and 89-7) in the Guinea Basin may be explained by the different ontogenetic stages of the specimens studied, e.g. the claw of PII in preparatory female (holotype ZMH K–43203, D2D023) with simple conate seta versus in juvenile ZMH K–43205 (D2D051) the claw of PII with serrated conate setae like in *C. rugosus* Brix & Riehl sp. nov. (see below). Other differences were found between the subadult male ZMH K–43204 (D2D072) and the preparatory female (ZMH K–43203, D2D023), which may be a sexual dimorphism. The sample size is however too small to be able to study the full range of variation or to distinguish between intraspecific variability and interspecific divergence. The high distance between individuals [range between 6.5 % uncorrected *p* distance (D2D051/D2D023) to about 15 % (D2D072/D2D051) in 16S and 18S and about 12 % in COI (D2D023/D2D051)] may indicate the presence of multiple cryptic species in *C. aequabilis*. Because of insufficient knowledge of ontogenetic variation, we cannot recognise these potential species morphologically, and we hence describe multiple individuals representing different ontogenetic stages.

Chelator rugosus Brix & Riehl sp. nov.

Material

Fifty specimens of *Chelator rugosus* sp. nov. from two epibenthic sledge stations (40-1, 41-2 in the Cape

Basin) during the DIVA-2 expedition were compared for description.

Holotype Female, preparatory, 2.4 mm; ZMH K–43228 (D2D002); designated here

Type locality Cape Basin, start position: 28°3.07'S, end position: 07°19.81'E, depth 5,055 m; RV “Meteor” M63/2; station 40-1; gear: EBS, 4 March 2005.

Paratypes 1 male, adult, 1.6 mm, ZMH K–43229 (D2D003, allotype), same locality as holotype.

4 juveniles ZMH K–43230 (D2D012, D2D013, D2D014, D2D016) from station 41-2 Cape Basin, 04.03.2005, start position 28° 3.98'S, end position 07° 20.49'E, depth 4,054 m, RV “Meteor” M63/2; station 41-2; gear: EBS, trawling distance 1,368 m.

Paratypes used for SEM pictures: ZMH K–43231 (D2D087) female, ZMH K–43232 (D2D105) male adult and ZMH K–43233 (D2D005) male subadult. All three specimens from same locality as holotype. ZMH K–43234 (D2D175) male adult, ZMH K–43235 (D2D197) female; both from station 41-2.

Other material ZMH K–43236 (23 specimens), same locality as holotype.

ZMH K–43237 (16 specimens), same locality as paratypes.

Etymology

The name refers to the “rugose” (Lat. wrinkled, folded or creased) cuticular structure, especially in the males.

Diagnosis

Body covered with deep cuticular folds, more in male than in female. Folds absent on the female and juvenile male plt tergites. Lateral margins of Prn1–7 smooth, without posterolateral spines in male and female. Mxp scale tip with a “hook” (stout seta-like structure) and fine setae. A1 of five articles. Lm with three teeth. Urp uniramous. Claw of PII with double serrated conate seta. Female operculum and male pleopods 2 with several small setae on distolateral margins (Fig. 25; SEM plate of ZMH K–43231).

Description of female

Habitus of female (ZMH K–43228; Fig. 18a, b) body 2.4 mm long, 3.8 longer than width of Prn2. Cephalon free, 0.8 longer than wide. Prn1 width 0.6 cephalon width. Prn1 length 1.4 Prn2 length. Lateral margins of Prn1–4 smooth. Prn5 width 1.3 length, anterior margin and lateral margins straight. Lateral

margins of Prn 6 and 7 convex. Coxae 1–4 produced, tipped with 1 stout seta. Plt length 0.8 width, lateral margins more straight than convex, posterior margin rounded.

Antennula (ZMH K–43228; Fig. 19d) 0.2 mm long, length 0.4 body length, with 5 articles. Article 1 with 3 broom setae and 1 small simple seta. Article 2 length 6.0 width; distally with 1 simple seta and 2 large broom setae. Article 3 distally without setae. Article 4 distally with 1 small simple seta. Article 5 with 1 small broom seta, 2 long slender setae and 1 aestetasc. Articles 2–5 length relative to article 1: 2.4: 0.5: 0.4: 0.4.

Antenna broken off.

Mandibles (ZMH K–43228; Fig. 19e–f) first article of rMd palp with 1 seta, palp of lMd broken off. Ip with 4 teeth. Lm of lMd with 3 teeth, lm like structure of rMd distally serrated, spine row containing 3–6 distally serrated spines bearing lateral setules. Mp triangular with 10–12 setae.

Maxillula (ZMH K–43228; Fig. 19g–g) inner lobe terminally with 8 setae, extensor marginally with 10 slender setae. Outer lobe length 7.0 width, terminally with 9 strong spines and row of 8 setae.

Maxilla (ZMH K–43228; Fig. 19h, h) with 3 lobes. Medial lobe slightly broader and stouter than outer lobes, covered with small slender setae, terminally with 3 serrated setae and 5 simple setae. Outer lobes length 9.0 width, terminally with 1 large serrated seta and 2 small serrated setae, dorsolaterally with several fine slender setae, ventrolaterally with row of 7–9 triangular shaped setae.

Maxilliped (ZMH K–43228; Fig. 19j–j) epipodite (scale) length 3.6 width, subequal length as endite, tipped with 2 long slender setae and 3 small slender setae next to 1 stout seta-like structure. Endite with 2 coupling hooks, terminally with numerous fine setae, 2 fan setae and 2 setulate setae, marginally with numerous fine setae. Outer margins of palp articles 1 and 2 fringed with fine setae. Palp article 1 with 1 seta on outer margin, article 2 with 1 seta on outer margin, article 3 with 9 setae on inner margin and 1 on outer margin. Article 4 with 3 setae on inner margin. Article 5 terminally with 4 setae.

Pereopod I (ZMH K–43228; Fig. 18c–c) basis length 3.9 width, dorsally with 1 broom seta, ventrally with several slender setae, distoventrally with 1 seta. Ischium length 1.2 width, without setae. Merus width 0.6 length, distodorsally with 1 distally setulate seta. Carpus produces at insertion of claw-seta, length 1.7 width, distodorsally with 1 fine seta, ventrally 3 fine setae. Propodus length 3.2 width, dorsomedially with 1 fine seta, distodorsally with 1 seta. Dactylus close to claw with 3 slender setae. Claw of dactylus with 2 conate and 2 slender setae inserting in between conate setae.

Pereopod II (ZMH K–43228; Fig. 20a–a) basis length 5.7 width, dorsally with 1 small broom seta and 1 small seta,

ventrally with 10 setae (6 simple and 4 long distally setulate setae), distoventrally with 1 long distally setulate seta. Ischium length 1.6 width, dorsally with 2 setae, ventrally with 4 setae. Merus length 0.9 width, dorsally without setae, ventrally with 3 distally setulate setae. Carpus length 2.9 width, medially with row of 12 setae, distodorsally with 1 broom seta and 1 slender seta, ventrally with row of 14 composed setae increasing in size towards propodus. Propodus length 1.8 width, dorsally with 3 setae, distodorsally 1 composed seta and 1 small broom seta, ventrally with row of 10 composed setae. Claw of dactylus consisting of 2 conate setae (the bigger one serrated) with 2 slender distally setulate setae inserting in between, medially on dactylus prior claw 3 fine slender setae.

Pereopod III (ZMH K–43228; Fig. 20b–b) basis length 4.4 width, dorsally with 5 setae (1 seta broken off, 1 broom seta, 2 simple setae and 1 distally setulate seta) ventrally with 7 setae (potentially 4 distally setulate and 3 simple setae), distoventrally 1 distally setulate seta. Ischium length 1.6 width, distodorsally with 1 seta, ventrally with 3 setae. Merus length 1.3 width, distodorsally with 1 seta, ventrally with 2 composed setae. Carpus length 2.4 width, medially with row of 15 setae, distodorsally 1 composed seta, ventrally with row of 12 composed setae increasing in size towards propodus. Propodus length 2.2 width, dorsally with row of 5 setae, distodorsally 1 simple slender, 1 broom and 1 composed seta, ventrally with row of 9 composed setae and distoventrally 1 small slender seta. Dactylus ventrally fringed with numerous fine setae in cuticular membrane, distomedially with 2 slender setae. Claw of dactylus comprising of 1 conate seta and 2 slender distally setulate setae.

Pereopod IV (ZMH K–43228; Fig. 20c–c) basis length 5.1 width, dorsally with 5 setae, ventrally with 6 setae (1 small broom and 5 small setae), distoventrally with 1 distally setulate seta. Ischium length 1.7 width, distodorsally with 1 seta, ventromedially 1 small seta. Merus length 1.2 width, distodorsally with 2 setae, ventrally with 2 composed setae (1 broken off). Carpus length 3.5 width, medially with row of 10 setae, dorsally with 1 small seta, ventrally with row of 9 composed setae increasing in length towards propodus. Propodus length 3.0 width, dorsally with row of 5 setae and 2 small setae, ventrally with row of 7 composed setae and 1 small slender seta. Dactylus ventrally fringed with numerous setae in cuticular membrane, 3 slender setae close to claw. Claw composed of 1 elongated conate seta, 1 small slender and 2 slender distally setulate setae.

Pereopod V (ZMH K–43228; Fig. 20d–d) damaged and shown in two parts, basis length 5.4 width, dorsally with 1 large broom seta and 1 small seta, ventrally with 4 broom setae and 4 small setae. Ischium length 2.0 width,

dorsally with 3 setae, ventrally without setae. Merus length 1.4 width, distodorsally with 1 small seta, distoventrally with 1 small seta. Carpus length 2.3 width, dorsally with row of 7 long slender distally setulate setae, distodorsally with 1 small broom seta and 1 distally setulate seta, ventrally with row of 8 long slender distally setulate setae. Propodus and dactylus broken off.

Pereopod VI (ZMH K–43228; Fig. 20e) basis and ischium only, rest broken off, basis length 6.4 width, dorsally with 1 seta, ventrally with 3 setae, distoventrally 1 distally setulate seta. Ischium length 2.8 width, dorsally with 1 distally setulate seta, ventrally with 1 slender seta.

Pereopod VII broken off.

Pleopod 2, operculum (ZMH K–43228; Fig. 19a) length 1.1 width. Lateral margins rounded and distal margin straight. Lateral margins with 7 setae each and distal margin without setae. Surface structure present.

Pleopod 3 (ZMH K–43228; Fig. 19b) endopod length 1.5 width, distally with 3 plumose setae. Exopod length 0.6 of endopod length, outer margin with small fine setae.

Pleopod 4 (ZMH K–43228; Fig. 19c) endopod length 1.6 width. Exopod length 4.6 width, 0.8 endopod length, outer margin fringed with fine setae, terminally with 1 plumose seta.

Uropods broken off.

Description of male

Differences in male are shown in Figs. 21, 22, 23 and 24.

Pleopod 1 (ZMH K–43229; Fig. 24c) length 2.2 width. Lateral margins more straight than slightly concave and distal margin convex on each half with each ending with 3 slender setae. Surface ventrally with 3 slender setae on each half.

Pleopod 2 (ZMH K–43229; Fig. 24b) length 1.5 width, oval form.

Remarks

The diagnostic characters used for species delimitation in *Chelator* are mainly features of the shape of the body, as well as setation and proportions of the pereopods. In the case of *C. aequabilis*, intraspecific morphological variation and high similarity to *C. rugosus* makes the species' diagnostic characters subtle. Both species can be distinguished from all other species of the genus by the diagnostic character states explained for *C. aequabilis* above. The PI of both species is highly similar. Subtle differences are however found in the claw of PII in adult stage: in the juvenile of *C. aequabilis* (ZMH K–43205, D2D051), the PII claw features a serrated conate seta as in the adult specimens of *C. rugosus*. Adult specimens, on the other hand, possess a simple conate seta.

The setation of the operculum can also be used to distinguish between both species. These differences are,

however, not present in the male pleopods 2. The second pleopods of the juvenile male of *C. rugosus* (ZMH K–43233) possess approximately seven setae on the posterior margin and is in this regard similar to the conspecific preparatory female (ZMH K–43228). In the adult male of *C. aequabilis* where the conspecific female operculum bears 2 small setae, pleopod 2 shows a pattern (ZMH K–43210) similar to that of *C. rugosus* (ZMH K–43232). A sexual dimorphism is present here and the species-distinguishing character states are only present in females. The numbers of collected adult specimens were, however, insufficient to be used for a thorough statistical or morphometric analysis.

The cuticular ornamentation (cuticular folds) is expressed in both species but seems to be more pronounced in *C. rugosus* (compare Figs. 16 and 17 with Figs. 25, 26 and 27), again with a sexual dimorphism where the males have a stronger-ornamented cuticle. Sexual dimorphisms in cuticular microstructure observed here resemble previous observations in some species of the family Macrostylidae Hansen 1916. In *Macrostylis papillata* Riehl, Wilson & Hessler, 2012, the ornamentation was found more strongly expressed in males than in females (Riehl et al. 2012). Riehl et al. (2012) report the ornamentation to occur in a species-specific arrangement and hypothesize it might be a useful diagnostic character. A comparably characteristic surface structure was previously observed in the desmosomatid species *Eugerdella serrata* Brix, 2006. In this Southern-Ocean species, cuticular microstructure was arranged in a completely different pattern compared to the *Chelator* species described here. The microstructural differences between *C. aequabilis* and *C. rugosus* became apparent only on SEM pictures. Considering the irregular use of SEM in desmosomatid taxonomy, cuticular microstructure might bear a so far unrealized potential for delineation of closely-related species in this isopod family.

While the expression of cuticular structures and the character states in the setation of the female operculum can be found consistently across individuals of each of the two species, other characters show intraspecific variation.

The maxilliped scale tip, for example, occurs with and without hook and fine setae in either of the two described new species. So far, subtle features of the maxilliped have not been considered as apomorphic characters in desmosomatid taxonomy. Their use can be regarded especially prone to bias caused by damage to the specimens which might be too small to be detected by the taxonomists. Insufficient information about ontogenetic changes and variability across individuals in *Chelator* limits our understanding and judgement whether the juvenile condition may be representative for these species in general.

Parvochelus Brix & Kihara gen. nov.

Type and only known species. *Parvochelus russus* Brix & Kihara sp. nov.

Diagnosis

Body length about 5.0 pereonite 2 width. Md palp absent, Ip with 5 teeth, Im of IMd with 4 teeth. PI with less robust carpo-propodo-chela than in any other desmosomatid genus comprising this type of chela, PI merus length approx. 2.0 width; carpus 3.7 times longer than wide, carpus clearly longer than propodus; not produced at basis of claw-seta, distally of claw-seta one long slender seta, length 0.5 claw-seta length propodus subparallel and only distally slightly narrowing. Plt margin serrated. PII–IV slender (propodus length about 4.0 width, carpus length about 8.0 width), setal rows with no more than 5 setae, carpus and propodus of posterior pereopods ventrally only with few long setae (2–3). Body covered with cuticular folds.

Etymology

Parvus (lat. small) refers to the small body size as well as the small chela compared to all other desmosomatid genera with a chela where the carpus width is about twice PII carpus width. The second part of the name refers directly to the chela of PI: *chela* (Lat. a claw). A carpo-chela is a common feature in desmosomatid isopods with many genera having “chela” as part of their names. Referring to the chela in the genus name follows therefore a tradition in desmosomatid taxonomy.

Remarks

The most important feature in desmosomatid taxonomy is the PI (Hessler 1970; Brix 2007; Brix and Bruce 2008). The genus and species determination is based on the shape and setation of its articles (p.e. Schnurr and Brix 2012). The new species *Parvochelus russus* Brix & Kihara sp. nov. is placed into a new genus mainly due to the unique features of this leg but also of the mandible, serration and body size. This combination of character states is not known from any other desmosomatid species and genus. The individuals found during the DIVA expeditions are all tiny in adult stage (not longer than 2 mm).

The cheliferous Eugerdellatinae bear a carpo-propodo-chela on the PI. Rather similar to the condition in *Chelator* are the genera *Prochelator* Hessler, 1970; *Reductosoma* Brandt, 1992; *Oecidiobanchus* Hessler, 1970; *Disparella* Hessler, 1970 and *Chelantermedia* Brix, 2006.

Chelator can be distinguished from *Prochelator* by the ventral projection at the base of the claw-seta. Furthermore, the first four body segments are more compact than in *Prochelator* (the first pereonite in *Chelator* twice as high as pereonite 5). *Reductosoma* Brandt, 1992 differs from all other desmosomatid genera including the novel genus *Parvochelus* by features of the mouthparts. *Disparella* possesses a unique large lateral cephalic spine at the insertion of the antennae. *Disparella* and *Chelator* share the presence of small setae on the ventral carpus margin, but in contrast to *Chelator* in *Disparella* there is always a row of composed setae present on the ventral carpus margin. *Oecidiobanchus* possesses a propodus that is longer than the carpus. The dactylus is able to fully oppose the flexor margin of the propodus. Furthermore, the small branchial chamber is unique to this genus (Hessler 1970).

In contrast to all groups discussed above, in *Parvochelus* the PI is relatively slender and not enlarged when compared to PII. Nevertheless, it bears a carpo-chela. Especially, the carpus is slender and long, and its width is smaller than the merus width. Furthermore, the merus is longer than wide while in all the above-mentioned genera it is the opposite. The slender and long seta that is situated laterally to the carpo-propodal articulation is another characteristic feature. Thus, we see justification to add a novel genus to the Desmosomatidae.

Parvochelus russus Brix & Kihara sp. nov.

Holotype Female, preparatory 1.3 mm; ZMH K–43238 (D2D031); designated here

Type locality Guinea Basin, start position: 0°13.27'S, end trawl: 2°29.91'W, depth 5,054 m; RV “Meteor” M63/2; station 64-5; gear: EBS; 15 March 2005.

Paratypes ZMH K–43239 (D2D035, preparatory female, St.64), ZMH K–43240 (D2D044, female, St.90), ZMH K–43241 (D2D061, preparatory female, St.90)

ZMH K–43242 (D2D294, St.63) and ZMH K–43243 (D2D392, St.64) were used for SEM pictures; ZMH K–43244 (D2D495, St. 64) and ZMH K–43245 (D2D391, St. 89) for CLSM pictures and are stored in the collection NT II ZMH.

DZMB HH 9421 (D3D151 female); Brazilian Basin, start position: 03°57.67'S, end trawl: 28°05.36'W, depth 5,180 m; RV “Meteor” M79/1; station 604-7; gear: EBS; 5 August 2009.

DZMB HH 9381 (D3D156 female), DZMB HH 9392 (D3D157 female); Brazilian Basin, start position: 03°57.49'S, end trawl: 28°04.67'W, depth 5,189 m; RV “Meteor” M79/1; station 605-8; gear: EBS; 6 August 2009.

The specimens from DIVA-3 are remaining in the DZMB storage at $-20\text{ }^{\circ}\text{C}$ and will not be given into voucher storage at the Senckenberg DNA Bank before work on the DIVA-3 isopods is finished. The DZMB number refers to the DZMB database, but is not equivalent to a museum number.

Other material ZMH K–43246 DIVA-2 St. 63: 17 specimens; ZMH K–43247 DIVA-2 St. 64: 18 specimens; ZMH K–43248 DIVA-2 St. 89: 9 specimens; ZMH K–43249 DIVA-2 St. 90: 7 specimens

Etymology

“Russus” (Lat. red) refers to the colour code given to the species during the determination process and also used in Fig. 1.

Description of female

Habitus (ZMH K–43238; Figs. 28a, b, 31a, b) body 1.3 mm long, 3.3 longer than width of Prn2. Cephalon free (d), without frons clypeal furrow, transverse ridge on frons present. Prn1 width 1.4 cephalon width. Prn1 length 0.7 Prn2 length, 0.9 Prn2 width. Lateral margins of Prn1–4 convex tapering towards next Prn. Prn5 width 1.4 length, anterior margin straight, lateral margins of Prn5 straight. Coxae 1–4 produced, tipped with 1 seta each. Plt length 1.1 width, serrated (Fig. 30b).

Antennula (ZMH K–43238; Fig. 30f) 0.1 mm long, length 0.1 body length, with 5 articles. Article 1 with 2 small broom setae. Article 2 length 4.0 width, 1.9 article 1 length; distally with 4 broom setae. Article 3 distally with 1 small slender seta. Article 4 distally with 1 small slender and 1 broom seta. Article 5 with 2 long slender setae, 1 small broom seta and 1 aestetasc.

Antenna broken off from holotype (ZMH K–43238).

Mandibles (ZMH K–43240; Fig. 30g, h) palp absent. Ip with 5 lobes. Lm of lMd with 4 teeth, lm like structure of rMd distally serrated. Md spine row containing 4 spines. Mp triangular with 7–9 setae.

Maxillula (ZMH K–43240; Fig. 30i) inner lobe terminally with 4 setae. Outer lobe length 3.5 width, terminally with 13 strong spines (i'), marginally with few fine setae.

Maxilla (ZMH K–43240; Fig. 30k) with 3 lobes. Medial lobe slightly broader than outer lobes, ventrally with 3 slender setae, terminally with numerous fine setae and 3 small setae. Outer lobes terminally with 3 setae.

Maxilliped (ZMH K–43240; Fig. 30l) epipodite length 2.4 width, length 1.3 endite length, tipped with 3 fine setae. Endite with 2 coupling hooks, terminally with numerous fine setae and 1 fan seta a. Outer margins of palp articles 1 and 2 with few fine setae. Palp article 1 with 1 seta on inner margin, article 2 with 1 seta on

inner margin and 1 seta on outer margin (1 on outer margin broken off), article 3 with 1 seta on inner margin, article 4 terminally with 3 setae, article 5 with 3 setae.

Pereopod I (ZMH K–43238; Fig. 29a; ZMH K–43240; Figs. 29b, 32a) carpo-chelat, basis length 6.5 width, distoventrally with 1 distally setulate seta. Ischium length 2.2 width, ventrally with 1 seta. Merus length 1.5 width, distodorsally with 2 setae, ventrally with 1 seta. Carpus length 3.7 width, not produced at base of claw-seta, ventrally 1 small midventral seta, another small seta proximal to claw-seta, between claw-seta and propodus 1 slender seta reaching slightly more than half of length of claw-seta (b'). Propodus length 4.6 width, ventrally with several small setulate setae and numerous fine setae inserting in a cuticular comb (a'). Dactylus distally with 3 slender setae close to claw. Claw of dactylus consisting of 2 conate setae and 2 small slender setae in between them.

Pereopod II (ZMH K–43238; Fig. 29c) basis length 6.9 width, dorsally with 1 broom seta, distoventrally with 1 distally setulate seta. Ischium length 2.9 width, ventrally with 1 seta. Merus length 3.1 width, distodorsally with 1 composed and 1 small seta, distoventrally with 1 composed and 1 small seta. Carpus length 8.4 width, medially with 3 slender setae, ventrally with row of 5 composed setae (first one broken off) increasing in size towards propodus, largest one slightly longer than propodus. Propodus length 4.3 width, dorsally with 2 composed setae and 1 broom seta, ventrally fringed with fine setae in a cuticular comb, 2 small composed setae and 1 small seta. Dactylus distally with 3 slender setae close to claw. Claw of dactylus consisting of 1 conate seta and 2 slender setae.

Pereopod III broken off from holotype (ZMH K–43238) and paratype (ZMH K–43240).

Pereopod V (ZMH K–43238; Fig. 29d) basis dorsally with 1 broom seta, ventrally with 2 setae. Ischium length 3.2 width, ventrally with 1 seta. Merus length 1.7 width, distodorsally with 2 composed setae, ventrally with 1 composed seta. Carpus length 5.7 width, distodorsally with 1 small seta, ventrally with 2 long slender setae. Propodus length 7.8 width, laterally with 3 slender setae, distodorsally with 1 small broom seta, ventrally with 2 small and 2 long slender setae. Claw of dactylus consisting of 1 long conate seta and 2 slender setae.

Pereopod VI (ZMH K–43238; Fig. 29e) basis length 6.2 width, dorsally with 1 broom seta, ventrally with 2 setae. Ischium length 2.7 width, ventrally with 1 seta. Merus length 2.1 width, with 5 setae. Carpus length 5.3 width, distodorsally with 1 small seta, ventrally with 2

long slender setae. Propodus length 8.5 width, dorsally with 2 slender setae, ventrally with 2 small and 2 long slender setae. Claw of dactylus consisting of 1 long conate seta and 2 slender setae.

Pereopod VII (ZMH K–43238; Fig. 30b) basis length 6.7 width, dorsally with 1 broom seta, ventrally with 1 seta. Ischium length 3.8 width. Merus length 2.0 width, distodorsally with 1 distally setulate seta, distoventrally with 1 seta. Carpus length 4.9 width, ventrally with 2 long slender setae. Propodus length 5.1 width, dorsally with 2 slender setae, ventrally with 1 slender and 2 long slender setae. Claw of dactylus with 1 slender conate seta and 3 slender setae.

Pleopod 2, operculum (ZMH K–43240; Figs. 30c, 32c) length 1.3 width. Oval, tapering distally, posterior margin with 4 setae. Surface covered with cuticular folds.

Pleopod 3 (ZMH K–43240; Fig. 30d) endopod length 1.1 width, distally with 3 plumose setae. Exopod length 0.7 of endopod length, marginally fringed with fine setae, terminally with 1 slender seta.

Pleopod 4 (ZMH K–43240; Fig. 30e) endopod oval-shaped, length 1.2 width. Exopod length 0.8 endopod length, outer margin with numerous fine setae, terminally with 1 plumose seta.

Uropod (ZMH K–43242; Fig. 40a) uniramous. Protopod with 3 setae (partly broken off). Endopod length 2.2 protopod length, endopod length 5.8 width, with 6 broom setae and 2 slender setae.

Differences in male are shown in Figs. 31, 32 and 33.

Remarks

In *Parvochelus russus*, the surface is structured with folds, most apparent on the pleopod 2 (operculum, Fig. 32c). Because of insufficient numbers of well-preserved material at hand, the distribution of the cuticular structures cannot be provided in full detail. In the CLSM pictures of the habitus of *Parvochelus russus* (Fig. 31a), we see the body appears spotted with reflecting “dots”. We could observe single setae originating from these dots leading us to assume that these dots may be setal articulations.

Molecular results retrieved from COI, 16S and 18S

PCR success was low (in the case of *Chelator rugosus* 18 %, for *C. aequabilis* about 50 % success rate). We obtained the best result for all species for COI and 16S, while 18S was less successful (Table 3). This phenomenon is common to tiny deep-sea samples (Brix et al. 2011). For several organisms, PCR was only successful for one or two of the three markers. Therefore, the datasets of the three genes differ in the number of sequences (Table 3).

Two COI *Parvochelus* sequences of the DIVA-3 expedition were rather short (D3D156: 411 bp, D3D157: 260 bp). Nevertheless, these were added to the multiple sequence alignment to allow comparison between COI and 18S, for which none of the DIVA-2 specimens of the novel genus could be amplified successfully. The ZMH K–43204 (D2D072) sequence was successfully amplified for COI, but was discarded due to contamination. The sequence alignment of the COI contained 21 taxa and was 562 bp long. The three outgroup species contained one additional codon in the alignment. The sequence alignment for the 16S rDNA gene contained 15 taxa and consisted of 494 bp. The 18S rDNA alignment contained 12 sequences and after removal of hypervariable regions using Gblocks, it comprised 2,010 bp.

Few species of each genus are represented in the trees (Fig. 34a–c). The monophyly of Desmosomatidae was strongly supported in analyses of COI with a posterior probability of 1.0 and a ML bootstrap support value of 82.5. However, support for Desmosomatidae was weaker in the 18S analysis. Here, *Eugerdella* and *Chelator* create a polytomy.

The genus *Eugerdella* (Kussakin 1965) was not resolved as monophyletic in COI. *Eugerdella huberti* Schnurr & Brix, 2012 is sister taxon to the *Chelator* monophylum while *E. theodori* Brix, 2007 has a basal position to all other desmosomatids in the tree. This, however, may be a result of insufficient taxon sampling and/or saturation in nucleotide variation due to the old age of the taxa. This can be visualized in a neighbour network (not shown here) created with SplitsTree (Huson 1998) based on the alignment: both *Eugerdella* species as well as *Parvochelus* are characterized by rather long branches; monophyly of *Eugerdella* is not supported in the data. With only two species in the dataset, the status of *Eugerdella* cannot be fully resolved, but results may hint to a paraphyletic genus.

The *Chelator* specimens, on the other hand, form a well-supported monophyletic clade (pp 1.0, ML BT 99.3) in COI with *C. insignis* situated most basally. *Chelator rugosus* is monophyletic with *C. aequabilis* from north of the Walvis Ridge as sistergroup. In 16S, the Cape Basin species *C. rugosus* forms a monophyletic group. With regard to ZMH K–43204 (D2D072), *C. aequabilis* is paraphyletic despite high morphological conformity. Interestingly, in 18S, the *C. aequabilis* sequence of ZMH K–43204 (D2D072) falls outside the *Chelator* sequences and clusters in the basal polytomy. *Chelator rugosus* comes out as one group with the *Chelator* sequence from the Southern Ocean (Raupach et al. 2004) as direct sistergroup. *Chelator aequabilis* represented by ZMH K–43203 (D2D023) is the sistergroup to the

Southern Ocean/Cape Basin clade. The dataset does not contain any *Chelator* sequences from the Southern Ocean.

Looking at COI and 16S, all specimens assigned to the new genus *Parvochelus* group together in one well-supported clade (pp 1.0, ML BT 100). Interestingly, the sequences of *P. russus* from the Brazil Basin (D3D156

and D3D157) are grouped together with the sequences from specimens of the Guinea Basin specimens (no signal of reciprocal monophyly). This could only be confirmed for the COI gene as for the other genes only sequences from either the Brazil Basin or the Guinea Basin were present.

Key to desmosomatid genera

- Pereonite 1 as large as or larger than pereonite 2, PI enlarged → **Eugerdellatinae**
 Pereonite 1 shorter or as long as pereonite 2, PI smaller or resembling PII, more slender than PII or subchelate → **Desmosomatinae**

Desmosomatinae

1. Body margins serrated → ***Echinopleura***
 Body margins smooth → **2**
2. Pleotelson enlarged (width more than pereonite 7 width, length 2 times or more pereonite 7 length), uropods inserting close to each other, uropod endopod short and nearly bulbous, PVII ischium dorsal hook present → ***Pseudomesus***
 Pleotelson not enlarged, uropods extending beyond posterior margin of pleotelson, PVII ischium dorsal hook absent → **3**
3. Pereopod I subchelate → ***Torwolia***
 Pereopod I not subchelate → **4**
4. Pereopod I elongated/attenuated (carpus length more than 5.0 width; propodus more than 6.0 width), carpus and propodus of elongated, ventrally and dorsally with 1–3 setae; pereopod slender (PI carpus and propodus length to width ratios < PII carpus and propodus length to width ratios), may be extremely attenuated (carpus length greater 10.0 width; propodus length greater 15.0 width) and without setae → ***Eugerdia***
 Pereopod I not elongated (carpus length smaller 5.0 width; propodus length smaller 6.0 width), pPereopods V–VII heavily built (basis width twice width anterior pereopods), carpi and propodi broad (laterally flattened), with rows of long natatory setae → ***Desmosoma***
 Carpi and propodi of PV–VII not broadened → **5**
5. Pereopod I to IV of similar shape, not extremely setose, setal rows present, coxae in males extremely anteriorly produced, longer than coxa itself, in females may be anteriorly produced PI to PIV extremely setose (more than 15 setae in setal rows), all pereopods long in relation to body length, coxae not extremely produced → ***Momedossa***

Eugerdellatinae

1. Pereopod I chelate → **2**
 Pereopod I raptorial → **5**
2. Pereonites 6, 7 and pleotelson with segmental borders not expressed (fused) → ***Chelantermedia***
 Pereonites all with segmental borders expressed → **3**
3. Pereopod I carpus with 1 midventral strong seta → **4**
 Pereopod I carpus with setae in other arrangement → **7**
4. Pleotelson posterolateral spines present (can be rudimentary), maxilliped palp with 5 articles, coupling hooks short → ***Prochelator***
 Pleotelson posterolateral spines absent, maxilliped palp number of articles reduced, coupling hooks elongated. → ***Reductosoma***

5. Pereopod IV natatory (enlarged, carpus and propodus of paddle-like shape, with numerous setae) → *Paradesmosoma*
Pereopod IV ambulatory (not paddle-like) → **6**
6. Pereopods I and II of similar size → *Whoia*
Pereopod I much larger than PII → *Eugerdella*
7. Pleotelson vaulted (higher than posterior peronites), operculum small and rounded → *Oecidiobanchus*
Pleotelson not vaulted, operculum as large as width of pleotelson → **8**
8. Head cephalic spines lateral to antennae present → *Disparella*
Head cephalic spines absent **9**
9. Pereopod I carpus with ventral row of composed setae increasing in length towards claw → *Cryodesma*
Pereopod I merus length = width or shorter, carpus anteriorly produced (except *C. stellae*),
ventrally small or slender setae, width subsimilar or exceeding merus width, length subsimilar
or shorter propodus, propodus wide proximally and strongly tapered distally → *Chelator*
Pereopod I merus longer than wide; carpus clearly longer than propodus, not anteriorly
produced, one slender seta laterally to carpo-propodal articulation between propodus and claw
seta, propodus subparallel and only distally slightly narrowing. → *Parvochelus*

Remarks

Besides *Thaumastosoma* Hessler 1970, the question about the systematic position of the genus *Pseudomesus* Hansen, 1916 is one of the most discussed systematic problems in the literature concerning Desmosomatidae and Nannoniscidae (e.g. Svavarsson 1984; Wägele 1989; Kaiser and Brix 2007). The affiliation of both genera has been questioned more than once

and by several authors (e.g. Hansen 1916; Hessler 1970; Svavarsson 1984; Wägele 1989). *Thaumastosoma* has been considered as member of Nannoniscidae by Siebenaller & Hessler (1977, 1981), was recently transferred back by Wilson (2008b) and thus is excluded from this key. *Pseudomesus* is included into this key due to the history of taxonomic discussion.

Key to the species of *Chelator* Hessler, 1970

1. Body shape: pereonite 5 broadest, pereonites 5 to pleotelson tapering towards pleotelson → **2**
Body shape: pereonite 5 of equal width or less width as pleotelson → **3**
2. Antennula with six articles → *C. chelatus*
Antennula with five articles → **4**
3. Antennula with six articles, pereopod II dactylus elongated → *C. brevicaudus*
Antennula with five articles, pereopod II dactylus not elongated → **5**
4. Pereonite 5 lateral margins straight, pereopod I carpus ventrally only one slender seta, not produced at base of claw-seta → *C. stellae*
Pereonite 5 lateral margins convex (broadest of whole body), pereopod I carpus with several slender setae (6 in type drawn by Hessler), produced at base of claw-seta → *C. insignis*
5. Pereopod I carpus with one midventral small seta and one or two setae (small, slender) at base of claw-seta → **6**
Pereopod I carpus about six small setae (type drawn by Hessler 1970) distributed from midventral to base of claw-seta and one slender seta directly at base of claw-seta, operculum with numerous small setae on lateral and posterior margins, pereonite 5 nearly square with nearly straight sides → *C. vulgaris*
6. Pereopod I carpus one small midventral seta and two slender setae proximal to claw-seta. Pereopod II slender (carpus length 4.5 width), its carpus and propodus less than 8 setae, operculum rounded with lateral margins clearly convex and 2 setae on posterior margin. → *C. verecundus*
Pereopod I carpus one small midventral seta and two setae (small, slender) proximal to claw-seta. Pereopod II carpus length about 3 to 3.5 width, setal rows with more than 8 setae → **7**
7. Claw of pereopod II with serrated conate seta, operculum with several small setae on lateral margins margin, cuticular structure in female and male visible → *C. rugosus*
Claw of pereopod II with simple conate seta, operculum only 2 small setae on posterior margin, cuticular structure in females less visible than in males → *C. aequabilis*

Remarks

Chelator striatus (Menzies 1962) is excluded from the key, because the description of the species is incomplete, for example a drawing of the PI is missing and other species distinguishing characters are not visible. The type is in a very bad condition, missing relevant appendages (PI) or being squeezed. Because an unequivocal species allocation is therefore not possible, this species should be henceforward regarded as nomen dubium.

The existence of *Chelibranchus* Mezhov, 1986 is questioned here. Mezhov (1986) presented the following characters in the generic diagnosis: PI with elongated articles: carpus more than 2 times longer than wide, distoventral seta almost as long as propodus (chela), propodus 1.5 times longer than dactylus. Although characters were described in the text, they were not illustrated and are completely missing in the described type specimen of *Chelibranchus canaliculatus* Mezhov, 1986. Two female specimens were documented, but both are without pereopods. No information is given about the developmental stage of the holotype. Due to the importance of PI, it is impossible to define a genus without describing the characters of this leg. Consequently, the drawings of the only species of this genus are insufficient and the designated type specimen is missing even generic characters.

When Mezhov (1986) described the genus, he used an example of another species for some characters, e.g. PI of *Chelator brevicaudus* (Menzies and George 1972). Mezhov (1986) also suggested that *Desmosoma lineare* G.O. Sars, 1864 should be reassigned to the genus *Chelibranchus*. This is astonishing, because this species is the type species of *Desmosoma*. Furthermore, the characters of PI of *Desmosoma lineare* are totally different from those of the species with a chelate PI. Kussakin (1999) added *Nymphodora fletcheri* (Paul & George, 1975) to *Chelibranchus*. This is noteworthy, because this species is a nannoniscid as redescribed by Kaiser (2009). This underlines even more the impression that *Chelibranchus* is badly defined due to missing characters and the whole definition of *Chelibranchus* as a new genus as presented by Mezhov (1986) is based on speculation. Thus, we suggest that *Chelibranchus* should be rejected and the genus and the type species should be called nomen dubium.

Discussion

Integrative species delimitation

The morphological species concept is most commonly applied in deep-sea isopod taxonomy. Cryptic (i.e. morphologically similar, but genetically distinct) species may lead to an underestimation of the true species

diversity in the deep sea (Vrijenhoek 2009). Unambiguous delineation of species remains thus a central problem in systematic and taxonomic studies but integrative approaches combining and comparing independent datasets can help to overcome such problems (Schwentner et al. 2011).

The genetic data available for deep-sea isopods are still very scarce and the relationships amongst Desmosomatidae and Eugerdelatinae remain elusive. We were able to show a clear distinctiveness between the genera *Chelator* and *Parvochelus*. Together with the above-mentioned morphological differences from all other genera of the family, we see justification for erecting a new, independent desmosomatid genus (see genetic results). DNA barcoding (Hebert et al. 2003) offers a promising alternative approach based on strict application of a distinct gap between intraspecific variability and interspecific variation in genetic distances of cytochrome-c-oxidase subunit I (COI). It was subsequently complemented by inclusion of other “barcoding” markers such as 16S. Threshold values are, however, not universal across different evolutionary lineages and thus genetic distance thresholds have to be applied carefully across taxa. While Hebert et al. (2003) proposed a 3 % threshold value, Radulovici et al. (2009), for example, considered intraspecific divergence greater than 3 %, like >13 % as potentially cryptic species in the case of gammarid amphipods. In spinicaudatan branchiopods, Schwentner et al. (2011) identified a 5–6 % threshold to discriminate between intra- and interspecific divergence. For asellote isopods few studies are yet known that applied genetic distances for species delimitation. In case of the Haplioniscidae and within the genus *Haplioniscus*, differences between species ranged from 9–20 % sequence divergence (uncorrected *p* distance; Brix et al. 2011) and from 25–28 % between genera. The high between-group divergence was contrasted by an intraspecific variability of below 1.8 %. Comparable patterns were observed for Munnopsidae (Osborn 2009). In Macrostylidae, interspecific distances of the 16S rRNA lay between 23 and 31 % and were thus not smaller than inter-familial distances while intraspecific diversity was close to zero (Riehl and Brandt 2013). The haplotypes of *C. rugosus* in the Cape Basin show a maximum of 0.4 % *p* distance in COI and 16S and hence fall within the range previously observed in haploniscids and munnopsids. Between the *C. rugosus* and *C. aequabilis* haplotypes and across all southeastern Atlantic basins, a *p* distance of 10.4–15.1 % was found in 16S and 15.6–18.6 % in COI which is again in accordance with observations in other families. Between the type specimens described above, the *p* distance varies from 7 to 15 % (Tables 6, 7 and 8) although they are very similar morphologically.

Table 6 Uncorrected pairwise genetic distances between individuals of the different species for the COI gene

| Specimen | 1 | 2 | 3 | 4 | 5 | 6 | 7 | 8 | 9 | 10 | 11 | 12 | 13 | 14 | 15 | 16 | 17 | 18 | 19 | 20 | 21 | |
|-----------------------------------|-------|-------|-------|-------|-------|-------|-------|-------|-------|-------|-------|-------|-------|-------|-------|-------|-------|-------|-------|-------|----|--|
| 1 D2D002_Chelator_rugosus | | | | | | | | | | | | | | | | | | | | | | |
| 2 D2D012_Chelator_rugosus | 0.004 | | | | | | | | | | | | | | | | | | | | | |
| 3 D2D014_Chelator_rugosus | 0.004 | 0.004 | | | | | | | | | | | | | | | | | | | | |
| 4 D2D003_Chelator_rugosus | 0.004 | 0.004 | 0.004 | | | | | | | | | | | | | | | | | | | |
| 5 D2D013_Chelator_rugosus | 0.005 | 0.005 | 0.005 | 0.005 | | | | | | | | | | | | | | | | | | |
| 6 D2D016_Chelator_rugosus | 0.011 | 0.011 | 0.011 | 0.011 | 0.013 | | | | | | | | | | | | | | | | | |
| 7 D2D023_Chelator_aequabilis | 0.172 | 0.174 | 0.174 | 0.174 | 0.174 | 0.176 | | | | | | | | | | | | | | | | |
| 8 D2D051_Chelator_aequabilis | 0.152 | 0.154 | 0.154 | 0.154 | 0.150 | 0.157 | 0.120 | | | | | | | | | | | | | | | |
| 9 Chelator_sp_(Southern_Ocean) | 0.161 | 0.161 | 0.161 | 0.161 | 0.161 | 0.161 | 0.195 | 0.202 | | | | | | | | | | | | | | |
| 10 IDesm064_Chelator_insignis | 0.270 | 0.268 | 0.270 | 0.272 | 0.270 | 0.267 | 0.256 | 0.267 | 0.245 | | | | | | | | | | | | | |
| 11 IDesm071_Chelator_insignis | 0.274 | 0.272 | 0.274 | 0.276 | 0.274 | 0.269 | 0.253 | 0.271 | 0.246 | 0.004 | | | | | | | | | | | | |
| 12 D3D156_Parvochelus_russus | 0.333 | 0.331 | 0.333 | 0.336 | 0.333 | 0.336 | 0.352 | 0.356 | 0.343 | 0.348 | 0.351 | | | | | | | | | | | |
| 13 D2D031_Parvochelus_russus | 0.342 | 0.340 | 0.342 | 0.343 | 0.342 | 0.343 | 0.360 | 0.363 | 0.349 | 0.336 | 0.339 | 0.015 | | | | | | | | | | |
| 14 D2D035_Parvochelus_russus | 0.347 | 0.345 | 0.347 | 0.349 | 0.347 | 0.349 | 0.360 | 0.369 | 0.343 | 0.331 | 0.333 | 0.022 | 0.023 | | | | | | | | | |
| 15 D2D044_Parvochelus_russus | 0.336 | 0.335 | 0.336 | 0.338 | 0.338 | 0.336 | 0.346 | 0.356 | 0.343 | 0.320 | 0.317 | 0.087 | 0.082 | 0.089 | | | | | | | | |
| 16 D3D157_Parvochelus_russus | 0.354 | 0.354 | 0.354 | 0.354 | 0.354 | 0.354 | 0.359 | 0.385 | 0.354 | 0.385 | 0.381 | 0.089 | 0.092 | 0.081 | 0.119 | | | | | | | |
| 17 HQ214677_Eugertella_huberti | 0.327 | 0.327 | 0.329 | 0.329 | 0.327 | 0.327 | 0.330 | 0.345 | 0.333 | 0.340 | 0.341 | 0.331 | 0.327 | 0.329 | 0.338 | 0.358 | | | | | | |
| 18 D2D050_Eugertella_theodori | 0.365 | 0.361 | 0.361 | 0.365 | 0.363 | 0.358 | 0.346 | 0.367 | 0.351 | 0.347 | 0.346 | 0.363 | 0.340 | 0.340 | 0.331 | 0.412 | 0.360 | | | | | |
| 19 JF283474_Haplionicus_rostratus | 0.390 | 0.392 | 0.388 | 0.392 | 0.388 | 0.395 | 0.364 | 0.404 | 0.340 | 0.349 | 0.348 | 0.336 | 0.331 | 0.335 | 0.338 | 0.381 | 0.360 | 0.335 | | | | |
| 20 EF682287_Paropsurus_giganteus | 0.365 | 0.367 | 0.367 | 0.367 | 0.367 | 0.367 | 0.337 | 0.343 | 0.358 | 0.331 | 0.330 | 0.343 | 0.322 | 0.320 | 0.333 | 0.396 | 0.322 | 0.333 | 0.247 | | | |
| 21 EF682297_Lipomerinae_sp. | 0.343 | 0.342 | 0.342 | 0.345 | 0.343 | 0.342 | 0.349 | 0.340 | 0.335 | 0.331 | 0.330 | 0.396 | 0.374 | 0.369 | 0.352 | 0.427 | 0.376 | 0.343 | 0.331 | 0.272 | | |

Table 7 Uncorrected pairwise genetic distances between individuals of the different species for the 16 s gene

| Species | 1 | 2 | 3 | 4 | 5 | 6 | 7 | 8 | 9 | 10 | 11 | 12 | 13 | 14 | 15 |
|------------------------------------|-------|-------|-------|-------|-------|-------|-------|-------|-------|-------|-------|-------|-------|-------|----|
| D2D023_ <i>Chelator_aequabilis</i> | | | | | | | | | | | | | | | |
| D2D051_ <i>Chelator_aequabilis</i> | 0.065 | | | | | | | | | | | | | | |
| D2D072_ <i>Chelator_aequabilis</i> | 0.150 | 0.146 | | | | | | | | | | | | | |
| D2D014_ <i>Chelator_rugosus</i> | 0.143 | 0.156 | 0.103 | | | | | | | | | | | | |
| D2D016_ <i>Chelator_rugosus</i> | 0.143 | 0.156 | 0.103 | 0.000 | | | | | | | | | | | |
| D2D003_ <i>Chelator_rugosus</i> | 0.141 | 0.158 | 0.105 | 0.002 | 0.002 | | | | | | | | | | |
| D2D012_ <i>Chelator_rugosus</i> | 0.141 | 0.154 | 0.101 | 0.002 | 0.002 | 0.004 | | | | | | | | | |
| IDesm064_ <i>Chelator_insignis</i> | 0.236 | 0.231 | 0.233 | 0.244 | 0.244 | 0.246 | 0.244 | | | | | | | | |
| IDesm071_ <i>Chelator_insignis</i> | 0.225 | 0.222 | 0.222 | 0.233 | 0.233 | 0.235 | 0.233 | 0.000 | | | | | | | |
| D2D031_ <i>Parvochelus_russus</i> | 0.313 | 0.309 | 0.297 | 0.299 | 0.299 | 0.301 | 0.299 | 0.306 | 0.299 | | | | | | |
| D2D044_ <i>Parvochelus_russus</i> | 0.307 | 0.311 | 0.295 | 0.297 | 0.297 | 0.300 | 0.297 | 0.298 | 0.292 | 0.038 | | | | | |
| D2D050_ <i>Eugerdella_theodori</i> | 0.304 | 0.304 | 0.284 | 0.274 | 0.274 | 0.272 | 0.274 | 0.280 | 0.272 | 0.301 | 0.310 | | | | |
| <i>Betamorpha</i> | 0.288 | 0.297 | 0.308 | 0.312 | 0.312 | 0.312 | 0.310 | 0.287 | 0.284 | 0.305 | 0.303 | 0.306 | | | |
| <i>Haploniscus</i> | 0.308 | 0.317 | 0.303 | 0.319 | 0.319 | 0.319 | 0.317 | 0.309 | 0.303 | 0.325 | 0.325 | 0.302 | 0.290 | | |
| <i>Eugerdella huberti</i> | 0.352 | 0.335 | 0.331 | 0.352 | 0.352 | 0.352 | 0.352 | 0.340 | 0.337 | 0.330 | 0.339 | 0.369 | 0.397 | 0.360 | |

The divergence between *C. rugosus* and the type species *C. insignis* was 26.8–27.5 % uncorrected *p* distance in COI and 22.9–25 % in 16S. For *C. aequabilis*, it ranged from 26.7 to 27.7 % for COI, and from 22.9 to 25.6 % uncorrected *p* distance for 16S. Between the genera *Chelator* and *Parvochelus*, a *p* distance of ~32 % was calculated in 16S, and 32–34 % in COI, regardless of the origin of the specimens. A distance of 32 % in the 16S gene has been found to be typical between different congeneric species (Riehl and Brandt 2013), isopod genera (Wetzer 2001) or even families (Riehl and Brandt 2013). The distinct gap between intra- and interspecific variability supports the morphologically defined species.

Within *C. aequabilis*, however, the observed divergence was relatively high [*p* distance between ZMH K–43203 (D2D023) and ZMH K–43205 (D2D051)=7.5 % in 16S and 12.2 % in COI]. According to the “DNA-barcoding” threshold value of 3 % suggested as a universal value for species delimitation (Hebert et al. 2003), this is indicative for the presence of another species not recognised by morphological means. Clearly, the application of a general threshold has its shortcomings (e.g. DeSalle et al. 2005; Meier et al. 2006; Schwentner et al. 2011; Sauer and Hausdorf 2012), e.g. due to the multiply presented overlap between inter-specific and intraspecific nucleotide variability (Will and Rubinoff 2004). Nevertheless, the divergence between *C. aequabilis*

Table 8 Uncorrected pairwise genetic distances between individuals of the different species for the 18S gene

| Species | 1 | 2 | 3 | 4 | 5 | 6 | 7 | 8 | 9 | 10 | 11 | 12 | 13 | 14 | 15 |
|---------------------------------------|-------|-------|-------|-------|-------|-------|-------|-------|-------|-------|-------|-------|-------|-------|----|
| 1 D2D023_ <i>Chelator_aequabilis</i> | | | | | | | | | | | | | | | |
| 2 D2D051_ <i>Chelator_aequabilis</i> | 0.065 | | | | | | | | | | | | | | |
| 3 D2D072_ <i>Chelator_aequabilis</i> | 0.150 | 0.146 | | | | | | | | | | | | | |
| 4 D2D014_ <i>Chelator_rugosus</i> | 0.143 | 0.156 | 0.103 | | | | | | | | | | | | |
| 5 D2D016_ <i>Chelator_rugosus</i> | 0.143 | 0.156 | 0.103 | 0.000 | | | | | | | | | | | |
| 6 D2D003_ <i>Chelator_rugosus</i> | 0.141 | 0.158 | 0.105 | 0.002 | 0.002 | | | | | | | | | | |
| 7 D2D012_ <i>Chelator_rugosus</i> | 0.141 | 0.154 | 0.101 | 0.002 | 0.002 | 0.004 | | | | | | | | | |
| 8 IDesm064_ <i>Chelator_insignis</i> | 0.236 | 0.231 | 0.233 | 0.244 | 0.244 | 0.246 | 0.244 | | | | | | | | |
| 9 IDesm071_ <i>Chelator_insignis</i> | 0.225 | 0.222 | 0.222 | 0.233 | 0.233 | 0.235 | 0.233 | 0.000 | | | | | | | |
| 10 D2D031_ <i>Parvochelus_russus</i> | 0.313 | 0.309 | 0.297 | 0.299 | 0.299 | 0.301 | 0.299 | 0.306 | 0.299 | | | | | | |
| 11 D2D044_ <i>Parvochelus_russus</i> | 0.307 | 0.311 | 0.295 | 0.297 | 0.297 | 0.300 | 0.297 | 0.298 | 0.292 | 0.038 | | | | | |
| 12 D2D050_ <i>Eugerdella_theodori</i> | 0.304 | 0.304 | 0.284 | 0.274 | 0.274 | 0.272 | 0.274 | 0.280 | 0.272 | 0.301 | 0.310 | | | | |
| 13 <i>Betamorpha</i> | 0.288 | 0.297 | 0.308 | 0.312 | 0.312 | 0.312 | 0.310 | 0.287 | 0.284 | 0.305 | 0.303 | 0.306 | | | |
| 14 <i>Haploniscus</i> | 0.308 | 0.317 | 0.303 | 0.319 | 0.319 | 0.319 | 0.317 | 0.309 | 0.303 | 0.325 | 0.325 | 0.302 | 0.290 | | |
| 15 <i>Eugerdella huberti</i> | 0.352 | 0.335 | 0.331 | 0.352 | 0.352 | 0.352 | 0.352 | 0.340 | 0.337 | 0.330 | 0.339 | 0.369 | 0.397 | 0.360 | |

haplotypes is substantial, although we should keep in mind the small number of specimens in the genetic analyses.

According to the phylogenetic species concept, a species is the “smallest monophyletic group worth of recognition” (Mishler and Brandon 1987; Wheeler and Platnick 2000). All species, except *Chelator aequabilis*, formed reciprocally monophyletic clades with high divergence between them. These thus qualify as distinct species according to the phylogenetic species concept. *C. aequabilis* was found paraphyletic in 16S (18S did not sufficiently resolve the tree and in the COI dataset only one of the two clades of *C. aequabilis* is represented). Thus, the possible existence of two morphologically cryptic species within the morphological coherent *C. aequabilis* as indicated by the DNA barcoding approach was confirmed in the phylogenetic analysis. To emphasize our doubt of only one species defined as *C. aequabilis*, we did draw all developmental stages present in the genetic analysis in detail. If future data show the presence of more species, the description for each individual could be used separately. The cuticular folds discussed for separating *C. rugosus* and *C. aequabilis* are variable and therefore not reliable to distinguish both species. This has been already noticed by Just and Wilson (2004). The serrated claw in the PII of *C. rugosus* is not trustworthy because a serrated claw is also present in the PII of a juvenile of *C. aequabilis*. The chaetotaxia of the operculum seems to be the only stable difference between these two species and is only visible in the female. Genetic analyses of individuals of *C. aequabilis* were only possible from the Guinea Basin while DNA amplification from the Angola Basin material (DIVA-1) was unsuccessful. All genetic studies on deep-sea isopods have in common that the datasets studied were rather small and the whole range of intraspecific variability was likely not nearly covered. These data should be treated with care.

Evidence for genetic connectivity across ocean basins

Within *Parvochelus*, specimens sampled from the Brazil Basin (western South Atlantic) form a clade together with specimens from the Guinea Basin (COI). In this clade, they do not form reciprocally monophyletic subclades (Fig. 34). The depth records for *Parvochelus russus* specimens from the Guinea and Brazilian Basins is similar: 5,047 and 5,189 m, respectively. Both basins are separated by the Mid-Atlantic Ridge (MAR), a substantial physical barrier with elevations of up to 3,000 m from the sea floor at abyssal depths and the Romanche Fracture Zone separating the North Atlantic part of the MAR from the South Atlantic part with maximal depth of 7,730 m through the Romanche trench just north of the equator at the narrowest part of the Atlantic between Brazil and West Africa, extending from 2°N to 2°S and from 16° to 20°W (Schlitzer et al. 1985; Bonatti et al. 1996). Both the Guinea and Angola basins are influenced by the southward

current of North Atlantic Deep Water (NADW; Reid 1996). Additionally, the bottom layer in the northern Guinea Basin is influenced by Antarctic Bottom Water (AABW) entering through the Romanche Fracture Zone from the Brazil Basin, while the western Guinea Basin is more influenced by NADW (Kröncke et al. 2013). AABW and NADW may function as potential vector for species distribution. While there is some substantial genetic variation present within *Parvochelus russus* (1.5–11.9 % *p* distances), the close relatedness of some specimens from either side of the MAR suggests sporadic connectivity across this barrier (Fig. 27; Tables 6, 7, 8). If species distribution is influenced by watermasses as suggested by Brix and Svavarsson (2010), the deep passages through the Romanche Fracture Zone may be the connection between populations.

The Cape Basin, on the other side of the Walvis Ridge, is under the influence of a different composition of water masses like the Circumpolar Deep Water (CPDW) and NADW partly passing the Walvis Ridge southwards, but northwards-flowing AABW underlies the more saline and about 2 °C warmer NADW, which mixes with CPDW (Bickert and Wefer 1996; Gage and Tyler 1992). *Chelator aequabilis* has been found only north of the Walvis Ridge in the Angola and the Guinea Basins. The Walvis Ridge potentially separates the species from *C. rugosus*. Due to very restricted sampling effort in the area and patchy distribution of deep-sea isopods (Kaiser and Barnes 2008), the occurrence of each species on both sides of the ridge cannot be excluded. We assume that the Guinea Rise is only a minor barrier to gene flow, if at all. Regarding the *Chelator* haplotypes, we might wonder if it would be possible that future sequences from the Angola basin specimens show a closer relatedness to both species (*C. aequabilites* and *C. rugosus*). If so, we might consider them as one species with variability among each population (Guinea, Angola and Cape basins) and not as cryptic species.

Acknowledgments We would like to thank all pickers and sorters during the DIVA expeditions to provide a unique set of specimens. Michael Raupach and Christoph Held introduced Saskia Brix into the molecular world and helped in the laboratory during her research stay at the Ruhr University Bochum in 2005. Without the technical assistance of Karen Jeskulke and Andrea Ormos working hard on producing high-quality PCR products at the Smithsonian, the whole work would have been much slower. Special thanks go to Amy Driskell for her support. Stefanie Kaiser put energy into discussing and improving the key to genus level. Marco Büntzow introduced the first author to the CLSM and spent much effort into explaining the techniques. Marina Maljutina kindly translated Kussakin's (1999) key to the Arctic *Chelator* species. Saskia Brix and Torben Riehl were supported by the German Research Foundation (DFG) under contract No. Br 1121/28-1 doing first steps in producing results from 2005–2007 in the working group of Angelika Brandt at the University of Hamburg. The Census of the Diversity of Abyssal Marine Life (CeDAMar) supported travels and the financial background for retrieving sequences in the frame of the project “DNA barcoding deep-sea Isopoda”. Torben Riehl was funded by the German National Academic Foundation (Studienstiftung des deutschen Volkes) while writing this article and acknowledges the support of the Marine

Invertebrates Department at the Australian Museum. Kevin Kocot kindly checked the English. Finally, we would like to thank the subject editor Gary Poore and four anonymous referees for their comments improving the quality of our manuscript.

References

- Bickert T, Wefer G (1996) Later quaternary deep water circulation in the South Atlantic: reconstruction from carbonate dissolution and benthic stable isotopes. In: The South Atlantic: present and past circulation. Springer, Heidelberg, pp 599–620
- Birstein JA (1963) Isopods from the ultra-abysal zone of the Bougainville Trench. Zool Zh 42:814–834
- Böttgermann M (2009) Polychaetes (Annelida) of the abyssal SE Atlantic. Org Divers Evol 9:251–428
- Bonatti E, Ligi M, Carrara G, Gasperini L, Turko N, Perfiliev S, Peyve A, Sciuto P (1996) Diffuse impact of the mid-atlantic ridge with the romanche transform: an ultracold ridge-transform intersection. J Geophys Res 101:8043–8054
- Brandt A, Brenke N, Andres H-G, Brix S, Guerrero-Kommritz J, Mühlhardt-Siegel U, Wägele J-W (2005) Diversity of peracarid crustaceans (Malacostraca) from the abyssal plain of the Angola Basin. Org Divers Evol 5:105–112
- Brandt A, Gooday AJ, Brandao SN, Brix S, Brokeland W, Cedhagen T, Choudhury M, Cornelius N, Danis B, De Mesel I, Diaz RJ, Gillan DC, Ebbe B, Howe JA, Janussen D, Kaiser S, Linse K, Malyutina M, Pawlowski J, Raupach M, Vanreusel A (2007) First insights into the biodiversity and biogeography of the Southern Ocean deep sea. Nature 447:307–311
- Brenke N (2005) An epibenthic sledge for operations on marine soft bottom and bedrock. Mar Technol Soc J 39:10–21
- Brix S (2006a) A new genus and new species of Desmosomatidae (Crustacea: Isopoda: Asellota) from the deep sea of south-eastern Australia. Mem Mus Vict 63:175–205
- Brix S (2006b) A new species of Desmosomatidae (Isopoda: Crustacea) from the deep Southern Ocean: *Eugerdella serrata* sp. nov. including remarks to the morphological variability within *Eugerdella* Hessler, 1970. Mitteilungen aus dem hamburger zoologischen Museum und Institut:69–84
- Brix S (2007) Four new species of Desmosomatidae Sars, 1897 (Crustacea: Isopoda) from the deep sea of the Angola Basin. Mar Biol Res 3:205–230
- Brix S, Bruce NL (2008) *Prochelator tupuhi* sp. nov., the first record of Desmosomatidae Sars, 1897 (Crustacea: Isopoda) from New Zealand waters. Zootaxa 1866:462–492
- Brix S, Svavarsson J (2010) Distribution and diversity of desmosomatid and nannoniscid isopods (Crustacea) on the Greenland–Iceland–Faeroe Ridge. Polar Biol 33:515–530
- Brix S, Riehl T, Leese F (2011) First genetic data for species of the genus *Haploniscus* Richardson, 1908 (Isopoda: Asellota: Haploniscidae) from neighbouring deep-sea basins in the South Atlantic. Zootaxa 2838:79–84
- Brökeland W (2010a) Description of four new species from the *Haploniscus unicornis* Menzies, 1956 complex (Isopoda:Asellota: Haploniscidae). Zootaxa 2536:1–35
- Brökeland W (2010b) Redescription of *Haploniscus rostratus* (Menzies, 1962) (Crustacea: Peracarida: Isopoda) with observations on the postmarsupial development, size ranges and distribution. Zootaxa 2521:1–25
- Castresana J (2000) Selection of conserved blocks from multiple alignments for their use in phylogenetic analysis. Mol Biol Evol 17:540–552
- Choudhury M (2009) Biodiversity and zoogeography of the Isopoda (Crustacea: Malacostraca) from the Victoria Land Coast, Ross Sea, Antarctica. Doktor dissertation, University of Hamburg, Hamburg
- Choudhury M, Brandt A (2007) Composition and distribution of benthic isopod (Crustacea, Malacostraca) families off the Victoria-Land Coast (Ross Sea, Antarctica). Polar Biol 30:1431–1437
- Crandall KA, Fitzpatrick JF (1996) Crayfish molecular systematics: using a combination of procedures to estimate phylogeny. Syst Biol 45:1–26
- DeSalle R, Egan MG, Siddall M (2005) The unholy trinity: taxonomy, species delimitation and DNA barcoding. Philos Trans R Soc Lond B 360:1905–1916
- Drummond AJ, Ashton B, Buxton S, Cheung M, Cooper A, Duran C, Field M, Heled J, Kearse M, Markowitz S, Moir R, Stones-Havas S, Sturrock S, Thierer T, Wilson A (2011) Geneious v.5.4, Available from <http://www.geneious.com>
- Folmer O, Black M, Hoeh W, Lutz R, Vrijenhoek R (1994) DNA primers for amplification of mitochondrial cytochrome c oxidase subunit I from diverse metazoan invertebrates. Mol Mar Biol Biotechnol 3: 294–299
- Gage JD, Tyler PA (1992) Deep-sea biology: a natural history of organisms at the deep-sea floor. Cambridge University Press, Cambridge
- Guindon S, Dufayard JF, Lefort V, Anisimova M, Hordijk W, Gascuel O (2010) New algorithms and methods to estimate maximum-likelihood phylogenies: assessing the performance of PhyML 3.0. Syst Biol 59:307–321
- Hansen HJ (1916) Crustacea Malacostraca: the order Isopoda. Dan Ingolf Exped 3:1–262
- Hebert PDN, Ratnasingham S, de Waard JR (2003) Barcoding animal life: cytochrome c oxidase subunit 1 divergences among closely related species. Proc R Soc Lond B 270:S96–S99
- Hessler RR (1970) The Desmosomatidae (Isopoda, Asellota) of the Gay Head-Bermuda transect. Bull Scripps Inst Oceanogr 15:1–185
- Hessler RR, Sanders HL (1967) Faunal diversity in the deep sea. Deep-Sea Res 14:65–78
- Huson DH (1998) SplitsTree: a program for analyzing and visualizing evolutionary data. Bioinformatics 14:68–73
- Just J, Wilson GDF (2004) Revision of the *Paramunna* complex (Isopoda: Asellota: Paramunnidae). Invertebr Syst 18:377–466
- Kaiser (2009) *Nymphodora* gen. nov., a new genus of *Nannoniscidae* Hansen, 1916 (Isopoda, Asellota) from the high Arctic. Zootaxa 2096:371–380
- Kaiser S, Barnes DKA (2008) Southern Ocean deep-sea biodiversity: sampling strategies and predicting responses to climate change. Clim Res 37:165–179
- Kaiser S, Brix S (2005) A new isopod species from the Southern Ocean: *Disparella maiuscula* sp. nov. (Isopoda: Asellota: Desmosomatidae). Mitt Hamb Zool Mus Inst 102:153–165
- Kaiser S, Brix S (2007) Two new species of the genus *Pseudomesus* Hansen, 1916 (Isopoda, Asellota) from the Southern hemisphere: *Pseudomesus pitombo* sp. nov and *Pseudomesus satanus* sp. nov. Zootaxa 1658:21–38
- Katoh K, Misawa K, Kuma K, Miyata T (2002) MAFFT: a novel method for rapid multiple sequence alignment based on fast Fourier transform. Nucleic Acids Res 30:3059–3066
- Kihara TC, Rocha C (2009) Técnicas para o estudo taxonomico de copépodos harpacticóides da meiofauna marinha. Asterisco, Porto Alegre
- Kröncke I, Reiss H, Türkay M (2013) Macro- and megafauna communities in three deep basins of the South-East Atlantic. Deep-Sea Res 1(81):25–35
- Kussakin OG (1965) On the fauna of the Desmosomatidae (Crustacea, Isopoda) of the Far-Eastern seas of the USSR. Issledovanija dal'nevostocnaya morej SSSR (Exploration of the Far-Eastern Seas of the USSR) 3:115–144
- Kussakin OG (1999) Marine and brackish-water Crustacea (Isopoda) of cold and temperate waters of the Northern

- Hemisphere. 3. Suborder Asellota 2. Families Joeropsididae, Nannoniscidae, Desmosomatidae, Macrostylidae. *Opredeliteli po Faune. Akad Nauk* 169:1–384
- Leese F, Agrawal S, Held C (2010) Long-distance island hopping without dispersal stages: transportation across major zoogeographic barriers in a Southern Ocean isopod. *Naturwissenschaften* 97(6):583–594. doi:10.1007/s00114-010-0674-y
- Maljutina MV, Kussakin OG (1996) Addition to the Polar Sea bathyal and abyssal Isopoda (Crustacea). Part 1. Anthuridea, Valvifera, Asellota (Ischnomesidae, Macrostylidae, Nannoniscidae). *Zoosyst Ross* 4:49–62
- Meier R, Shiyang K, Vaidya G, Ng PKL (2006) DNA barcoding and taxonomy in Diptera: a tale of high intraspecific variability and low identification success. *Syst Biol* 55:715–728
- Menzel L, George KH, Martinez P (2011) Submarine ridges do not prevent large-scale dispersal of an abyssal fauna: a case study of Mesocletodes (Crustacea, Copepoda, Harpacticoida). *Deep Sea Res Part I* 58:839–864
- Menzies RJ (1962) *Abyssal Crustacea*. Columbia University Press, New York
- Menzies RJ, George RY (1972) Isopod Crustacea of the Peru-Chile Trench. *Anton Bruun Rep* 9:1–124
- Mezhov BV (1986) Bathyal and abyssal Nannoniscidae and Desmosomatidae (Isopoda, Asellota) from Alaska Bay. *Arch Zool Mus Moscow State Univ* 24(1986):126–167
- Michels J, Büntzow M (2010) Assessment of Congo red as a fluorescence marker for the exoskeleton of small crustaceans and the cuticle of polychaetes. *J Micros* 238:95–101
- Mishler BD, Brandon RN (1987) Individuality, pluralism, and the phylogenetic species concept. *Biol Philos* 2(4):397–414
- Osborn KJ (2009) Relationships within the Munnopsidae (Crustacea, Isopoda, Asellota) based on three genes. *Zool Scr* 38:617–635
- Palumbi S, Martin A, Romano S, Stice L, Grabowski G (1991) The simple fool's guide to PCR, version 2.0. Spec Pub University of Hawaii, Department of Zoology and Kewalo Marine Laboratory
- Posada D (2008) jModelTest: phylogenetic model averaging. *Mol Biol Evol* 25:1253–1256
- Radulovici AE, Bernard S-M, Dufresne F (2009) DNA barcoding of marine crustaceans from the Estuary and Gulf of St Lawrence: a regional-scale approach. *Mol Ecol Resour* 9:181–187
- Raupach MJ, Held C, Wägele J-W (2004) Multiple colonization of the deep sea by the Asellota (Crustacea: Peracarida: Isopoda). *Deep Sea Res Part II* 51:1787–1795
- Reid J (1996) On the circulation of the South Atlantic Ocean. In: *The South Atlantic: present and past circulation*. Springer, Heidelberg, pp 13–44
- Rex M, Etter R (2010) *Deep-sea biodiversity. Pattern and scale*, 1st edn. Harvard University Press, London
- Riehl T, Brandt A (2010) Descriptions of two new species in the genus *Macrostylis* Sars, 1864 (Isopoda, Asellota, Macrostylidae) from the Weddell Sea (Southern Ocean), with a synonymisation of the genus *Desmostylis* Brandt, 1992 with *Macrostylis*. *Zookeys* 57:9–49
- Riehl T, Brandt A (2013) Southern Ocean Macrostylidae reviewed with a key to the species and new descriptions from Maud Rise. *Zootaxa* 3692(1):160–203
- Riehl T, Kaiser S (2012) Conquered from the deep sea? A new deep-sea isopod species from the Antarctic shelf shows pattern of recent colonization. *PLoS ONE* 7(11):e49354
- Riehl T, Wilson GD, Hessler RR (2012) New Macrostylidae Hansen, 1916 (Crustacea: Isopoda) from the Gay Head-Bermuda transect with special consideration of sexual dimorphism. *Zootaxa* 3277:1–26
- Sanders HL, Hessler RR (1969) *Ecology of the deep-sea benthos*. Science (New York) 163:1419
- Sanders HL, Hessler RR, Hampson GR (1965) An introduction to the study of deep-sea benthic faunal assemblages along the Gay Head-Bermuda transect. *Deep Sea Res Oceanogr Abstr* 12:845–867
- Sars GO (1897) Isopoda. Part VII, VIII. Desmosomidae, munnopsidae. An account of the crustacea of Norway with short descriptions and figures of all the species, Oslo, 117–144
- Sauer J, Hausdorf B (2012) A comparison of DNA-based methods for delimiting species in a Cretan land snail radiation reveals shortcomings of exclusively molecular taxonomy. *Cladistics* 28:300–316
- Schlitzer R et al (1985) A meridional 14C and 39Ar section in northeast Atlantic deep water. *J Geophys Res* 90:6945–6952
- Schnurr S, Brix S (2012) *Eugerdella huberti* sp. nov.—a new species of Desmosomatidae Sars, 1897 (Crustacea, Isopoda) from the deep-sea of the South Atlantic Ocean. *Mar Biodivers* 42:13–24
- Schwentner M, Timms BV, Richter S (2011) An integrative approach to species delineation incorporating different species concepts: a case study of *Limnadopsis* (Branchiopoda: Spinicaudata). *Biol J Linn Soc* 104(3):575–599
- Svavarsson J (1984) Description of the male of *Pseudomesus brevicornis* Hansen, 1916 (Isopoda, Asellota, Desmosomatidae) and rejection of the family Pseudomesidae. *Sarsia* 69:37–44
- Svavarsson J (1988) Bathyal and abyssal Asellota (Crustacea, Isopoda) from the Norwegian, Greenland and North Polar Seas. *Sarsia* 73:83–106
- Svavarsson J, Stromberg JO, Brattegard T (1993) The deep-sea asellote (Isopoda, Crustacea) fauna of the Northern Seas: species composition, distributional patterns and origin. *J Biogeogr* 20:537–555
- Vrijenhoek RC (2009) Cryptic species, phenotypic plasticity, and complex life histories: assessing deep-sea faunal diversity with molecular markers. *Deep Sea Res Part II* 56:1713–1723
- Wägele JW (1989) Evolution und phylogenetisches System der Isopoda. *Stand der Forschung und neue Erkenntnisse*. *Zoologica* 140:1–262
- Wetzer R (2001) Hierarchical analysis of mtDNA variation and the use of mtDNA for isopod (Crustacea: Peracarida: Isopoda) systematics. *Contrib Zool* 70:23–39
- Wheeler QD, Platnick NI (2000) The phylogenetic species concept (sensu Wheeler and Platnick) Quentin D. Wheeler and Norman I. Platnick. *Species concepts and phylogenetic theory: a debate*, 55
- Will KW, Rubinoff D (2004) Myth of the molecule: DNA barcodes for species cannot replace morphology for identification and classification. *Cladistics* 20:47–55
- Wilson GDF (2008a) Local and regional species diversity of benthic Isopoda (Crustacea) in the deep Gulf of Mexico. *Deep-Sea Res II* 55:2634–2649
- Wilson GDF (2008b) A review of taxonomic concepts in the Nannoniscidae (Isopoda, Asellota), with a key to the genera and a description of *Nannoniscus oblongus* Sars. *Zootaxa* 1680:1–24
- Wilson GDF, Hessler RR (1987) Speciation in the deep sea. *Annu Rev Ecol Syst* 18:185–207